NOVEL DEVICES FOR ANALYTICAL-SCALE ISOELECTRIC TRAPPING

SEPARATIONS

A Dissertation

by

PENIEL JASON LIM

Submitted to the Office of Graduate Studies of
Texas A&M University
in partial fulfillment of the requirements for the degree of

DOCTOR OF PHILOSOPHY

December 2006

Major Subject: Chemistry

NOVEL DEVICES FOR ANALYTICAL-SCALE ISOELECTRIC TRAPPING

SEPARATIONS

A Dissertation

by

PENIEL JASON LIM

Submitted to the Office of Graduate Studies of
Texas A&M University
in partial fulfillment of the requirements for the degree of

DOCTOR OF PHILOSOPHY

Approved by:

Chair of Committee,	Gyula Vigh
Committee Members,	Hung-Jue Sue
	Paul A. Lindahl
	Manuel P. Soriaga
Head of Department,	David Russell

December 2006

Major Subject: Chemistry

ABSTRACT

Novel Devices for Analytical-Scale Isoelectric Trapping Separations. (December 2006)

Peniel Jason Lim, B.S., University of San Carlos, Philippines

Chair of Advisory Committee: Dr. Gyula Vigh

Isoelectric trapping (IET), has proven to be one of the most successful electrophoretic techniques used for separations of ampholytic compounds. IET is carried out in multicompartment electrolyzers (MCEs) in which adjacent compartments are joined through buffering membranes whose pH values bracket the pI of the ampholytic component to be trapped in the compartment. The present small-scale instruments use plastics as their structural materials, which causes poor Joule heat dissipation. The separation compartments have cylindrical or pear-shaped interiors with large internal diameters, which create long heat transfer paths. The long electrode distances yield low field strengths that lead to low electrophoretic velocities for the analytes. These factors interrelatedly limit the electric power that can be applied to the system, contributing to long separation times. Furthermore, these devices do not offer a realistic solution to the problems associated with the detection of low abundance proteins.

To address these problems, two novel IET devices have been developed for small-scale IET separations. The first device, named MSWIFT, was constructed using thermally conductive, high-purity alumina as the structural material of the separation compartments. By creating narrow, 0.1- or 0.2-mL channels in thin alumina blocks, the

heat transfer path from the center of the compartment to the wall was significantly decreased; and the distance between electrodes was greatly shortened. MSWIFT achieved 6 to 50 times faster IET separations compared to other MCEs. The second device, named ConFrac, was developed to simultaneously fractionate and concentrate ampholytic components from a complex sample into 0.1-mL collection compartments. By designing a system with a 2-dimensional pH gradient and allowing recirculation of the sample feed, the ConFrac demonstrated enrichment of analytes by a factor of 100 and greater.

To my wife, Becca, for her unfailing love, unceasing support, and for enduring with me the often unpredictable challenges of being a graduate student

To my parents, Pedro and Patricia, for raising God-fearing children; they still teach me the things that matter most - those that are eternal

ACKNOWLEDGEMENTS

TABLE OF CONTENTS

Page

Page

LIST OF FIGURES

NOMENCLATURE

2DE	Two-Dimensional Electrophoresis
ACAD	Automated computer-aided design
Asp	Aspartic acid
AU	Absorbance units
BDMASP	1,3-bis(N,N-dimethylamino)-2-O-sulfopropane
BDPASP	1,3-bis(N,N-dipropylamino)-2-O-sulfopropane
BE	Background electrolyte
BMSP	1,3-bis(4-morpholino)-2-O-sulfopropane
BzS^-	Benzenesulfonate ion
BzSA	Benzenesulfonic acid
$BzTMA^+$	Benzyltrimethylammonium ion
BzTMAOH	Benzyltrimethylammonium hydroxide
CA	Carrier ampholytes
Carn	Carnosine
CE	Capillary electrophoresis
cIEF	Capillary isoelectric focusing
ConFrac	Concentration-Fractionation device
ESI-MS	Electrospray ionization-mass spectrometry
Glu	Glutamic acid
HEPES	4-2-hydroxyethyl-1-piperazineethanesulfonic acid
His	Histidine

HMMB	4-hydroxy-3-(morpholinomethyl)benzoic acid
HBMMB	4-hydroxy-3,5-bis(morpholinomethyl)benzoic acid
IDA	Iminodiacetic acid
IEF	Isoelectric focusing
IET	Isoelectric trapping
IPG	Immobilized pH gradient
MCE	Multi-compartment electrolyzer
MeLys	Methyl lysine
MSA	Methylsulfonic acid
MSWIFT	Membrane-separated wells for isoelectric focusing and trapping device
NDA	Naphthalene dialdehyde
pI	Isoelectric point
pK_a	Negative logarithm of the acid dissociation constant
PTS^-	*p*-toluenesulfonate ion
PTSA	*p*-toluenesulfonic acid
PVA	Poly(vinyl alcohol)
PVC	Poly(vinyl chloride)
QDBA	N,N-bis(carboxypropanyl)diethylammonium hydroxide
TRIS	Tris-(hydroxymethyl)aminomethane
UV	Ultraviolet

1. INTRODUCTION

1.1. Ampholytes and isoelectric points

An ampholyte generally has one or more weakly acidic and weakly basic groups. The charge state of an ampholyte depends on the pK_a values of each group and the pH of the environment. In a highly basic environment (*i.e.,* when the pH is greater than the pK_a of the most basic group), all carboxylic and amino groups of the ampholyte are completely deprotonated giving the ampholyte a net negative charge. Under highly acidic conditions, (*i.e.,* when the pH is lower than the pK_a of the most acidic group), all ionizable groups are completely protonated giving the ampholyte a net positive charge. Somewhere along the pH range, there is a pH where the net charge of the ampholyte is zero; at this state, the ampholyte is said to be isoelectric and the pH is equal to the pI value (isoelectric point) of the ampholyte. The pI of a simple ampholyte is calculated as the average of the nearest pK_a values which surround the neutral point, as long as any additional pK_a values of the ampholyte are at least 2 pH units different from that of the pI [1].

For proteins, calculation of the accurate pI value is complicated because proteins fold in solution and this may cover some of the functional groups and prevent them from protonation and deprotonation. Moreover, thiol groups can easily oxidize, thus cannot contribute to the net charge. Nevertheless, reasonable approximation of the pI value can obtained from the net charge versus pH plot for a protein, calculated with the equation:

This dissertation follows the style and format of *Electrophoresis.*

$$\text{Net charge} = \sum_i \frac{n_i}{\left(\dfrac{K_i}{c_{H+}}\right) + 1} - \sum_j \frac{n_j}{\left(\dfrac{c_{H+}}{K_j}\right) + 1}$$

where subscripts i refer to the basic groups and subscripts j refer to the acidic groups, K is the equilibrium constant of each ionizable group, and c_{H+} is the hydrogen ion concentration. In most approximations, the ionizable groups listed in Table 1 are assumed to have the same pK_a value at any position in the large molecule [2-3]. Currently, most pI values of known proteins are determined experimentally using techniques described in the next section.

Table 1. pK$_a$ values of the acidic and basic functional groups that contribute to the net charge of the protein [2]

Functional group (amino acid residue)	pK$_a$
α-amino	9.7
ε-amino (Lys)	10.5
guanidino (Arg)	12.4
imidazole (His)	6.0
α-carboxyl	2.3
β-carboxyl (Asp)	3.9
γ-carboxyl (Glu)	4.3
SH (Cys)	8.3
phenolic OH (Tyr)	10.0

1.2. Isoelectric focusing

Among the techniques capable of separating ampholytic components, electrophoretic methods such as isoelectric focusing (IEF) and isoelectric trapping (IET) are the most suitable due to their high resolving power. In an IEF experiment, an ampholytic sample is mixed with a series low molecular mass polycarboxy-polyamino compounds known as carrier ampholytes (CA) and placed in between the anode and the cathode [4-5]. Carrier ampholytes have high buffering capacity at their individual isoelectric points and adequate conductivity in the vicinity of their pI to carry the electric current (pK_a values of the functional groups responsible for buffering in each ampholyte are close to the pI value) [6]. Upon application of an electric potential, the carrier ampholytes and the ampholytic sample migrate electrophoretically until they reach the position where the pH of the medium is equal to their pI values and their electrophoretic mobilities approach zero. Since there are in excess of 1000 different CA species per pH unit [7], the carrier ampholytes create a continuous pH gradient between the two electrodes, with the pH increasing from the anode to the cathode [7-12]. The analytes get focused in different locations in that pH gradient, thus are separated [13-15]. Any movement away from this point in the gradient, brought about by diffusion or convection, causes the ampholyte to acquire a positive or negative net charge and hence forces it to migrate back to the location where the pH is equal to its pI. According to Svensson's model [5], if the electric field and the pH gradient are kept constant, the system will reach a steady state where the proteins will remain focused in sharp bands, constantly opposing the effects of diffusion and convective mixing. Strong electrolytes present in the sample are electrophoretically transported to the electrolyte chambers (*i.e.,* strong anions migrate to the anode chamber;

strong cations migrate to the cathode chamber) and remain there throughout the

separation process.

The smallest ΔpI value that can be distinguished by IEF is expressed by the equation

[16]:

$$\Delta pI = 3 \sqrt{ D\left[\frac{d(pH)}{dx}\right] \Big/ E\left[\frac{d\mu}{d(pH)}\right] }$$

In this equation, D is the diffusion coefficient of the ampholytic substance, $d(pH)/dx$ is

shape of the pH gradient across the separation axis, E is the field strength during

electrophoresis, and $d\mu/d(pH)$ is the slope of the mobility as a function of the pH.

Many devices have been designed to perform analytical- and preparative-scale isoelectric

focusing. Typically, an anti-convective medium is used as an electrolyte support system,

such as gels (slabs or beads) or capillaries. In other cases, a hydrophilic polymer such as

hydroxypropylmethyl cellulose, polyethylene glycol or poly(vinyl alcohol), *etc*., is added

to the sample solution to mitigate diffusive and convective mixing during IEF. Some of

the preparative-scale IEF devices include the Octopus (Weber GmBH, Kirchheim,

Germany) [17], and the Rotofor® (BioRad Laboratories, Hercules, CA) [18]. For

analytical-scale IEF, one can use CA-filled gels, such as the Novex IEF gels (Invitrogen,

Carlsbad, CA) or capillary electrophoretic systems, such as the MDQ (Beckman –

Coulter, Fullerton, CA), the ChemCE (Agilent, Little Falls, PA) or the iCE280

(Convergent Bioscience, Ontario, Canada) [19]. Experimentally, inherent, time-

dependent anodic and cathodic drifts distort the slope of the pH gradient [20-23], thus the

IEF process actually does not reach a true steady state. Furthermore, the separated

fractions obtained from IEF contain carrier ampholytes which, in certain applications, can be a major disadvantage. In analytical studies, if further investigation of the fraction is required, the carrier ampholytes have to be removed, which often leads to sample loss. In addition, FDA has banned the administration of proteins and other ampholytes which are mixed with CAs, into a human subject; hence, material produced by IEF is not suitable for clinical studies.

The introduction of immobilized pH gradients (IPGs) [24-25] was unquestionably a step forward in the area of IEF. By using a density gradient mixer, measured amounts of acrylamido buffers and titrants, called Immobilines, were copolymerized with acrylamide and bisacrylamide to form a gel in which the shape of the pH gradient can be adjusted for a specific use. Since in an IPG the buffering components are fixed in the gel, the anodic and cathodic drifts experienced in IEF are eliminated and the use of carrier ampholytes can be avoided. However, other problems arose: (i) the sample capacity of IPG stripts is low; (ii) protein precipitation or streaking occurs in IPG strips; (iii) comigration and spot fusion are frequently observed; and (iv) the separation speed is slowed down compared to CA-based IEF. Ironically, to mitigate these setbacks, a small amount of CA is added to the sample to help keep the proteins in solution, provide more buffering capacity, and enhance the conductivity in the system.

1.3. Isoelectric trapping

A way to prefractionate ampholytic samples without the use of carrier ampholytes is by isoelectric trapping. The concept of isoelectric trapping is similar to IEF except that

buffering membranes are used to generate a step-wise pH gradient between the anode and the cathode. IET is carried out in multi-compartmental electrolyzers (MCEs). A schematic diagram of a simple MCE device is shown in Figure 1. In a conventional MCE device, each compartment is separated by a semi-permeable, buffering membrane. The pore sizes of the membranes are large enough to allow ampholytes, even large proteins, with sizes up to 1500 kDa, to pass through, but still small enough to prevent convective mixing of the liquid between the adjacent compartments. The buffering membranes are typically made of polymeric hydrogels where measured amounts of buffering compounds are covalently bound into the polymer matrix and define a single pH value throughout the
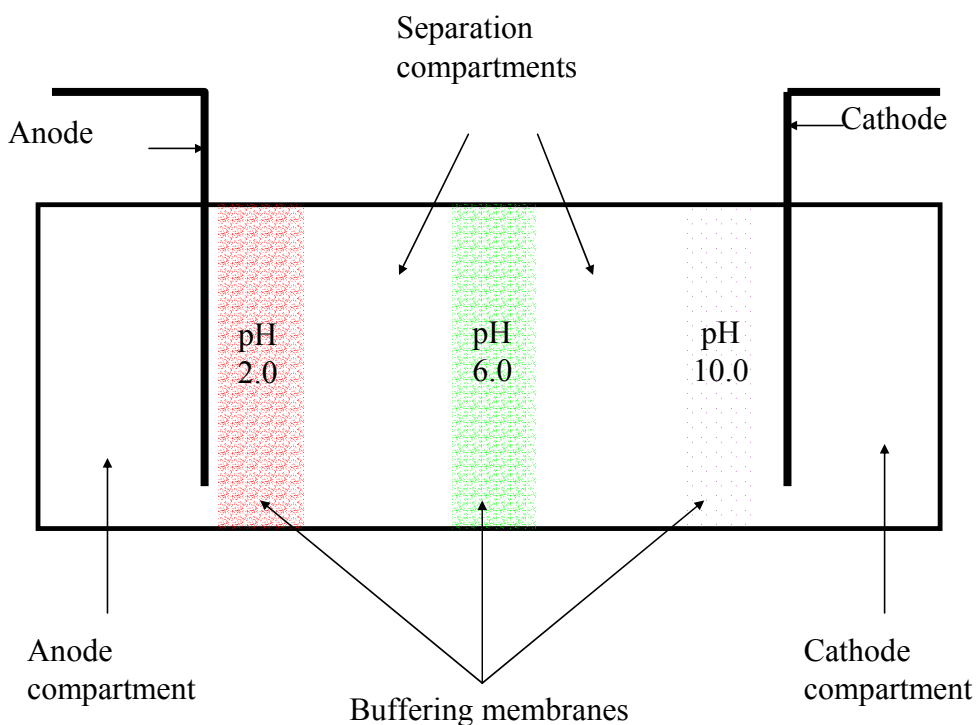
Figure 1. A schematic diagram of a simple MCE device.

membrane structure. The buffering membranes are arranged serially in the MCE, with the pH increasing from anode to cathode. The first and last compartments hold the anode and the cathode, respectively. The anode contains the most acidic electrolyte; the cathode contains the most basic electrolyte. The ampholytic sample is loaded in the compartments between the electrodes. In Figure 2, the separation of a hypothetical sample made up of two ampholytic components is shown. When the concentrations of the ampholytic components are high enough, the pH of the solution is somewhere between the pI values of the ampholytes. Hence, in a mixture of two ampholytic components, one having a pI of 5 and the other a pI of 8, the solution has a pH of 6.5. At this pH, the components with pI 5 become deprotonated and acquire a net negative charge (*i.e.*, they become anions),
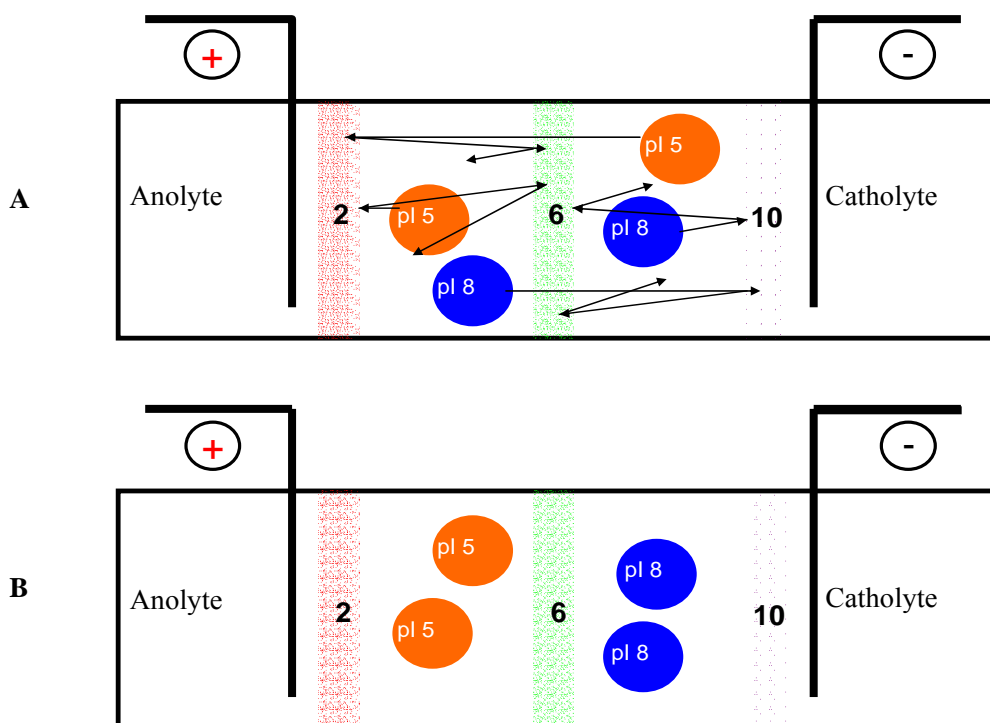
Figure 2. A schematic diagram showing an IET process: (A) electrical potential is applied and ampholytes start to migrate; (B) ampholytes are trapped in the chamber delimited by membranes with pH values bracketing the pI value of the ampholyte.

while the components with pI 8 become protonated and acquire a net positive charge (*i.e.*, become cations). When an electric potential is applied, the anionic ampholytes migrate toward the anode. When these negatively charged ampholytes meet a buffering membrane with a pH lower than their pI value, the ampholytes get titrated and become positively charged, thereby become attracted toward the cathode. When these cationic ampholytes meet a buffering membrane with a pH greater than their pI value while moving toward the cathode, they get titrated and become anionic again. A similar scenario will be experienced by the pI 8 ampholytes. Hence, the ampholytes become eventually trapped in the compartment where the bounding buffering membranes bracket their pI values [26].

IET was first described by Martin *et al.*, who covalently attached weak acids and weak bases to an agarose membrane to generate a certain pH (*e.g.*, they attached acetic acid and different amounts of diethanolamine to an agarose gel to generate a membrane with pH 4.8 to 5.5) [27]. When the concentration of the weak electrolytes is high enough, the membranes possess a sufficiently high buffering capacity to prevent any anodic or cathodic sample drift. However, the lack of reproducibility in membrane preparation and the lack of membranes covering the entire useful pH range, have limited the utility of IET. Opportunely, Righetti used his Immobiline chemistry and brought a solution to the problem Martin had with his buffering gels [24]. By using the Henderson-Hasselbach equation, the proper ratio of acrylamido weak acid or base and titrant can be calculated to yield a membrane with a desired pH and adequate buffering capacity [28]. By 1987,

Righetti successfully demonstrated the viability of his buffering membranes over the 3 < pH < 10 range [29-32]. Yet, useful as they are, acrylamide-based membranes still suffer from hydrolytic instability. At pH < 4 and pH > 8, polyacrylamide gels hydrolyze and yield bound carboxylate groups. Moreover, hydrolysis of the bisacrylamido cross-linker destroys the mechanical integrity of the membranes. Recently, the development of a series of hydrolytically-stable poly(vinyl alcohol)-based buffering membranes provided a new promise for IET [33-35]. A schematic representation of the synthesis of PVA-based buffering membranes is shown in Figure 3. These PVA-based buffering membranes can be reproducibly manufactured in the 1.7 < pH < 13 range; they have been used in solutions of 1 M strong acids and up to 3 M strong bases.
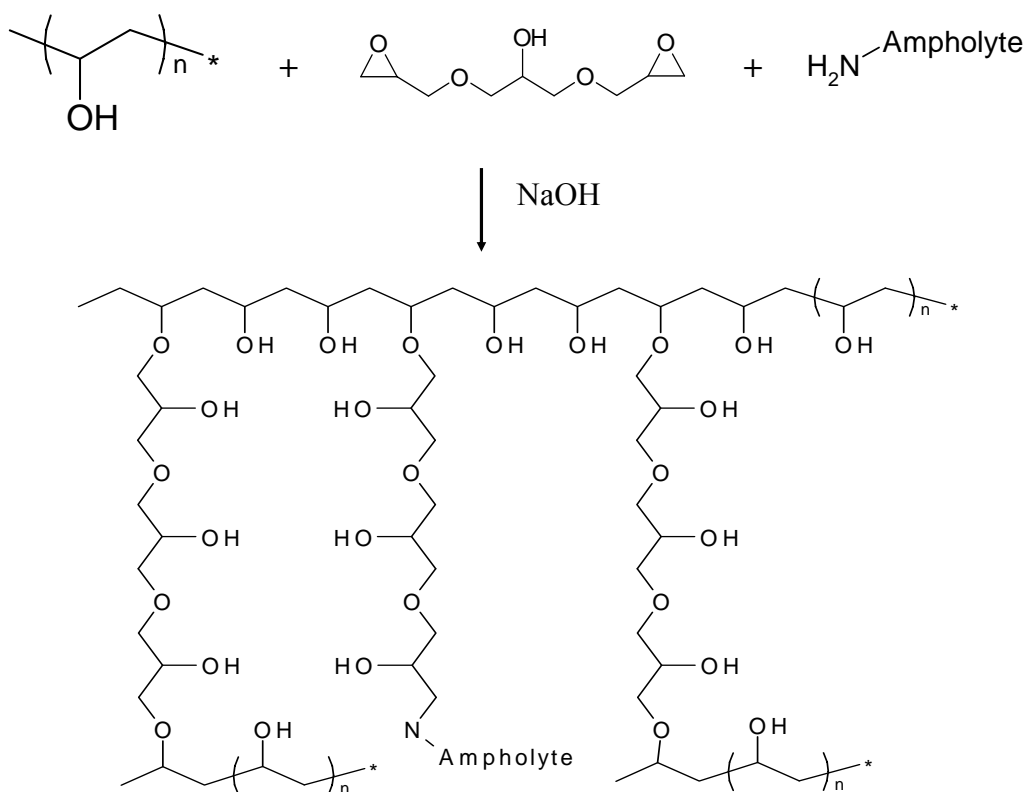
Figure 3. Schematic representation of the synthesis of a hydrolytically stable PVA-based buffering membrane.

1.4. pH-biased isoelectric trapping

During a classical IET separation, an ampholyte approaches its pI value, thus its net charge approaches zero. This increases the possibility of precipitation especially if the ampholyte is large (*i.e.*, proteins) and decreases the electrophoretic velocity of the ampholyte, thus lengthening the required separation time. Recently, a technique called pH-biased IET was developed to overcome these shortcomings [36]. By controlling the solution pH inside the compartments of an MCE, such that the pH is sufficiently far from analytes' pI values, the problems of classical IET can be mitigated. The pH is controlled by adding an isoelectric buffer (sometimes called pH-biaser) to the sample solution and the isoelectric buffer is trapped along with the analytes during IET. In this manner, the analytes are maintained in a more soluble cationic or anionic charge state over the course of the entire separation. Also, in this charged configuration, the elecrophoretic mobility of the analytes will not approach zero, therefore, the separation time is shortened [36]. A pH biaser is selected to satisfy two requirements: (i) its pI value must be between the pH values of the buffering membranes delimiting the respective compartment, and (ii) its pI value is sufficiently different from the pI values of the target component to insure that the target components are kept in charged state throughout the entire separation process. Practically useful biasers should also have the following properties: (i) high solubility even in their isoelectric state; (ii) high buffering capacity, that is, $|\,pI - pKa\,| < 1.5$; and (iii) UV transparency to facilitate analyses. Some amino acids that can be used as good pH biasers include: iminodiacetic acid (pI 2.2), aspartic acid (pI 2.7), glutamic acid (pI 3.2), histidine (pI 7.5), methyl lysine (pI 9.9), and arginine (pI 10.7). A series of novel synthetic isoelectric buffers were synthesized recently including N,N-

bis(carboxypropanyl)diethylammonium hydroxide (QDBA, pI 4.2), 1,3-bis(4-morpholino)-2-O-sulfo-propane (BMSP, pI 5.6), 1,3-bis(N,N-dimethylamino)-2-O-sulfo-propane (BDMASP pI 7.7), and 1,3-bis(N,N-dipropylamino)-2-O-sulfo-propane (BDPASP, pI 8.4) providing more buffering options in the operational pH range of IET [37-38].

1.5. Large-scale IET devices

The apparatus used for IET also evolved as solutions to the technical problems were found over a period of time. In 1978, Martin reported an early version of an IET device [39]. At that time, he could not obtain reproducible results since the agarose-based buffering membranes were not well characterized. One of the first commercially available MCEs used for IET is a large-scale device called the Isoprime [40]. It holds 0.1 cm thick polyacrylamide-based buffering membrane disks with a diameter of 4.7 cm. Seven different buffering membranes are selected to make eight compartments. Two of these compartments, the first and the last, are used for the anode and cathode solutions. In between the anodic and cathodic compartments, there are six separation compartments. The volume of each separation compartment is 5 ml and is bounded by buffering membranes 1 cm apart from each other, making the anode-to-cathode distance 10 cm. The Isoprime can process up to 100 mg of total proteins and can separate a complex sample into 6 fractions in 24 to 48 hours. A group led by McEwen, modified the Rotofor® which was originally intended for IEF into an IET device [41]. It was equipped with buffering membranes and was used to trap myoglobin into a compartment. They also demonstrated the separation of a yeast protein mixture, dissolved in 30% isopropanol

in water, into fractions. Another preparative apparatus, the Gradiflow BF200 (Life

Therapeutics, Frenchs Forest, Australia), designed to perform size-based binary

separations of proteins, brought an improved design to the MCE [42-53]. In the

Gradiflow BF200, the sample is pumped through two shallow separation channels formed

by three non-buffering polyacrylamide hydrogel membranes, perpendicular to the electric

field. 1 mm-thick spacer grids prevent the collapse of the membranes onto each other and

keep the flow unobstructed through the channels. The total distance from anode to

cathode is 8- mm. The instrument was designed to perform size-based binary separations

of proteins. The outer anode and cathode membranes have a small pore size (nominal cut-

off 5 kDa) to prevent proteins from leaving the separation compartment. The pore-

diameter of the middle membrane is chosen to discriminate the target proteins according

to size. To migrate the proteins from one chamber to the other (or keep them away from

each other), the pH of the medium is adjusted to make the proteins cationic or anionic.

For example, if a sample contains two proteins, one with 14kDa (pI 9.6) and one with

65kDa (pI 7.1), and the solution is kept at pH 11, both proteins will have a net negative

charge and will be attracted toward the anode. If the middle membrane has a cut-off size

of 20kDa, and the sample is passed through the upper feed stream (*i.e.*, the channel near

the cathode), the smaller protein will be able to pass through the 20kDa membrane and

into the lower stream, while the larger 65kDa protein will be prevented from passing and

remains in the upper feed stream. If the lower stream is also kept at pH 11, the 14kDa

protein will be kept negatively charged and prevented from going back towards the

cathode, thus it will remain in the lower stream. The electrolyte streams and the feed

streams are recirculated through their respective compartments and returned to the same

respective temperature-controlled external reservoirs. In this mode of separation, the electrolyte composition for the anode and cathode is the same (there is only a single electrolyte reservoir). The Gradiflow unit was significantly improved by Shave and Vigh, who made it suitable for IET separations [24, 36]. The main changes include the redesign of the entire cooling system, and the elimination of the parasitic pressure drops in the separation head which previously caused bulk liquid transport across the membranes and lead to cross-contamination of the streams. The new cooling system can maintain proteins at 5 °C and prevent burn-ins of the buffering membranes. The new system, called the Twinflow, exhibited superior, reproducible protein separations.

1.6. Small-scale IET devices

There is also interest in analytical-scale IET devices, especially since the concept of lab-on-a-chip became popular. The ability to perform laboratory operations in miniaturized devices has several advantages: small volumes reduce the time taken to process or analyze a sample or product; reagent costs and the amount of chemical waste can be much reduced; and compact devices allow samples to be analyzed at the point of need rather than in a centralized laboratory [54-56]. The benefits are compelling, but designing and fabricating devices of reduced size that operate effectively is challenging. Nevertheless, a few small-to-medium-scale IET devices have been made and are available commercially.

In 2000, Proteome Systems (Sydney, Australia) released an MCE instrument called the IsoelectriQ^2 (IQ^2). The IQ^2 can hold up to 7 polycarbonate separation compartments, each

one with an inter-membrane distance of 2.2 cm and a volume of 5 ml [57-58]. The total

anode-to-cathode distance is 22.2 cm. Stir bars provided in the bottom of each

compartment keep the sample compartments mixed during electrophoresis. The device is

placed on a magnetic stirring plate which also provides cooling through a Peltier system.

The IQ^2 can fractionate 50 – 500 mg protein, typically in 24-48 hours using a maximum

electric power of 1 watt. A schematic diagram of the MCE used in the IQ^2 system is

shown in Figure 4. In the same year, a smaller IET device, the ZOOM™ (see Figure 5),
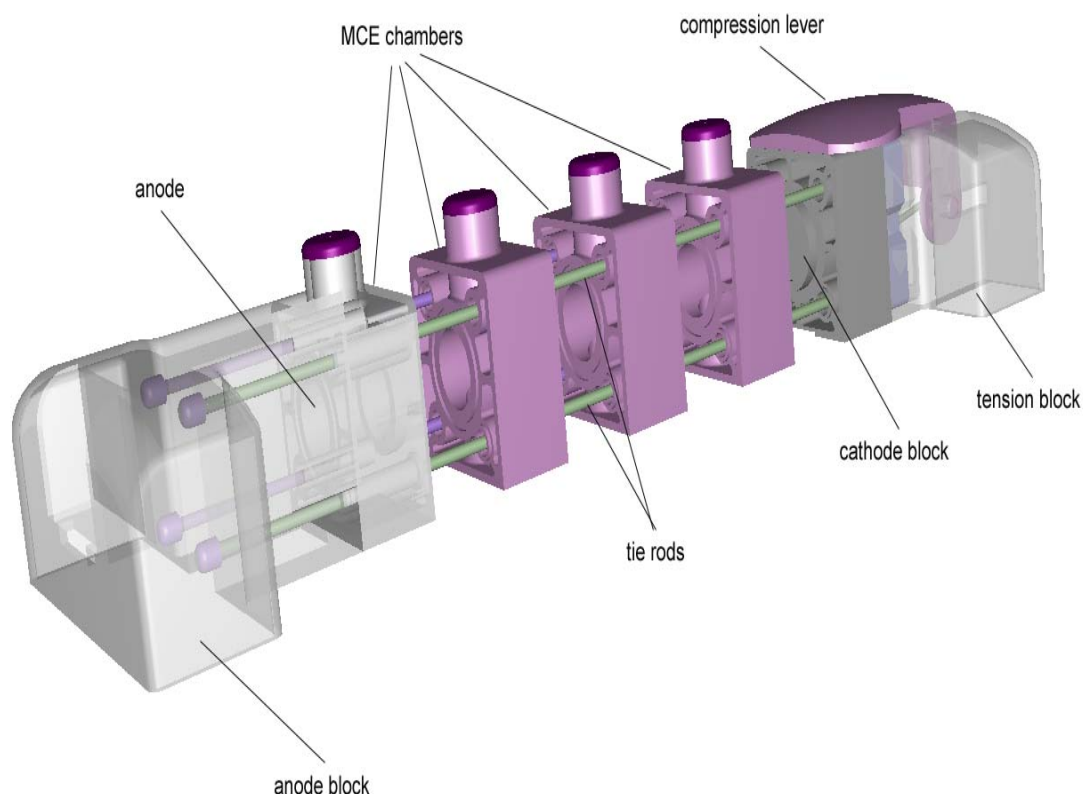
Figure 4. A schematic diagram of the MCE used in the IQ^2 system [57].

developed by Zou and Speicher, became commercially available from Invitrogen

(Carlsbad, CA) [59-60]. It holds 7 separation compartments, made of Teflon. The pear-

shaped interior of each compartment has 0.5 cm center-to-wall distance and holds 0.64

mL solution. The length of each compartment (*i.e.*, the approximate inter-membrane distance) is 1.4 cm. The total electrode distance in the ZOOM™ is 20 cm. The maximum electric power that can be applied in the ZOOM™ is only 1 watt. The device has been used to prefractionate, in 4 hours, up to 50 mg of *E. coli* lysate before two-dimensional gel analysis [61]. Both the IsoelectriQ^2 and the ZOOM can operate with field strength around 100 Vcm^{-1}. If 3 watts of power are applied to these instruments, the solutions in the compartments boil.

Figure 5. A schematic diagram of the ZOOM™ system [61].

Karger's group developed a 96-well miniaturized device for IET [62]. The 96 chambers were arranged in eight rows, similarly to those of a standard microtiter plate. Adjacent chambers in a given row were separated by 0.4 cm inner diameter, 0.3 cm long glass

tubes, into which Immobiline gels of predetermined pH values were polymerized. Each

chamber contained 0.075 mL of solution and all eight rows shared the same anodic and

cathodic solution reservoirs. High-throughput fractionation (12 fractions in each row) of a

complex peptide mixture was achieved in 3 hours. In Figure 6 a multi-chamber IET

device is shown with its parts: (1) anode socket; (2),(2') threaded rods for fastening; (3),

(3') nuts; (4) cathode socket (5), (5') electrode Pt wires; (6) cathodic reservoir; (7), (7')

holes for electrolyte access, within which are anodic and cathodic membranes; (8) 96

separation wells separated by buffering gels within rows, and acrylic plastic between

columns. A drawback in this design is that only one anode is used for 8 rows of channels

that act as individual resistors. The current would preferably flow through the channel

with the least electric resistance and result in uneven amounts of electrical work exerted

in each channel.
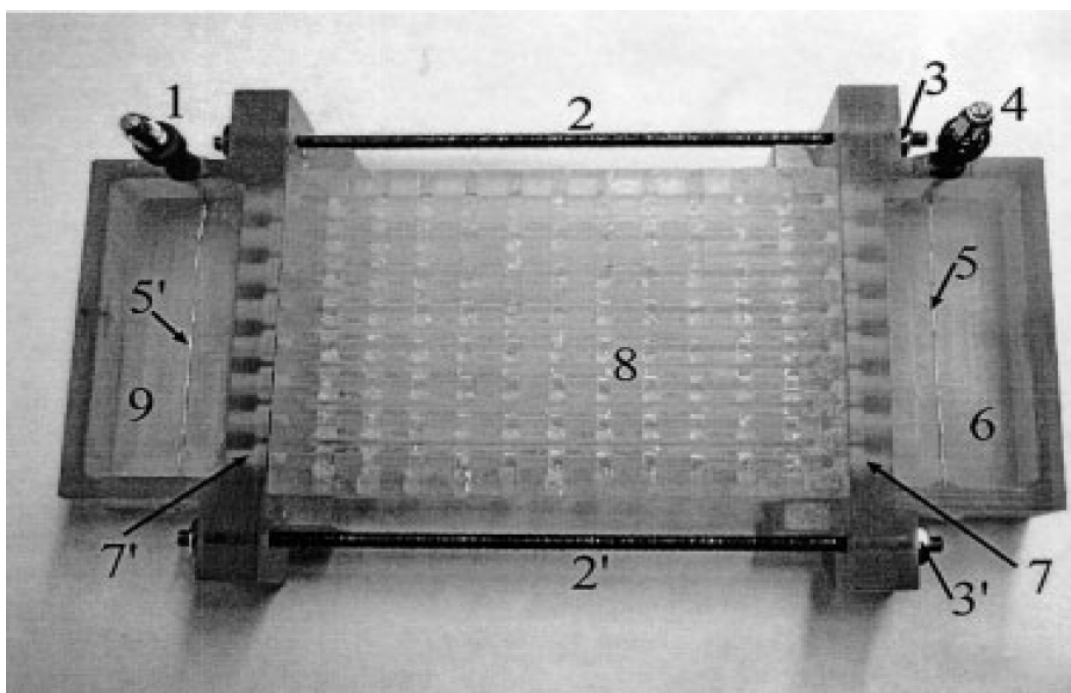
Figure 6. A photograph of a multi-chamber IET device [62].

In Europe, Rossier and co-workers placed cylindrical or square glass sample compartments on top of an IPG strip. Each compartment held 0.1 to 0.3 mL of volume and had a diameter of 5 mm. On a typical, 11 cm-long IPG strip, they could fit up to 7 compartments. This off-gel multicompartmental device was used to isolate cytochrome C and prefractionate an *E. coli* lysate in 48 to 72 hours [63]. They simulated the electric field vectors in their IET setup and showed that a significant amount of dead volume inside the chambers could not be covered by the electric field, which resulted in long separation times. Figure 7 shows a picture of an off-gel MCE setup. Recently, a commercial version of the off-gel device became available from Agilent Technologies, Santa Clara, CA [63].
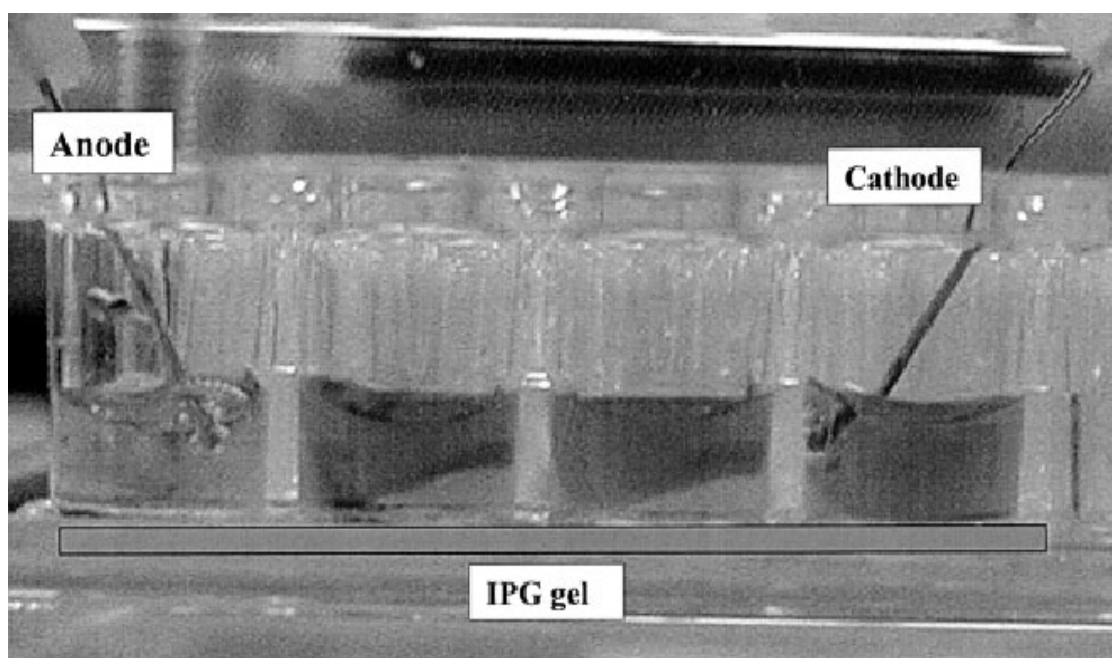
Figure 7. A picture of the Off-Gel IET setup. Glass cylinders are placed on top of an IPG strip to create the electrolyte and sample compartments [63].

These prefractionation devices, useful as they are, suffer from interrelated and critical limitations. One is poor Joule heat dissipation that limits the electric power that can be applied to the system to 1-to-2 watts. The poor heat transfer characteristics stem from the design of the separation compartments: (i) cylindrical or pear shape interiors with diameters 9 to 12 mm create long heat transfer paths; (ii) the structural materials used for these devices are plastics which are inherently poor thermal conductors (0.1–0.5 W/m-K) and have very low specific heats (0.03-0.05 cal/g °C); (iii) and the long anode-to-cathode distances (electrodes are 75 mm to 200 mm away from each other) bring low field strength and lead to low electrophoretic velocities. Hence, these devices require at least 3 to 48 hours to complete the IET process.
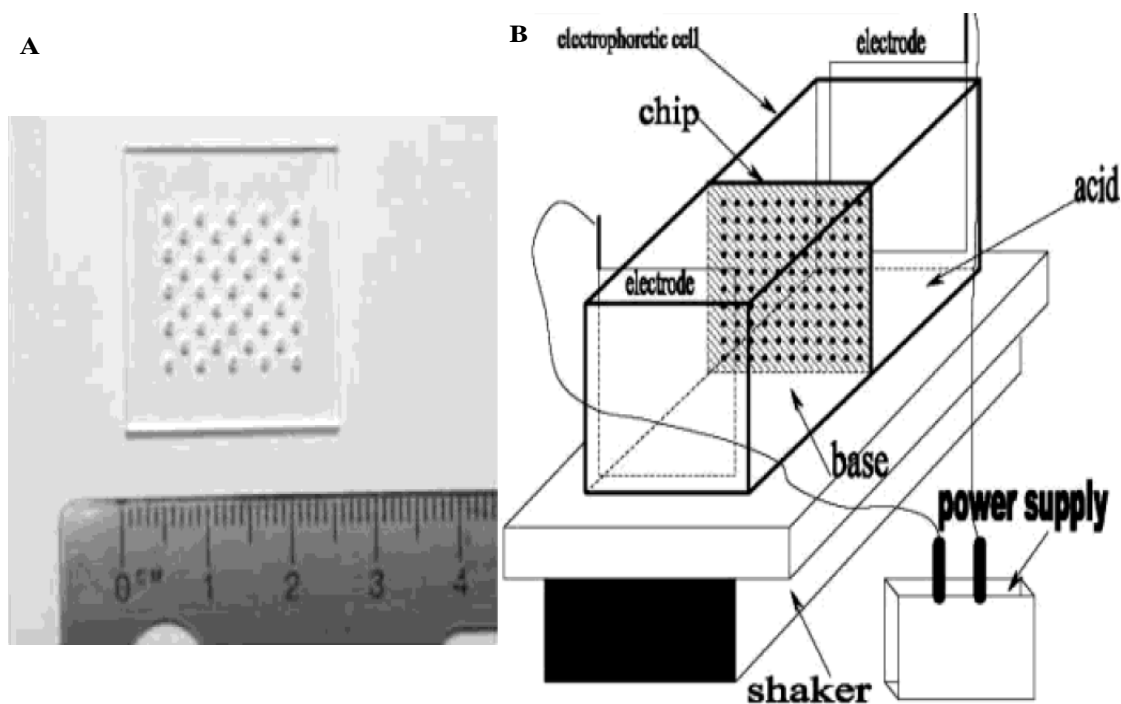
Figure 8. A. A picture of the plexiglass plate with 41 through-holes. Each hole accommodates acrylamide gels with different buffering pH. B. A schematic diagram of the parallel IET device [64].

A proteomics company in Rehovot, Israel, introduced a parallel IET chip (see Figure 8) [64]. The concept is similar to Karger's 96-well device except that instead of assembling the buffering gels serially to make the rows, they arranged the gels parallel to each other. In this configuration, a pH gradient orthogonal to the electric field and another step-wise pH gradient along the electric field are formed. Furthermore, the anode-to-cathode distance was greatly lessened, and the field strength during electrophoresis was enhanced. The device showed high-resolution separations on a standard protein mixture in 30 minutes. Even though this parallel chip offers a promising solution to long separation times, it cannot eliminate the detection problems associated with the analysis of low abundance proteins.

2. MEMBRANE-SEPARATED WELLS FOR ISOELECTRIC FOCUSING AND TRAPPING (MSWIFT): SOLUTION TO POOR HEAT DISSIPATION

2.1. Construction principles

This section describes the design and manufacture of an analytical-scale IET system that mitigates some of the limitations of the currently available IET devices. The objectives of the new system were as follows: (i) facilitate fast and efficient heat dissipation by selecting a structural material with high thermal conductivity and high specific heats comparable to metals; (ii) minimize the heat conduction path from center of the separation chamber to the wall and/or the environment; (iii) minimize the distance between the electrodes to provide high electric field strength during electrophoresis. These construction principles were expected to lead to separations that match the capabilities of the present tools but in much shorter separation time.

2.2. MSWIFT: design and manufacture

The next sections describe the structural components that were designed and manufactured to create the device called membrane-separated wells for isoelectric focusing and trapping (MSWIFT). This first system was built in the conventional MCE format.

2.2.1. Alumina compartments

Each compartment was made from 99.8% non-porous ceramics-grade alumina (Al_2O_3) blocks, which were purchased from Coorstek Inc. (Golden, CO). Alumina is non- toxic, and is more tolerant of acids and bases than other ceramics, such as AlN, Macor and

BeO. The thermal conductivity of this alumina is about 30 W/mK, and has a specific heat of about 0.3 cal/g °C. Compared to plastics, alumina is 100-fold, and 10-fold better in terms of thermal conductivity and specific heat, respectively. The manufacturing of these alumina blocks involves a firing process that produced a slightly curved surface. Precision lapping and polishing were done at Accumet Engineering Corp. (Hudson, MA), to produce sets of 0.250" x 0.500" x 1.000" and 0.125" x 0.500" x 1.000" blocks with perfectly flat surfaces. After polishing, 0.080" wide and 0.750" deep grooves were perpendicularly cut through the 0.500" surface of the blocks using a diamond-coated grinding wheel. This process was aided with a support system made of poly(vinyl chloride) (PVC) designed to create the grooves in a single pass (Figure 9). Pre-cut, 0.1
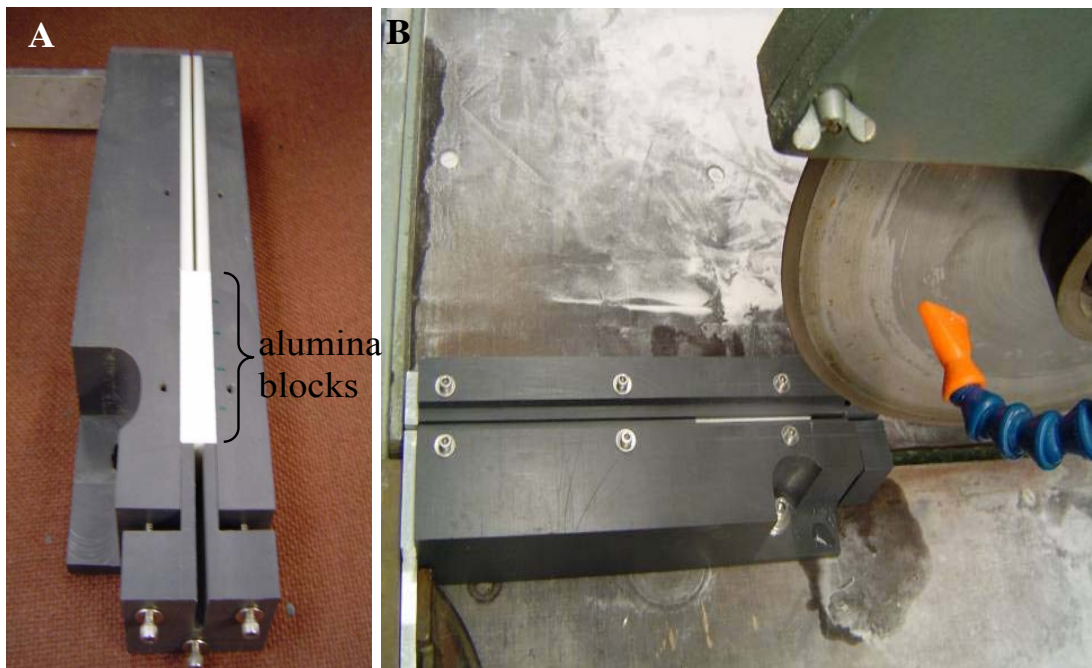
Figure 9. A. A picture of the PVC support system containing an array of alumina blocks. **B.** The support system is fixed on a flat table and aligned with the diamond-coated grinding wheel just before creating the grooves.

mm-thick, low-density polypropylene spacers were placed in between the alumina blocks to reduce vibration during grinding. By selecting alumina blocks of different thicknesses, the electrophoretic migration distance in the wells can be adjusted easily. The groove depth, grinding wheel width and the thickness of the alumina block can be varied easily to set the volume of the compartments. Wells that hold 100 μL and 200 μL of volume were made to perform the experiments needed in this project. A photograph of a typical MSWIFT compartment is shown in Figure 10.
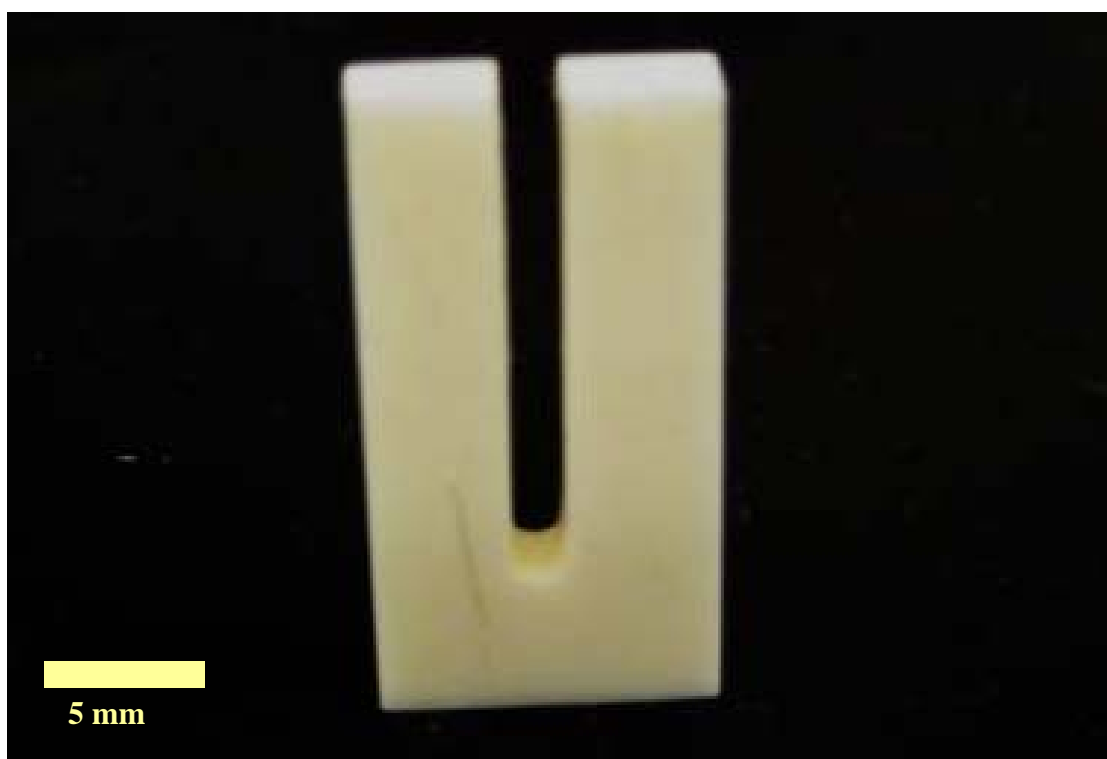
Figure 10. A picture of a 99.8% pure alumina block in which a groove has been created.

2.2.2. Membranes, gaskets and pouches

Semi-permeable buffering membranes that were used throughout this project were made of hydrolytically stable poly(vinyl-alcohol) (PVA). Buffering compounds were

covalently attached to the PVA matrix to create the buffering membranes [33-35]. The membranes were placed in between the alumina blocks to create the wells (separation compartments). In order to avoid seepage of liquid toward the sides of the membranes, causing some loss of sample volume, the membranes were installed into silicon rubber pouches. 0.020" thick, 8" by 11" silicon rubber sheets were cut to 0.50" x 1.00" using a CO_2 laser (Universal Laser Systems Inc., Scottsdale, AZ) to make the silicone gaskets. The gaskets were designed in automated computer-aided design (ACAD) software and the files were uploaded to the laser cutting system. A 0.080"-wide by 0.60"-long window was created in the middle of the gaskets to expose an area of the membrane to the electric field. By controlling the laser power and the X-Y velocities, the laser beam width was kept at 20 μm. A photograph of a silicon gasket is shown in Figure 11.
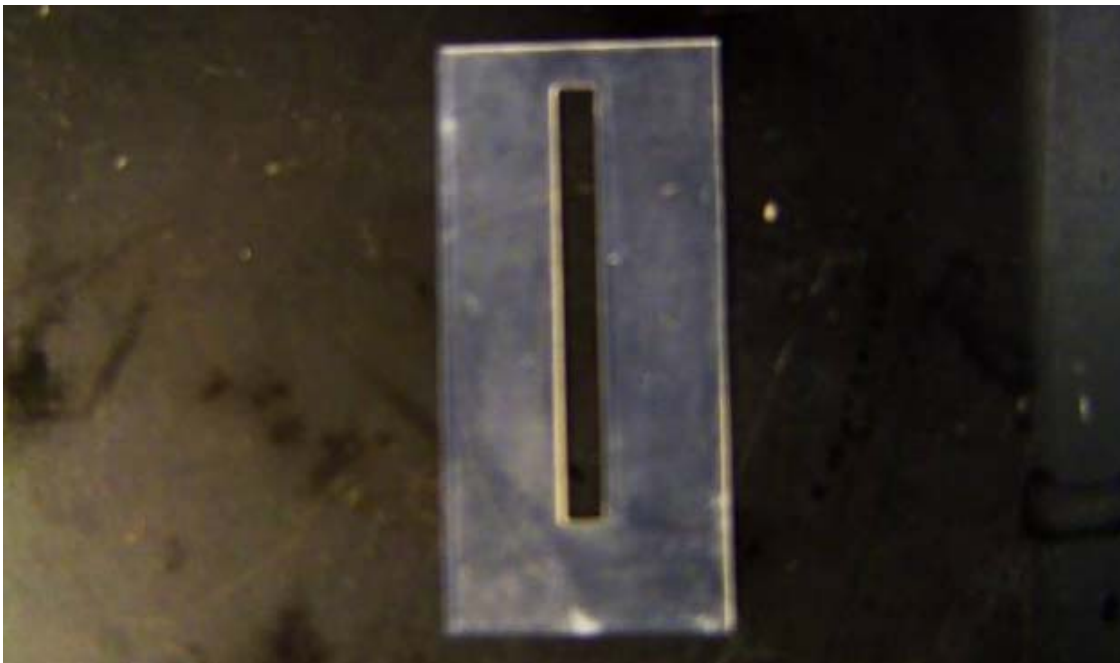
Figure 11. A picture of a silicone gasket.

Two silicone gaskets were precision glued to create a silicone pouch. An aluminum mold

system (photograph shown in Figure 12) was fabricated to aid the gluing process. The

whole process involved six steps: (i) a silicone gasket was placed to fit on a 1.001"-long,

0.501"-wide and 1.0"-deep cavity in the mold; (ii) a 1.5"-long, 0.450"-wide, and 0.005"-
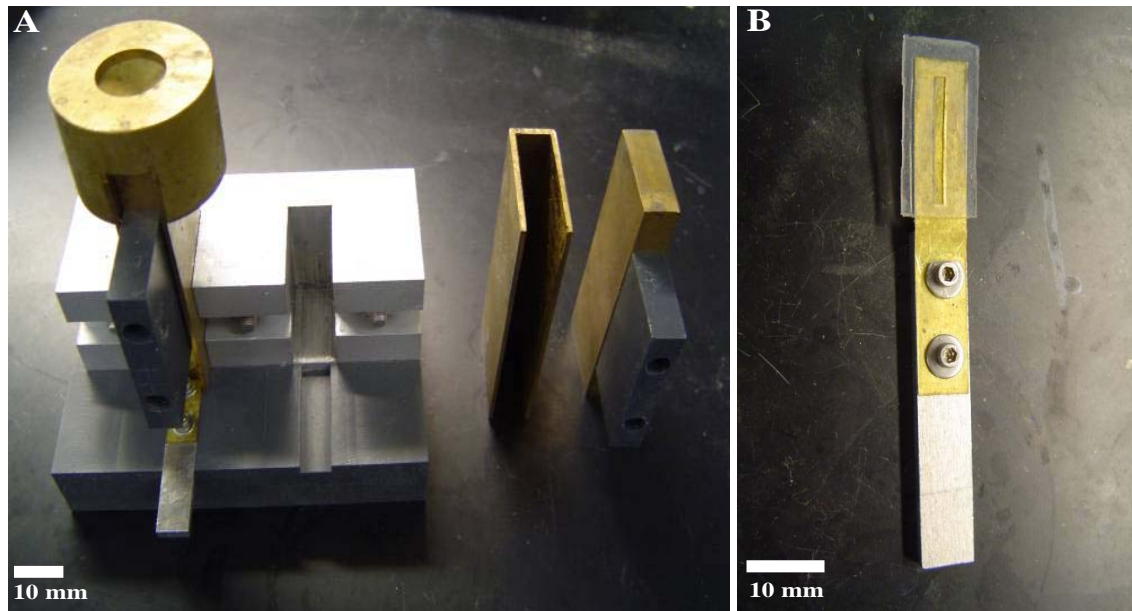
Figure 12. A. *Left*. The mold system used to make the silicone pouches. *Middle*. U-shaped brass used as weight to seal the sides of the gaskets. *Right*. Solid block used as a weight to keep the glue from getting into the shim stock. **B**. Finished silicone pouch still attached to the brass shim stock.

thick brass shim stock (see Figure 12B) was placed on top of the silicone gasket such that

a 0.025"-wide, U-shaped area of the gasket was exposed; (iii) a thin line of Dow Corning

silicone glue was carefully applied on the U-shaped, exposed edges of the gasket by a

syringe needle; (iv) a second silicone gasket was placed on top of the brass shim stock;

(v) a 1.0"-long, 0.450"-wide, and 3"-high brass block was placed above the second

gasket such that it was exactly over the area covered by shim stock; (vi) a U-shaped

brass weight was also placed on top of the second gasket such that it was over the area covered by the glue. After 2 hours of curing, a silicone pouch was formed. A picture of an empty silicone pouch and a silicone pouch containing a PVA-based buffering membrane are shown in Figure 13.
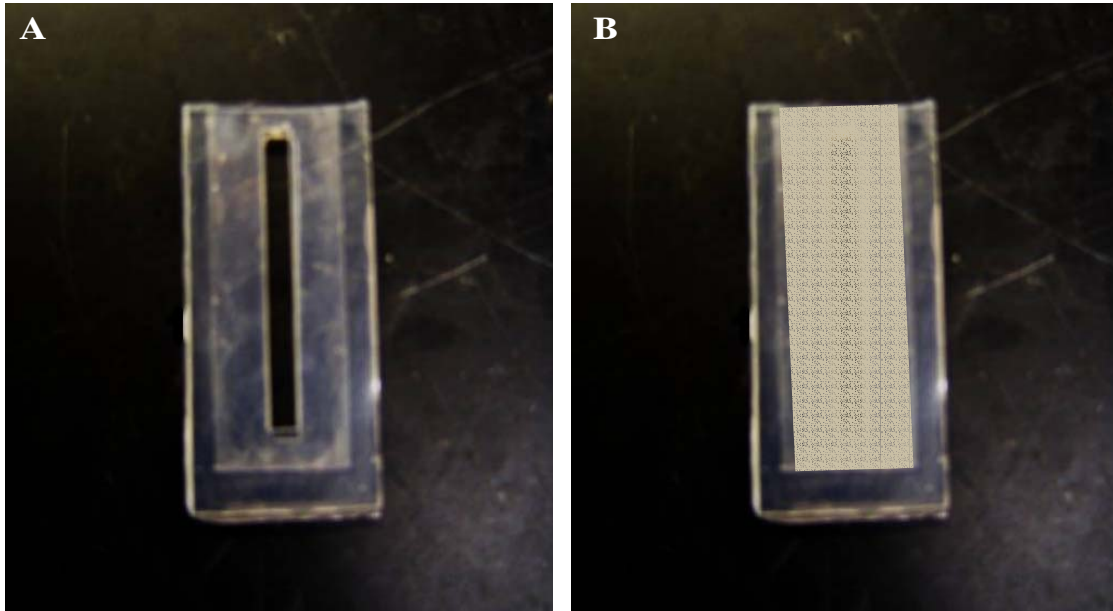
Figure 13. A. Picture of an empty silicone pouch. **B**. Picture of a silicone pouch containing a buffering membrane.

2.2.3. Main holder

A holder was fabricated to contain the alumina compartments, the gaskets and membrane-loaded pouches. Two end pieces (compression pieces) were also provided to create water-tight seals between the alumina chambers, the gaskets and the membranes. Efficient sealing was achieved with the help of four threaded brass rods, nuts and wing nuts to connect the main holder and the end pieces together. The main body was precision machined to insure good alignment of the neighboring compartments. A 0.500" wide and 1.000" deep groove was milled along the middle of a pre-cut 5.000" long, 2.250

wide, and 1.375" high, polycarbonate (Lexan) block. A 3.000" long, 0.500" wide oval

window was machined on top of the block to provide access for loading the alumina

blocks, the gaskets, the membranes and, ultimately, the sample. Along the sides of the

Lexan block, 4 grooves were provided to hold the threaded brass rods. A half inch-thick,

4.000" long and 2.250" wide aluminum block was machined to serve as the heat sink of

the device. It was installed at the bottom of the main holder. To prevent electric current

leaks and short circuits that may occur, a 1 mm-thick 4.00"x2.25" alumina plate was

placed in between the main holder and the aluminum base. Figure 14 shows the ACAD

generated diagrams and photographs of the MSWIFT.
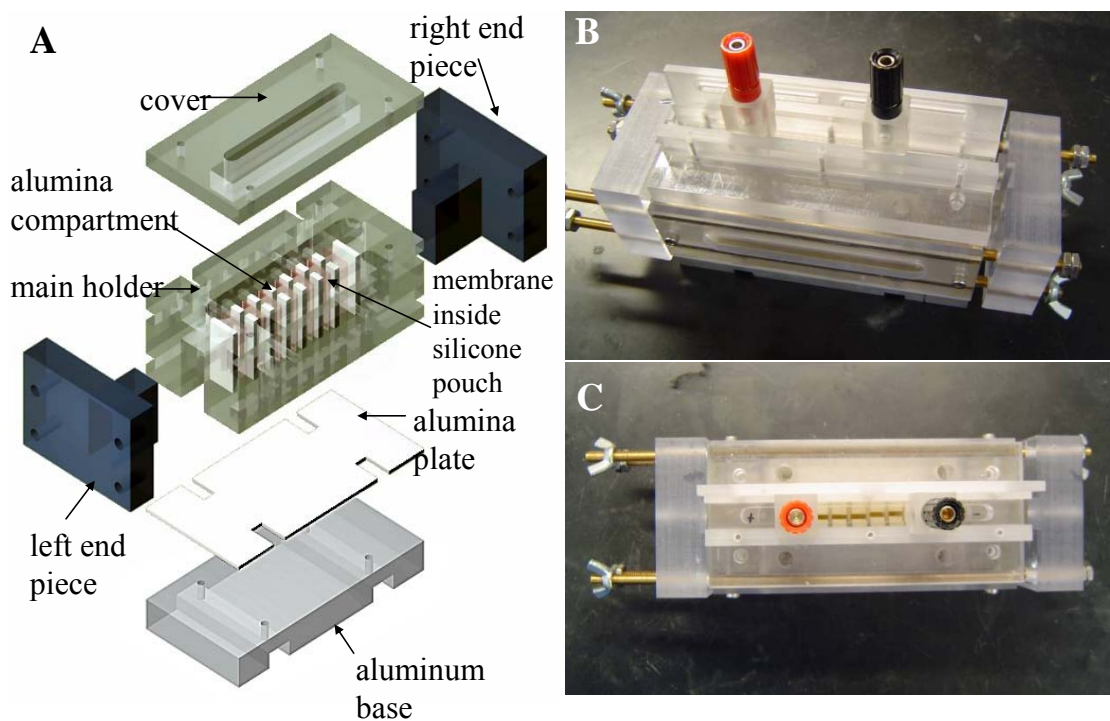
Figure 14. A. ACAD generated diagram of the MSWIFT showing the essential parts. **B**. A digital side view picture of the MSWIFT showing the electrode sockets. **C**. Top view picture of the MSWIFT showing the accessibility of the compartments.

The MSWIFT is a versatile analytical tool that can be used for rapid fractionation of ampholytic samples, because the number of compartments to be used and the membranes with the appropriate pH values can be selected as needed. A series of experiments showing the applicability of this device are shown in the next section.

3. FAST IET SEPARATIONS IN SMALL VOLUMES: APPLICATIONS OF MSWIFT

3.1. Desalting experiment on the MSWIFT

3.1.1. Background and objective

Protein samples derived from biological sources contains large amounts of salts (*e.g.,* a physiological solution of 154 mM aqueous NaCl is isotonic with blood plasma). In many protein analyses, salt removal is necessary during the sample preparation steps prior to many downstream analyses. Some of the conventional desalting approaches used include centrifugal force-assisted dialysis, electrodialysis, and pressure-mediated tangential flow dialysis. In these methods, a salty solution is forced through a membrane with a pore size small enough to let the salt pass, but prevent large proteins from passing. The typical nominal cut-off size used in dialysis is 10 kDa. Dialysis has disadvantages including: (i) permanent adsorption of large proteins onto the membrane; (ii) comigration and loss of proteins and peptides with a molecular weight smaller than 10 kDa with the salt. These problems lead to non-quantitative assessment of the protein sample. In cases where the salt is not forced to pass through a membrane, such as in passive dialysis, the desalting process is very long. An ion exchange column can also be used to desalt biological samples, but the technique dilutes the sample (rendering the low abundance proteins undetectable) and it is not suitable for small-scale desalting.

In IET, the removal of salts from the sample compartment is inevitable and usually precedes the trapping of the ampholytic components. This is due to the fact that strong electrolytes present in high concentration have a high transference number and carry the

bulk of the electric current through the system in the early stages of IET. Since the charges of strong electrolytes are permanent, the buffering membranes cannot trap them; the anions and cations migrate toward the anode and cathode compartments, respectively, and remain there throughout the entire process. Thus, IET is an excellent substitute to the current dialysis techniques. To study the desalting capabilities of the MSWIFT, UV-absorbing salts and ovalbumin were used. The aim was to quantitatively measure the rate of salt removal while keeping the proteins in solution inside the separation compartments.

3.1.2. Instrument set-up, materials, and method

The MSWIFT unit described in the previous section was used for the desalting experiment. Five compartments were used in the experimental setup, the two outside ones were the electrode compartments, the three middle ones the separation compartments. To create 400 µL volume compartments, two 200-µL volume alumina compartments were coupled with a silicone gasket in between them (*i.e.*, there was no buffering membrane in the silicon gasket). The four PVA-based buffering membranes used to separate the five compartments were pH 2.0, pH 4.1, pH 6.3 and pH 10; their pH increased from anode to cathode. The total anode-to-cathode distance was 5.8 cm. The UV-absorbing salt was prepared by titrating benzyltrimethylammonium hydroxide (BzTMAOH) with benzenesulfonic acid (BzSH), until the pH of the solution was 7.0. To prepare the feed solution (sample), the UV absorbing salt solution was added to N,N-bis(carboxypropanyl)diethylammonium hydroxide (QDBA, pI 4.2), and ovalbumin (SIGMA, St. Louis, MO, USA): the final aqueous feed solution contained 9 µM of protein, 2 mM of isoelectric buffer, and 65 mM of salt. Initially, 400 µL of 30 mM

methanesulfonic acid (MSA) solution was added to the anode chamber; 400 µL of 0.5

mM iminodiacetic acid (IDA) to the first separation chamber, 400 µL of the salt-laden

sample (feed) to the second separation chamber; 400 µL of 0.5 mM lysine to the third

separation chamber and 400 µL of 100 mM sodium hydroxide solution to the cathode

chamber. The separation was run with a constant power of 3 W using a BioRad Pac3000

power supply. The compartments were sampled every 5 minutes. The schematic diagram

of the desalting experiment with the MSWIFT is shown in Figure 15. The fractions were
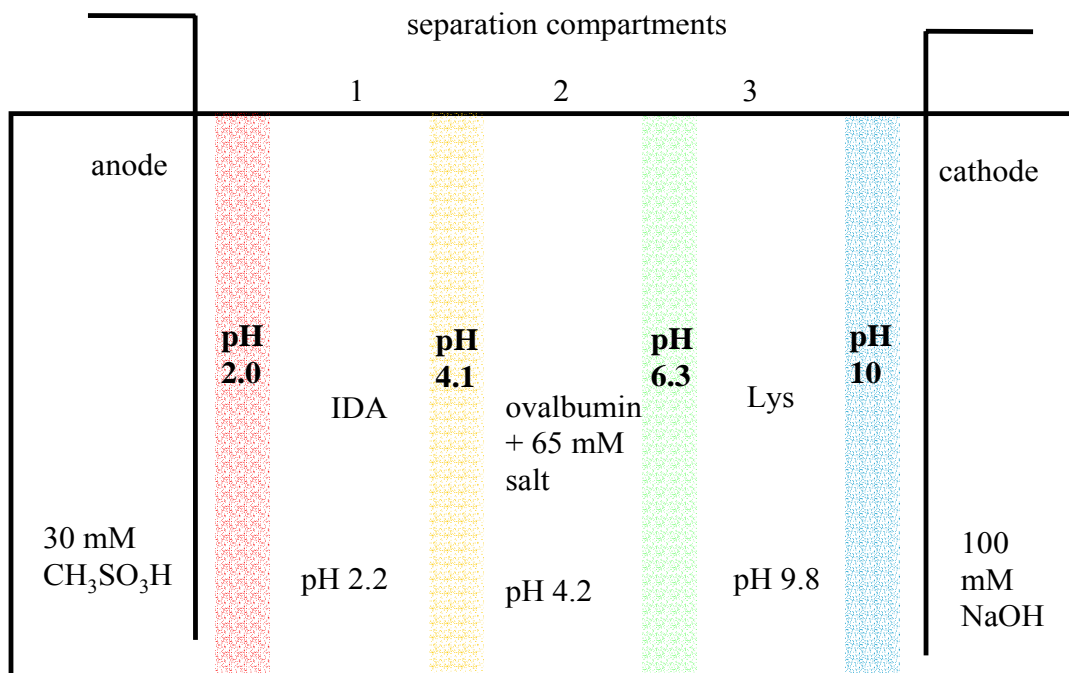
Figure 15. A schematic diagram of the desalting experiment setup in the MSWIFT.

analyzed by capillary electrophoresis (CE) with the UV detector wavelength set at 200

nm. All CE runs were done in a 26.5 cm long (L_t) fused silica capillary with a 50 µm

internal diameter, at a potential of 25 KV, using a 20 mM boric acid solution that was

titrated with LiOH to pH 9.6 as the background electrolyte (BE). The anode was at the inlet side, the cathode at the outlet side of the capillary (also referred to as 'plus-to-minus' polarity). The detector window was 19.5 cm away from the inlet (L_d). About 25 to 50% of the liquid in each MSWIFT compartment (about 50 to 100 µL) was needed to fill sample microvials of the P/ACE for CE analysis. Therefore, the following procedure was developed to acquire representative data for each 5-minute fraction: (i) after the first 5 minutes of electrophoresis, the first set of fractions were taken and analyzed by CE; (ii) without disassembling the MSWIFT, the compartments were rinsed several times with deionized water (DI) and reloaded with fresh anolyte, pH-biasers, sample and catholyte from the original stock solutions; (iii) the IET was resumed for an electrophoresis time, t_{elec}, where, t_{elec} = (previous electrophoresis time + 5 minutes), then the second set of fractions were taken and analyzed; (iv) the process in step (iii) was repeated (rinse with DI water, refill the compartments with the stock solutions, IET, collect aliquots and analyze them by CE) until the IET process was deemed complete.

3.1.3. Results and discussion

Calibration curves were made by plotting the normalized CE peak area against the concentrations of BzTMA$^+$ and BzS$^-$, (Figure 16) and ovalbumin. The linear fits yielded r-values of r = 0.999 or higher. A CE trace of the feed solution (sample) is shown in Figure 17. The components in the MSWIFT fractions can be easily tracked by CE by calculating the effective mobility, $\boldsymbol{\mu}^{eff}$, of each component with respect to a neutral marker, N. The effective mobilities of BzTMA$^+$, ovalbumin, and the BzS$^-$ were +18.0x10^{-5} cm^{2}V^{-1}s^{-1}, -14.2x10^{-5} cm^{2}V^{-1}s^{-1}, and -22.1x10^{-5} cm^{2}V^{-1}s^{-1}, respectively. Since QDBA is

UV-transparent, no peak was observed for it in the electropherograms. Significant amounts of the strong electrolytes accumulate in the electrode chambers already in the first 5 minutes of electrophoresis. After 15 minutes, almost all of the salt was removed from the feed solution. Desalting was complete (salt concentration undetectable by CE) after 20 minutes of IET, while all the protein remained in the middle separation compartment.

A

$$y = 1.19e^{-4}x - 6.08e^{-5}$$

$$r = 0.9994$$

B

$$y = 1.52e^{-4}x - 5.42e^{-5}$$

$$r = 0.9994$$
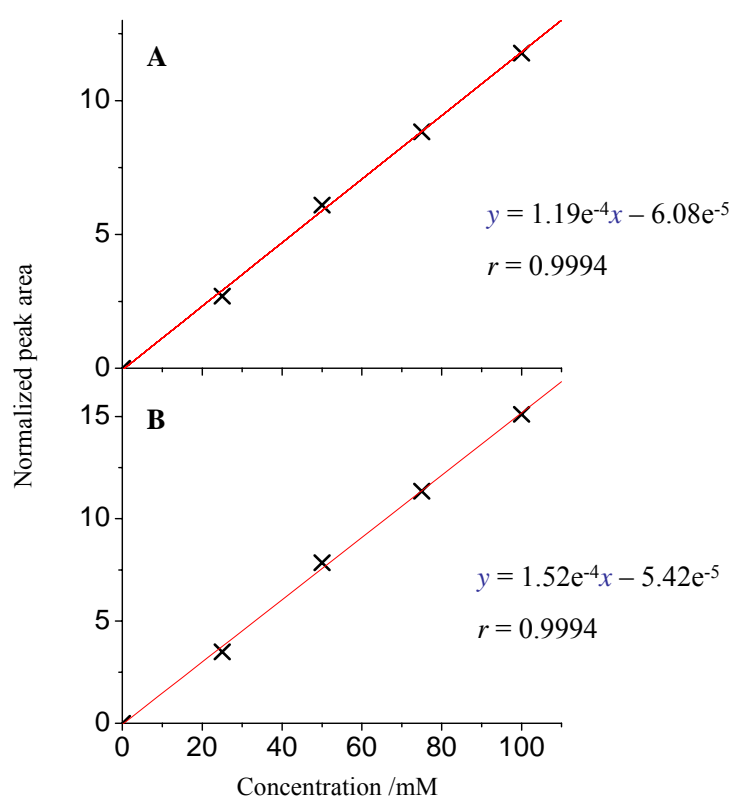
Figure 16. Calibration curves for **A**. BzTMA$^+$, and **B**. BzS$^-$.

Analyses of the fractions obtained from the middle separation compartment (feed compartment) indicated that the peaks of the UV-absorbing strong electrolytes disappeared rapidly, confirming the efficacy of the MSWIFT as a microscale desalting device. The CE traces are shown in Figure 18. After 5 minutes, only 12.5 mM of BzS$^-$

and 16.4 mM of BzTMA$^+$ were left with the protein. At 10 minutes, 4.3 mM of BzS$^-$ and

6.8 mM of BzTMA$^+$ were observed. After 15 minutes of IET, 0.94 mM of BzS$^-$ and 2.7

mM of BzTMA$^+$ remained. The 20-minute fraction (bottom panel) suggests that desalting

is complete. The ovalbumin concentration remained around 9 μM during the entire

experiment. It should be noted that BzS$^-$ has a faster transfer rate compared to BzTMA$^+$.
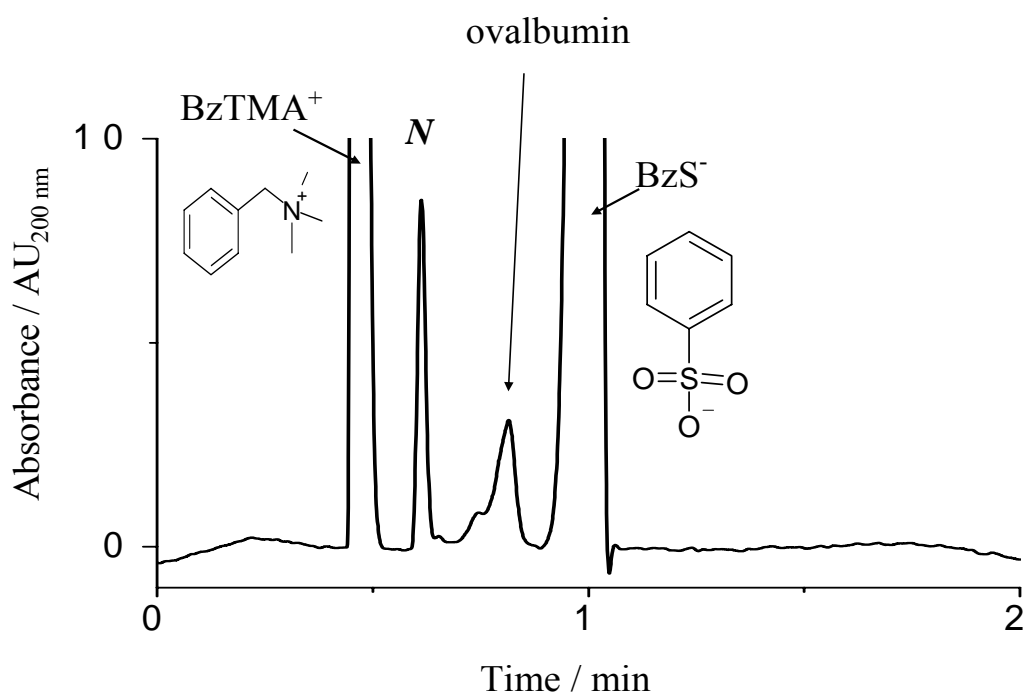
Figure 17. CE trace of the sample containing BzTMA$^+$, ovalbumin, and BzS$^-$. In CE, their effective mobilities can easily be tracked using a neutral marker, *N*.

This can be explained by the μ^{eff} difference between the two ions: the effective mobility

of BzS$^-$ is 4.1x10^{-5} cm^{2}V^{-1}s^{-1} (about 19%) larger than that of BzTMA$^+$, thus BzS$^-$ is able to

electrophoretically migrate to the anode at a shorter time. The plot in Figure 19 illustrates

the rate of salt removal and retention of the protein in the separation compartment. The

current and electric potential profiles during IET, along with the conductivity in the feed

compartment are plotted in Figure 20. The current and conductivity continually decrease
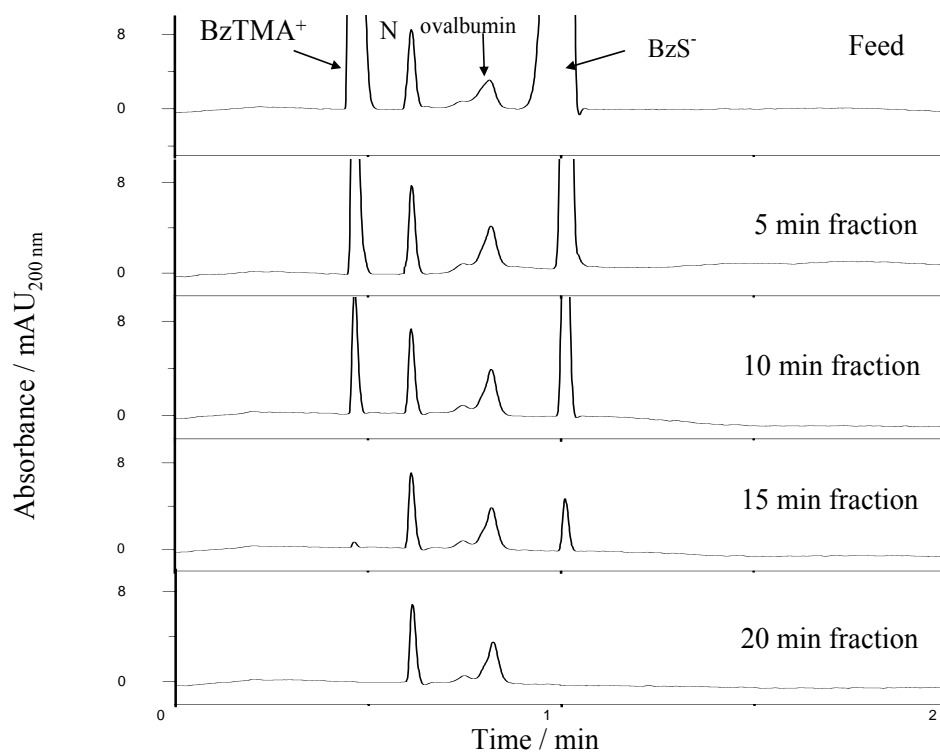
Figure 18. CE analysis of the feed compartment as a function of the separation time.
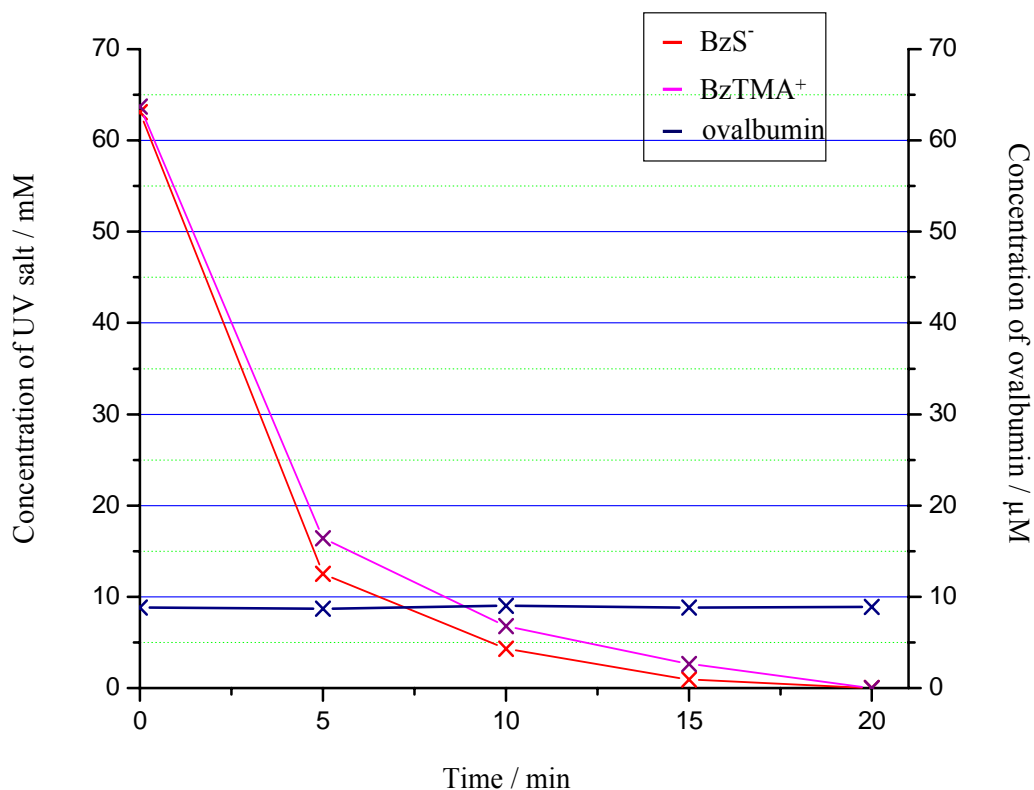
Figure 19. Concentration of the strong electrolytes and ovalbumin in the feed compartment as a function of the separation time.

as the amount of salts remaining in the middle separation compartment decreases; they leveled off at a minimum value once the desalting process was completed. Since the power was kept constant at 3 W, the potential gradually increased at the beginning of the run and leveled off at a maximum value once desalting was completed.

Figure 21 shows the CE traces of the fractions obtained from the anode compartment. Before electrophoresis (time zero), no BzS⁻ was found in the anode chamber. After 5 minutes, 42.7 mM of the UV-active anion was detected; at 10 minutes, 57.2 mM was observed; after 15 minutes, the concentration of BzS⁻ plateaued at around the 63 mM
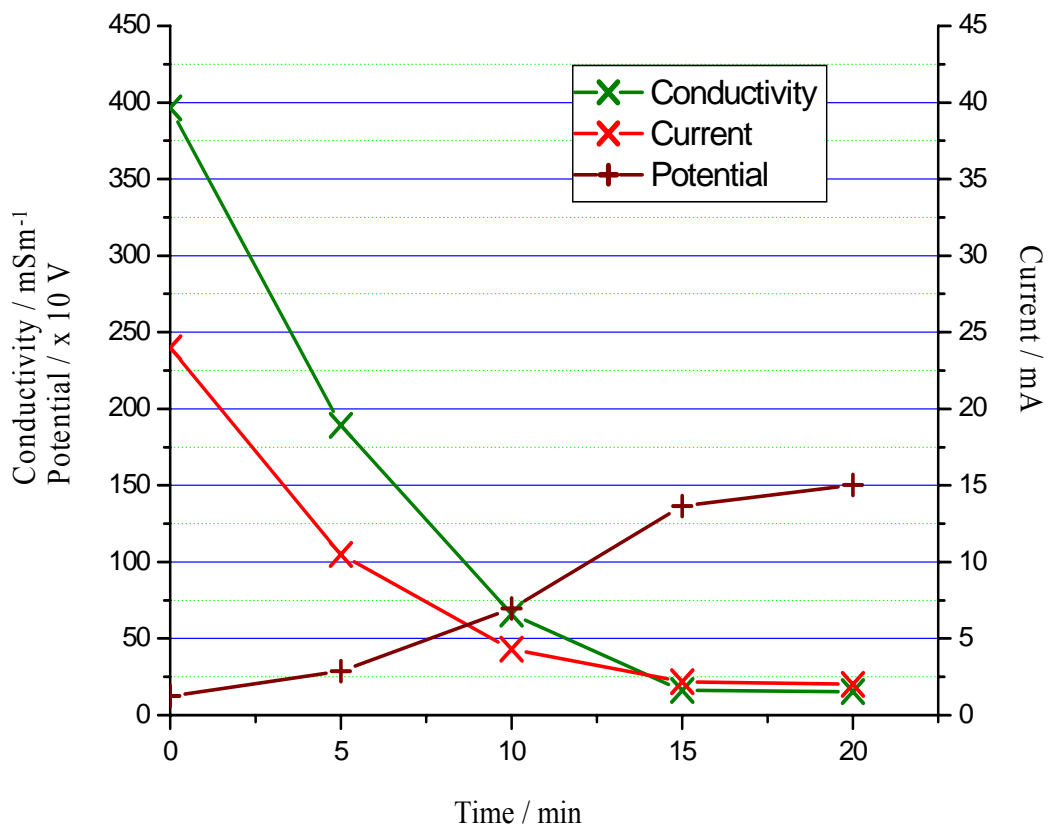
Figure 20. Current and voltage profile and conductivity of the feed fraction during desalting.
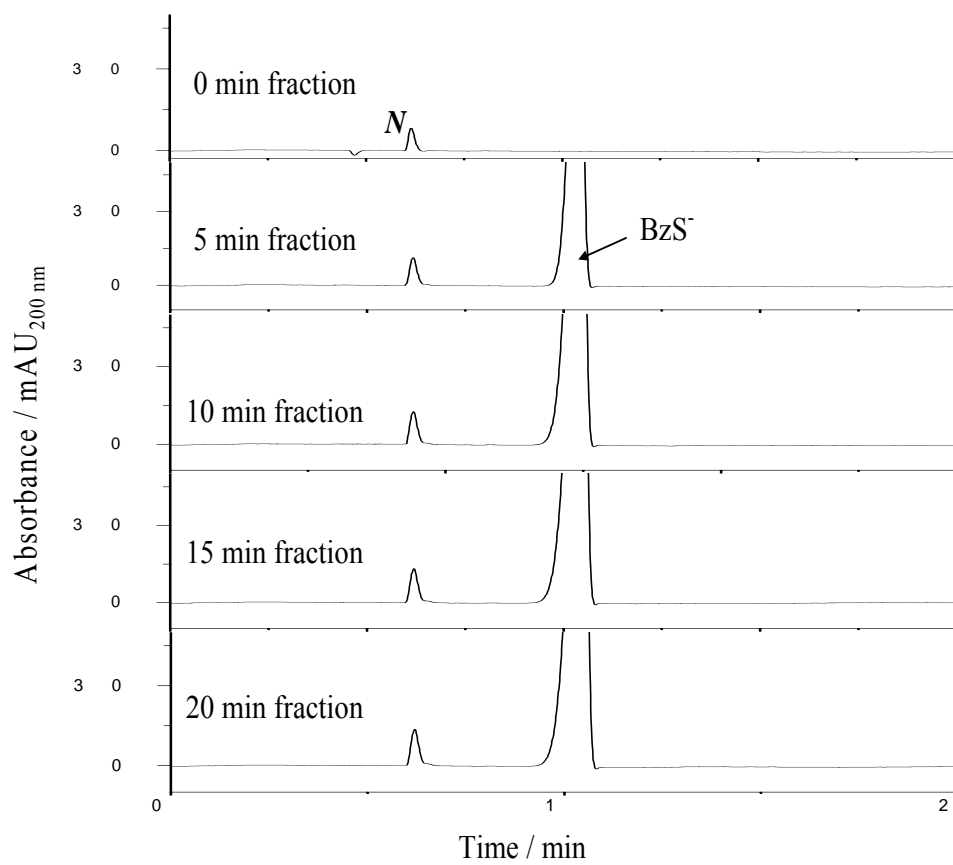
Figure 21. CE analysis of the anode compartment as a function of the separation time.

mark (65 mM was in the sample at start). The small decrease in concentration may be due

to the 5% increase in anolyte volume observed at the end of the run due to transport of

water. Minor sample injection errors during the CE analysis could also indirectly

contribute to the small concentration difference. The anolyte, MSA, has no chromophore

group and was invisible at 200 nm. A similar scenario was observed in the cathode

compartment. The CE traces (Figure 22) show BzTMA$^+$ accumulation in the cathode
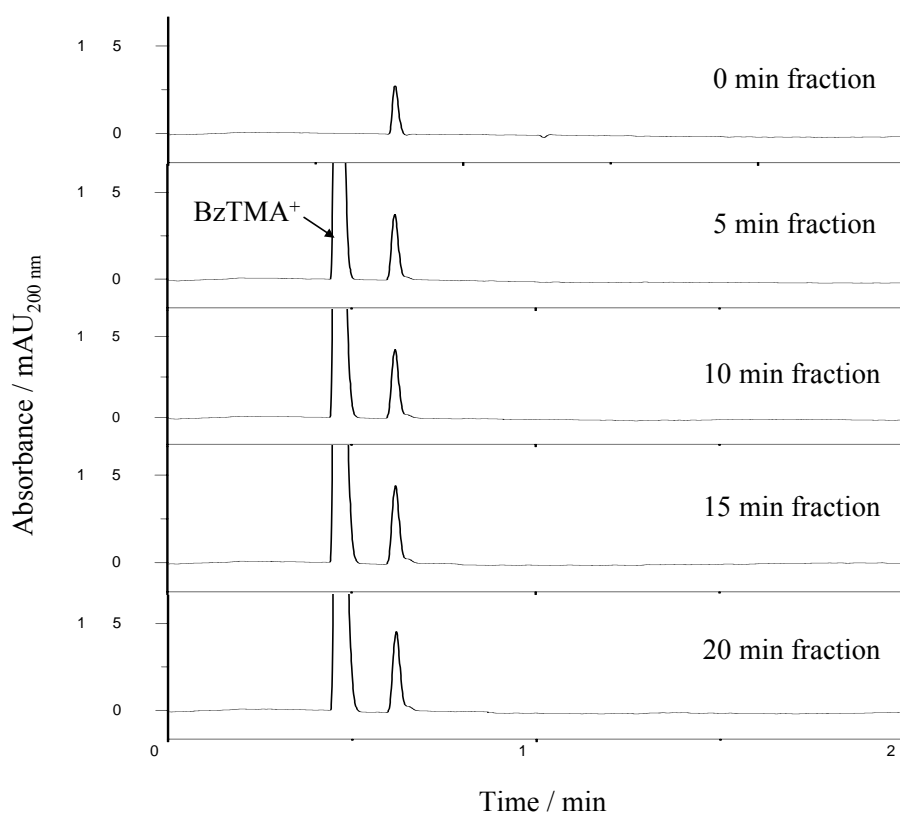
Figure 22. CE analysis of the cathode compartment as a function of the separation time.

compartment. The fractions obtained after 5, 10, 15 and 20 minutes show concentrations

of 35.6 mM, 53.3 mM, 60.9 mM, and 61.1 mM. A 7% increase in the volume of the

catholyte was observed at the end of IET, which again may be due to water transport. In

Figure 23, the concentrations of BzS$^-$ and BzTMA$^+$ in the anode and cathode
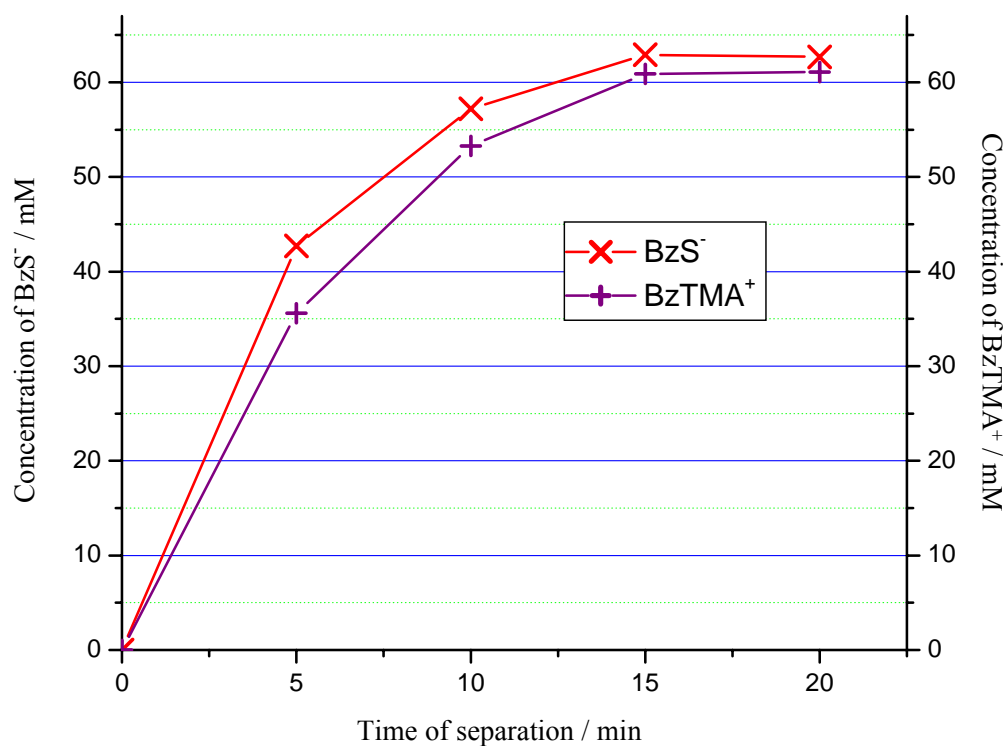
Figure 23. Concentration of BzS$^-$ and BzTMA$^+$ in the anode and cathode compartments, respectively as a function of separation time.

compartments are plotted as a function of separation time. The fractions from the first

and third separation compartments were also monitored by CE. Results revealed the

concentration transients of the UV-absorbing strong electrolytes as they migrated from

the feed compartment toward the electrode compartments. Figures 24 and 25 show the

CE traces of the fractions from the first and third separation compartments, respectively.

There was no salt before electrophoresis in the first and third compartments (top panels).

The electropherograms of the 5-, 10-, and 15-minute fractions (middle panels)

subsequently revealed the presence of about 16 mM, 7 mM, and 4 mM of each

component (BzS$^-$ in the first and BzTMA$^+$ in the third separation compartment). The

bottom panels also indicate that desalting was complete by 20 min.
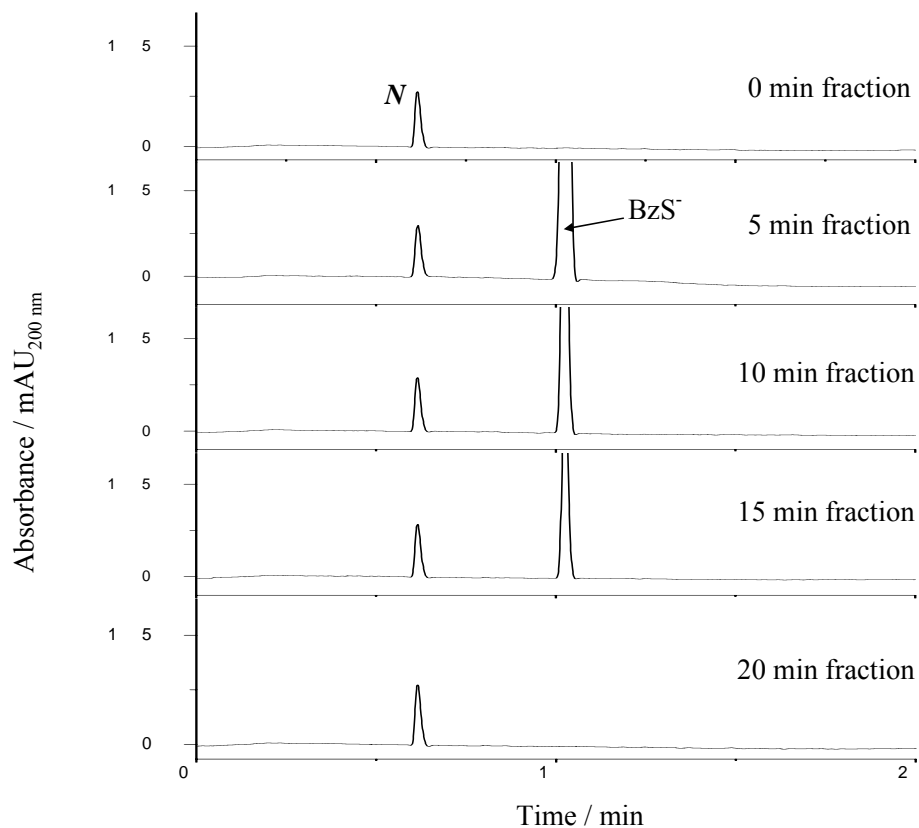
Figure 24. CE analysis of the fractions from separation compartment 1 as a function of the separation time.

Another important observation in this experiment was that the MSWIFT handled 3 watts

of power without causing the solutions to boil in the respective compartments throughout

the whole desalting process. In this experimental setup, the total anode-to-cathode

distance was 4 times shorter than in the IsoelectriQ^2 and the ZOOM™. The field strength

at the end of the run reached about 260 Vcm^{-1}. Finally, since the electrolytes in biological

samples have effective mobilities 3 times faster than that of the salt components used in

this experiment, the total desalting time of 20 minutes should be adequate for biological samples.
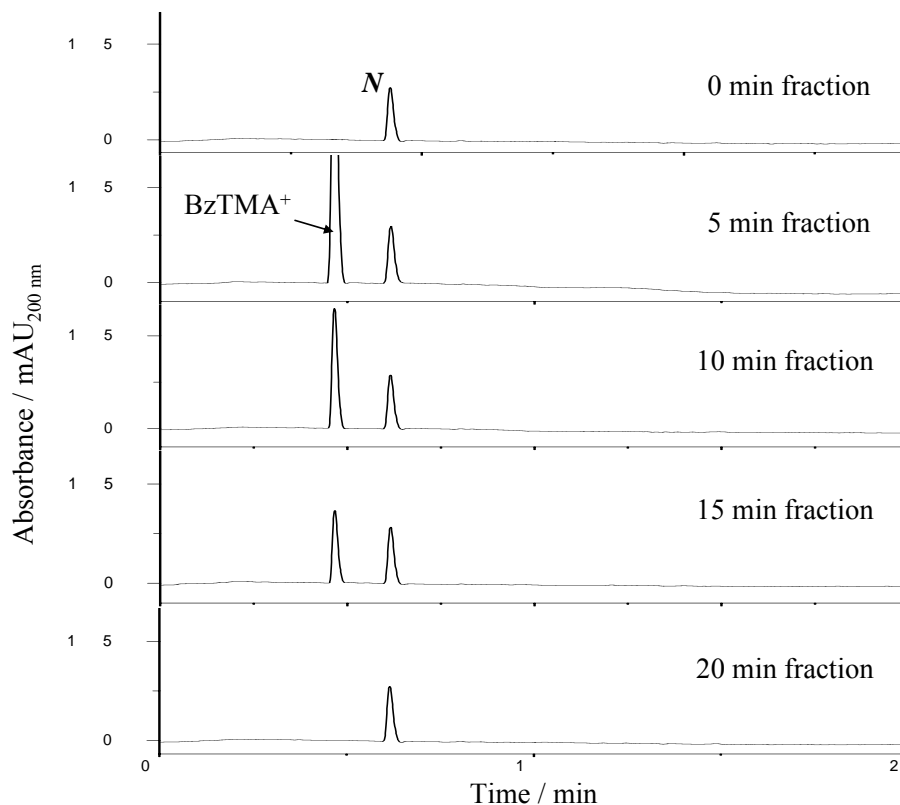
Figure 25. CE analysis of the fractions from compartment 3 as a function of the separation time.

3.2. Separation of five ampholytic components

3.2.1. Background and objective

The desalting experiment proved that MSWIFT could: (i) remove salts rapidly; (ii) keep a protein trapped in between pre-selected membranes; and (iii) handle 3 watts of power effectively. Its success quickly raised additional questions. Can the device rapidly separate ampholytes? Can the MSWIFT tolerate higher electrical power? When 4 watts of power was applied to the same setup described in Section 3.1, the power supply

reported an error due to rapid resistance change. Thus, the primary goal of the next experiment was to quantitatively investigate the efficiency of the MSWIFT to separate ampholytes using a higher wattage. For the first attempts, water-soluble ampholytic small-molecules were selected as ideal sample components. A more dilute sample mixture was used than in the previous experiment to avoid short-circuiting. There was a downside for this sample selection. Small, soluble ampholytes, especially when dilute, are typically undetectable in CE with UV-detectors. Therefore, the secondary objective for this experiment was to provide a sensitive method to detect the ampholytes during CE analyses.

3.2.2. Instrument set-up, materials, and method

Five different ampholytic components: aspartic acid (Asp, pI 2.7), glutamic acid (Glu, pI 3.2), histidine (His, pI 7.5), carnosine (Carn, pI 8.1), and methyl lysine (MeLys, pI 9.8) were chosen to be the sample components. Except for carnosine, which is a dipeptide, the rest of the ampholytes in the sample were amino acids. All of them were commercially available from SIGMA (St. Louis, MO). 100-mL stock solutions with known concentrations of 0.05, 0.10, 0.25, 0.50, 1.0, and 2.0 mM for each ampholyte were prepared. 200-µL aliquots from each stock solution were added to 200 µL of 25 mM boric acid/LiOH buffer (pH 10.5), 5 µL of 40 mM KCN, and 35 µL of 10 mM naphthalene dialdehyde (NDA). The mixtures were shaken and left at room temperature for 10 minutes. Each mixture was then analyzed by CE. The effective mobilities for each analyte were calculated. The normalized peak areas from the electropherograms were

plotted against the known concentrations to obtain a set of calibration curves for all

sample components.
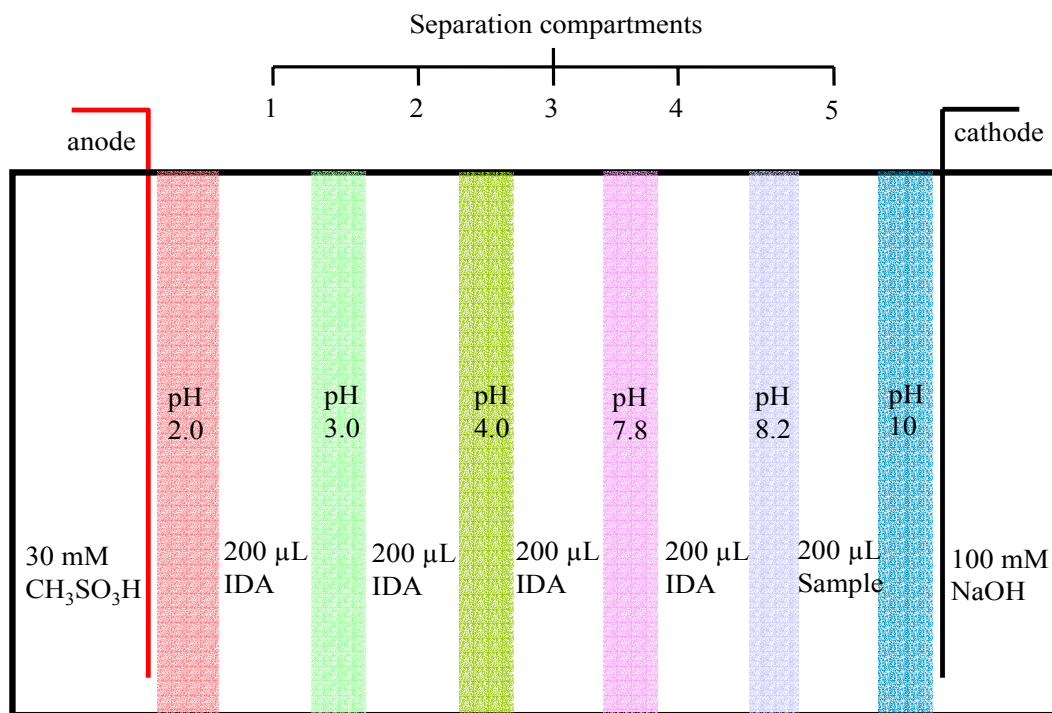
Figure 26. Schematic diagram of the MSWIFT setup for the fractionation of 5 ampholytic compounds. The sample was loaded in the 5th separation compartment.

A 100-mL sample stock solution was made such that the concentration for each

ampholytic component was 0.5 mM. The pH of the mixture was 6.1. The MSWIFT was

set up with 7 compartments (See Figure 26). The first and last compartments were used

as the electrode chambers, in between of them there were five separation chambers. All

compartments were separated by PVA-based buffering membranes with pH 2.0, 3.0, 4.0,

7.8, 8.2, and 10.0. The membranes were arranged such that their pH increased from

anode to cathode. The total anode-to-cathode distance was 4 cm. The anode compartment

was filled with 400 μL of 30 mM CH_3SO_3H, and the cathode compartment was filled

with 400 µL of 100 mM NaOH. 200 µL of the sample stock solution was loaded in the 5th

separation chamber (closest to the cathode chamber). The rest of the 200-µL separation

chambers were filled with 0.1 mM iminodiacetic acid (IDA, pI 2.2) solution. The

separation was done at constant 4 W power, fractions were collected from every

compartment every 5 minutes. Each fraction was treated with NDA following the

procedure described above. The NDA-treated fractions were analyzed by CE with the UV

detector wavelength set at 280 nm. All CE runs (during the calibration and fraction

analyses) were completed in a 50 µm internal diameter fused silica capillary (L_t = 46.5

cm; L_d = 39.5 cm) with a potential of 30 KV, using a 30 mM piperidine/ 10 mM HEPES,

pH 10.9 buffer as the background electrolyte. The polarity used was plus-to-minus.

A.

B.
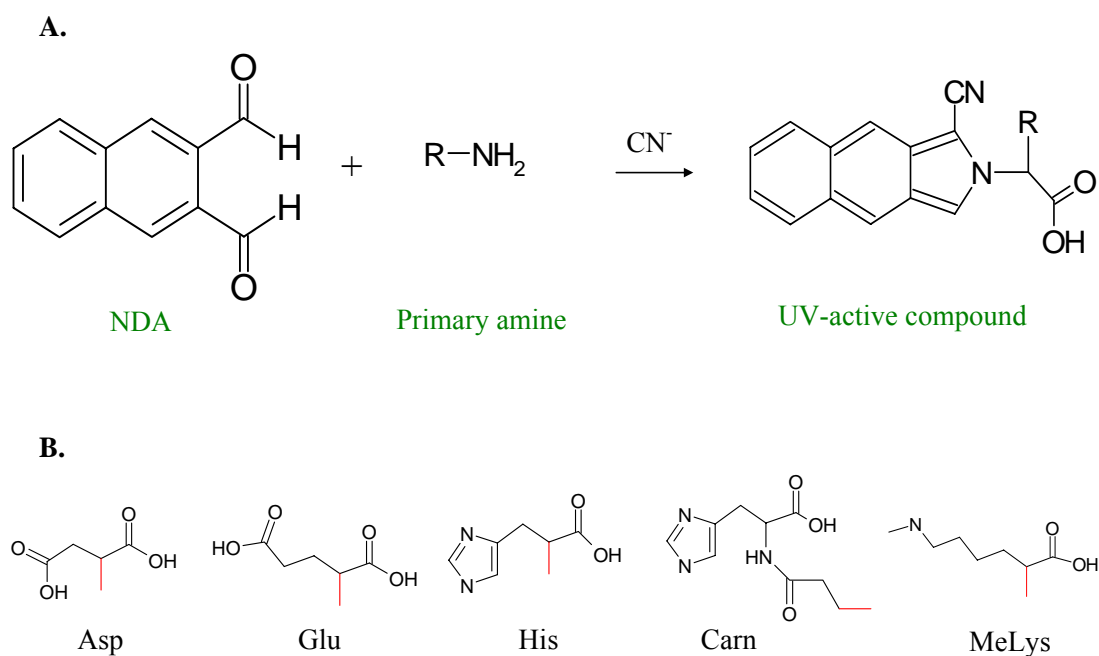
Figure 27. A. Chemical equation for the reaction of naphthalene dialdehyde with a primary amine. **B**. Different R groups used in the experiment.

3.2.3. Results and discussion

NDA, in the presence of cyanide ions, reacts with the primary amino functionality of the

analytes and converts them into UV absorbing derivatives (Figure 27). The reaction was

done in an environment basic enough (pH 10.5) to deprotonate the primary amines of the

sample components. It should be noted that the NDA-ampholyte reaction products will

no longer be ampholytic. After 30 seconds of reaction, a bright green color was observed

for each fraction. In 10 minutes, the reaction was found to be complete. Even at low
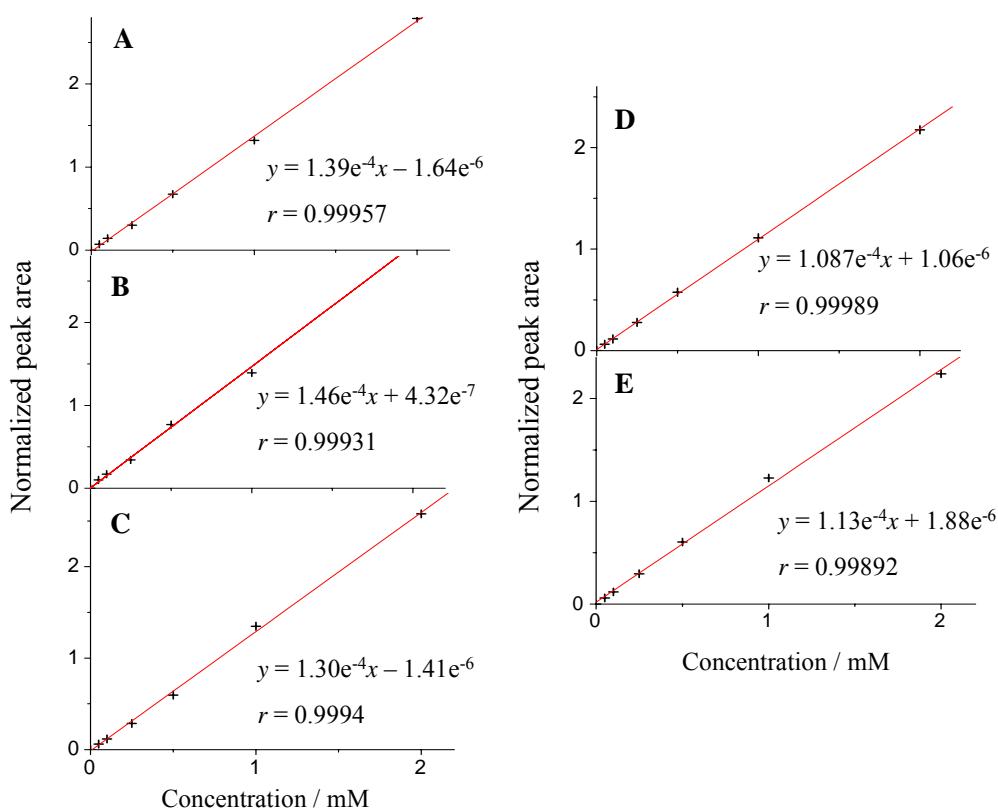
Figure 28. Calibration curves of NDA-amino acids: (**A**) Asp; (**B**) Glu; (**C**) His; (**D**) Carn; and (**E**) MeLys.

micromolar concentrations, the NDA-derivatized analytes were detected at 280 nm

wavelength with a signal-to-noise ratio (S/N) of 10 or greater. This way, the

concentrations of the UV-transparent ampholytes that were isolated in the respective MSWIFT fractions could be quantitatively monitored by CE. The normalized peak area versus concentration calibration curves were linear with correlation coefficients of $r =$ 0.999 or greater for all ampholytes. These results indicated that the NDA reaction was efficient. The calibration curves are shown in Figure 28.

The exact initial concentrations of the sample components were determined by treating an aliquot of the sample stock solution with NDA. From the normalized CE peak areas and the respective calibration curves, the concentrations for Asp, Glu, His, Carn, and MeLys were found to be 0.517 mM, 0.475 mM, 0.451 mM, 0.554 mM and 0.545 mM, respectively.

Before the start of IET, the sample was loaded into compartment 5. IDA was loaded in all other separation compartments to provide an initial conductivity. The buffering membranes were chosen to trap Asp, Glu, His and Carn in compartments 1, 2, 3 and 4, respectively. MeLys was expected to remain in the feed compartment. IDA was also anticipated to be trapped in the first separation compartment. Figure 29 shows the CE results for the fractions obtained from separation compartment 1. Evidently, aspartic acid accumulated in this compartment. Its concentration increased in the 5-, 10-, and 15-minute fractions from 0.426 mM through 0.473 mM to 0.485 mM, respectively and leveled off around 0.5 mM (0.498 mM, and 0.501 mM after 20 and 30 minutes). The amount of Asp recovered was 97%. Since IDA does not react with NDA, no peak was seen for it in the CE traces.
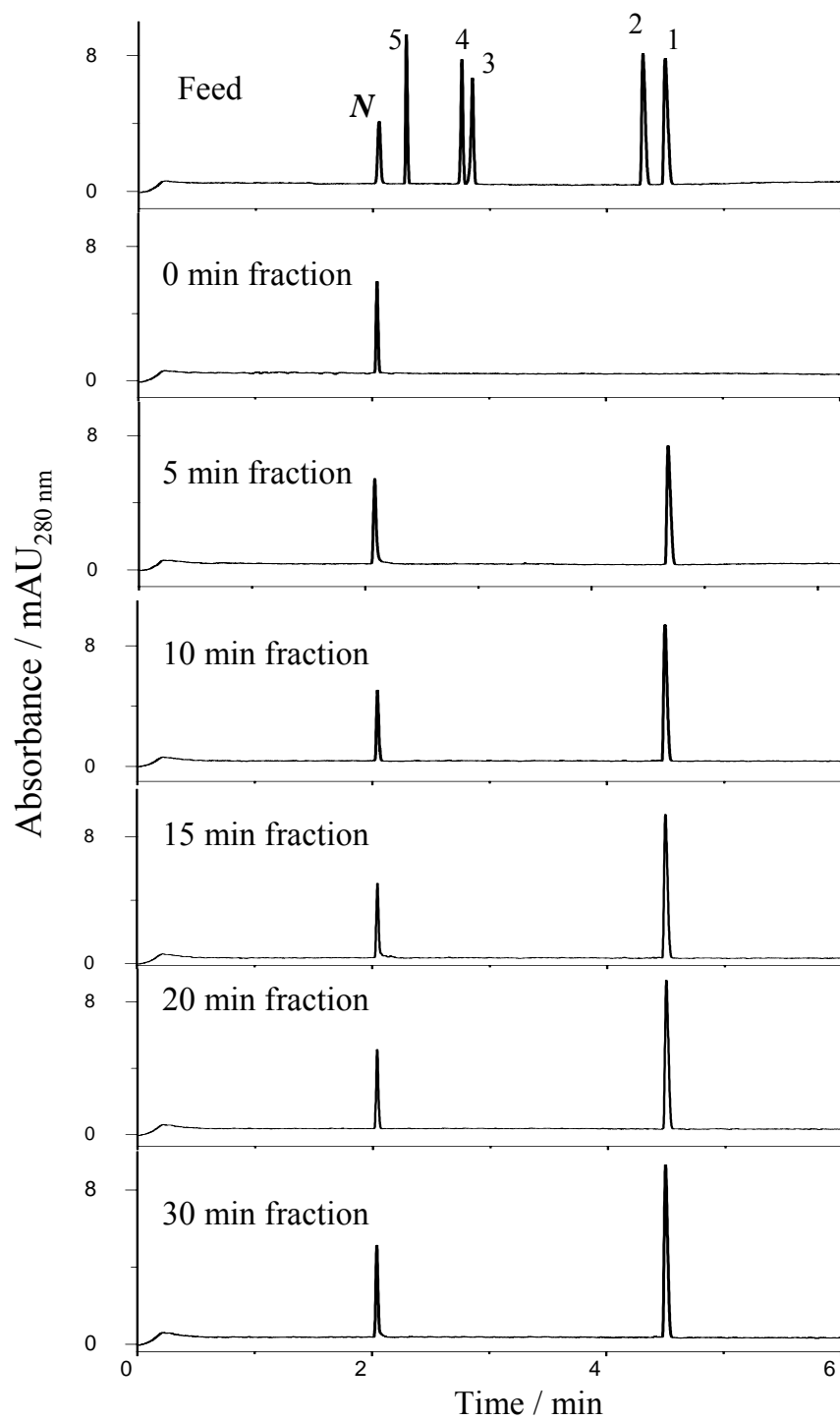
Figure 29. CE analysis of the fractions from compartment 1 as a function of the separation time. NDA derivatives of 1. Asp, 2. Glu, 3. His, 4. Carn, and 5. MeLys.

Figure 30 shows the CE traces for the fractions obtained from separation compartment 2. Clearly, Glu was trapped in this compartment. Its concentrations increased in the 5-, 10-, and 15-minute fractions from 0.368 mM through 0.445 mM to 0.467 mM, respectively. The concentration leveled off at around 0.47 mM (20 and 30 minutes of IET). About 99% of the Glu was isolated in the second separation compartment. The transient peaks of aspartic acid were also found in the 5- to 15-minute fractions.

The electropherograms for the fractions collected from separation compartment 3 are shown in Figure 31. Histidine was trapped in this chamber, its concentrations were 0.289 mM, 0.348 mM, and 0.414 mM in the 5-, 10-, and 15-minute fractions, respectively. The concentration started to leveled off around 0.45 mM (0.449 mM and 0.456 after 20 and 30 minutes of IET). Since the pH of the sample solution at the start was pH 6.1, the imidazole group of the His was partially protonated and gave the whole molecule a net positive charge. This would mean that the ampholyte was initially attracted toward the cathode, but could not reach the cathode chamber due to the presence of the pH 10 buffering membrane. In the early stages of electophoresis, the negatively charged Asp and Glu rapidly left the feed compartment and migrated toward the anode. As a consequence, the pH of the feed compartment increased to a value that was high enough for His to acquire a net negative charge. At this point, His began to move anode-bound. This explains why the accumulation of His in compartment 3 was slower compared to those of Asp and Glu. Nonetheless, all of His was recovered in the third separation

compartment by 30 minutes. The transient peaks of aspartic and glutamic acid were also found in the 5- to 15-minute fractions.
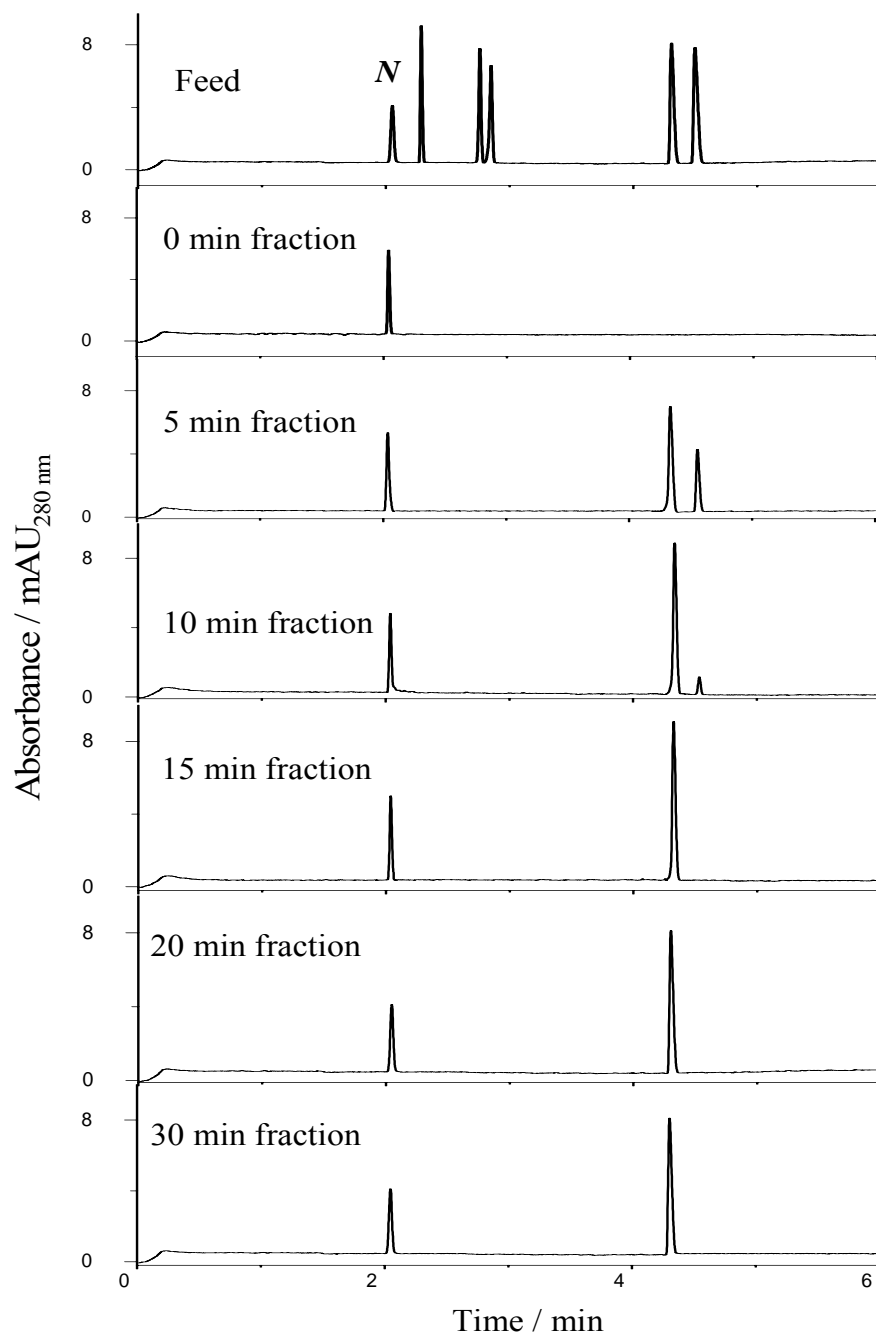
Figure 30. CE analysis of the fractions from compartment 2 as a function of the separation time
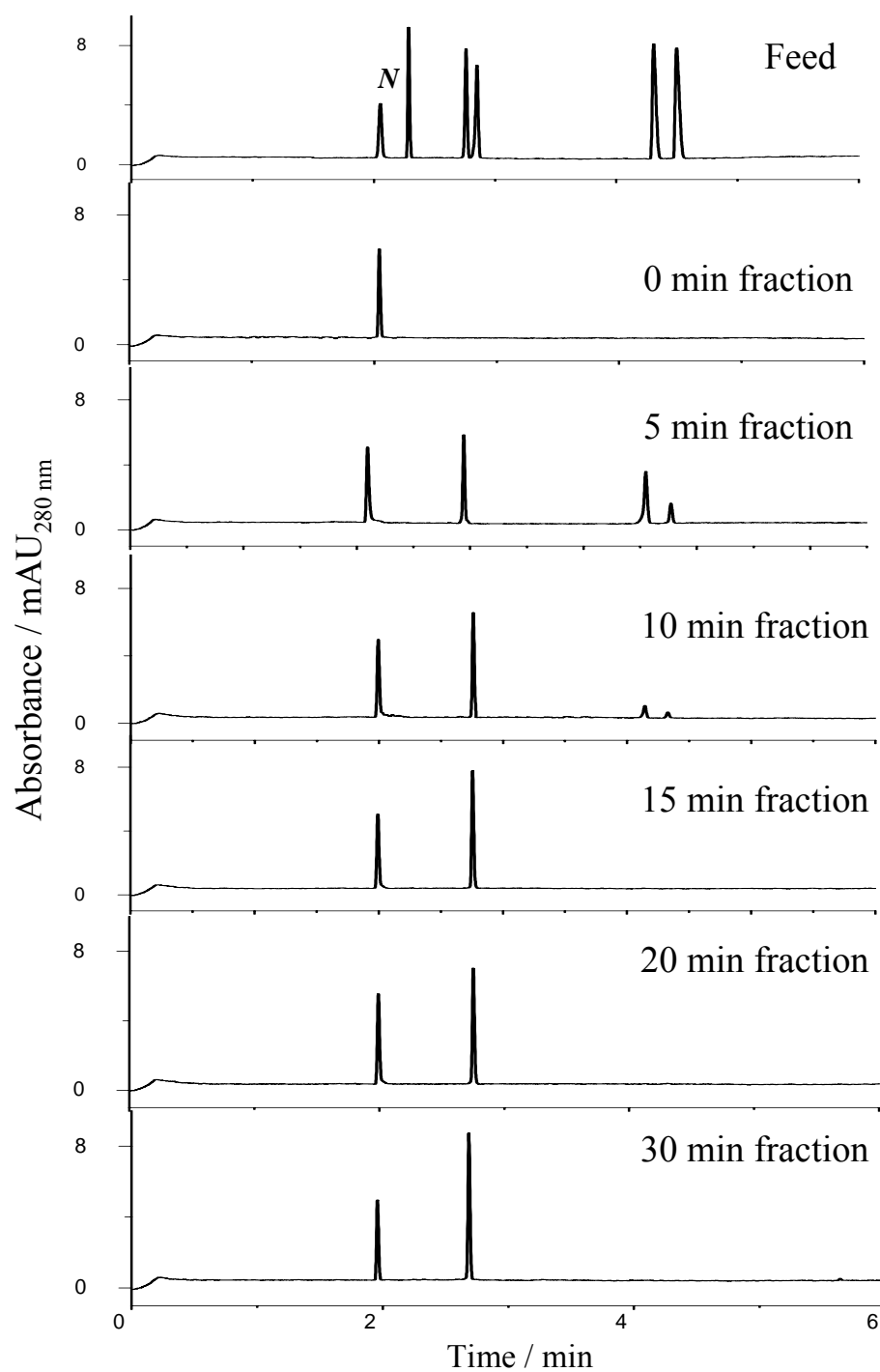
Figure 31. CE analysis of fractions from compartment 3 as a function of the separation time.

Figure 32 shows the CE results for the fractions obtained from separation compartment 4. Carnosine was isolated in this compartment, its concentrations in the 5-, 10-, and 15-minute fractions were 0.199 mM, 0.360 mM, and 0.476 mM, respectively. The concentration leveled off at 0.52 mM (20 and 30 minute fractionations). The slow trapping of Carn in the fourth separation compartment was observed and was similar to the behavior of histidine. About 95% of Carn was isolated in compartment 4. The transient peaks of Asp, Glu, and His were seen in the 5- to 15-minute fractions.

MeLys remained trapped in the feed compartment throughout the entire IET process (Figure 33). The calculated concentrations were constant at around 0.55 mM.
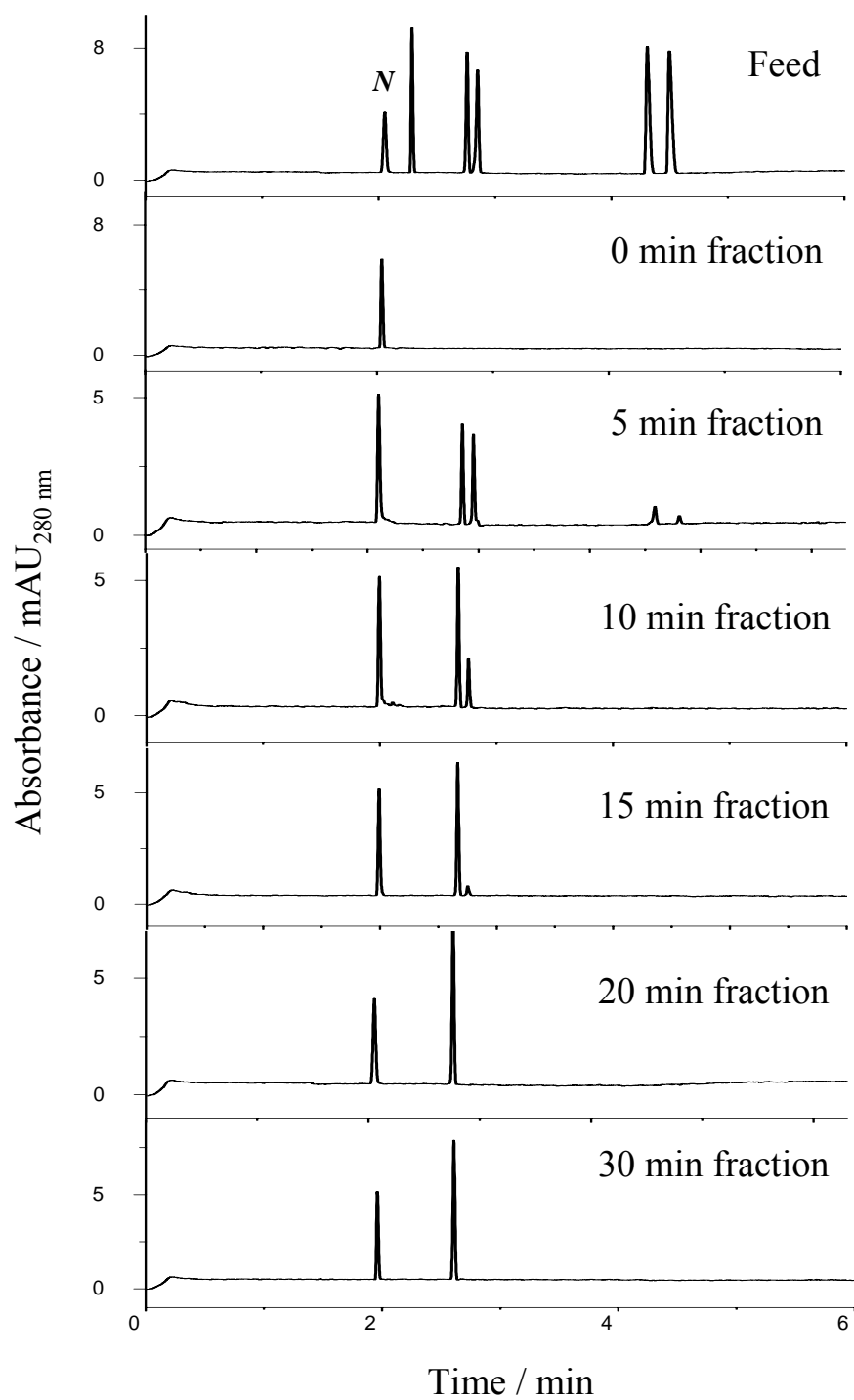
Figure 32. CE analysis of the fractions from compartment 4 as a function of the separation time.
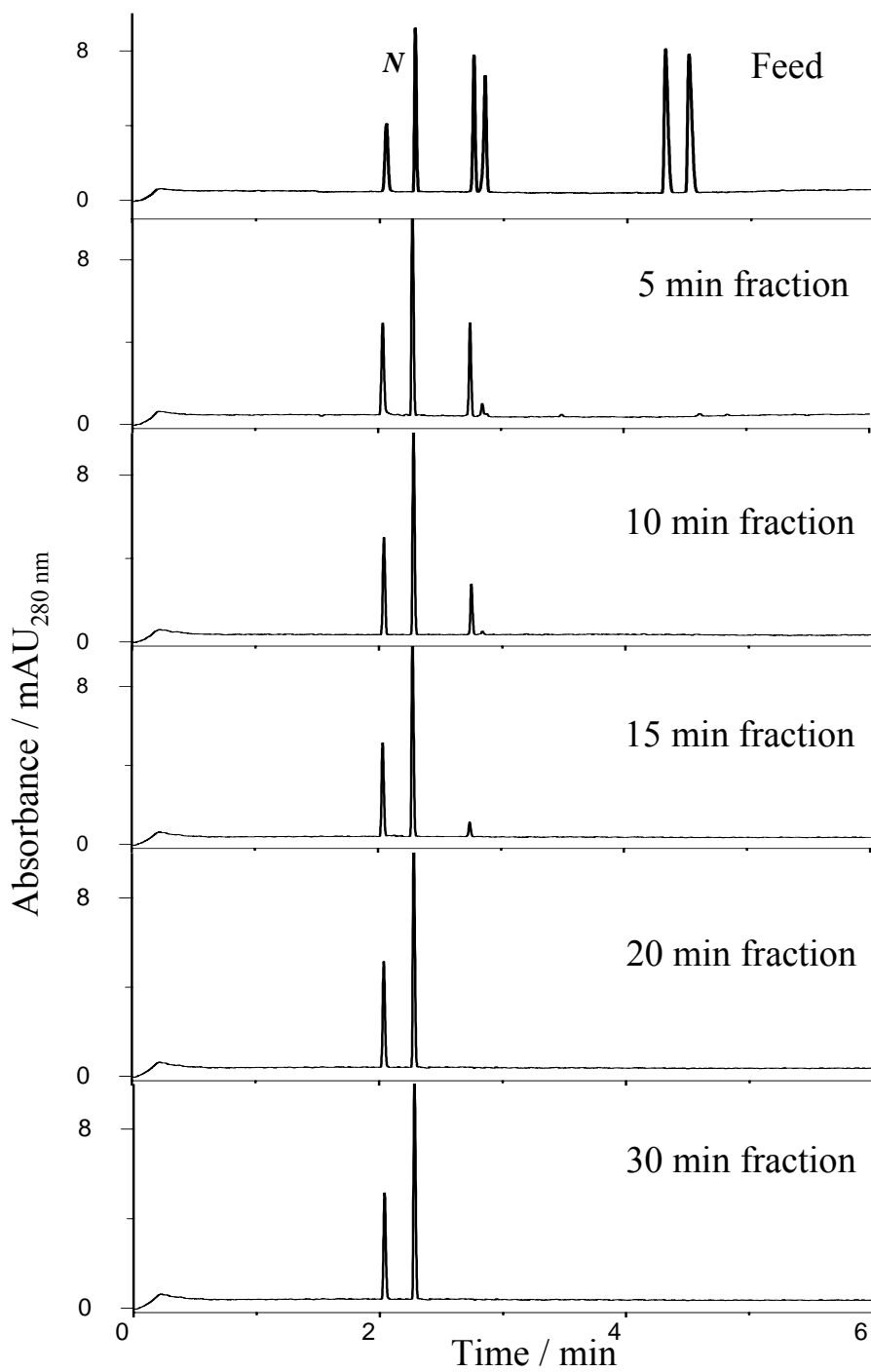
Figure 33. CE analysis of the fractions from compartment 5 as a function of the separation time.

Figure 34 shows the concentrations as a function of the separation time for each isolated component. The volumes of all the fractions at the end of the run remained about 200 μL (± 5 μL). The slight volume changes changes (Figure 35) may be due to water transport during the IET process. When all the volume differences are taken into account, the percentage recoveries for the isolated ampholytes are about 100%. The pH values of each fraction were also measured (Figure 36): the pH profile supports the hypothesis about the charge state of His and Carn in the early stages of the IET process. Figure 37 shows the current and voltage profiles for the entire separation. At the end of the run, the corresponding current and potential were 1.9 mA and 2115 V. The final field strength reached about 530 Vcm^{-1}. This experiment also showed that MSWIFT can tolerate 4 watts of power. It also provided the first set of quantitative data for IET fractionation in a small-scale instrument.
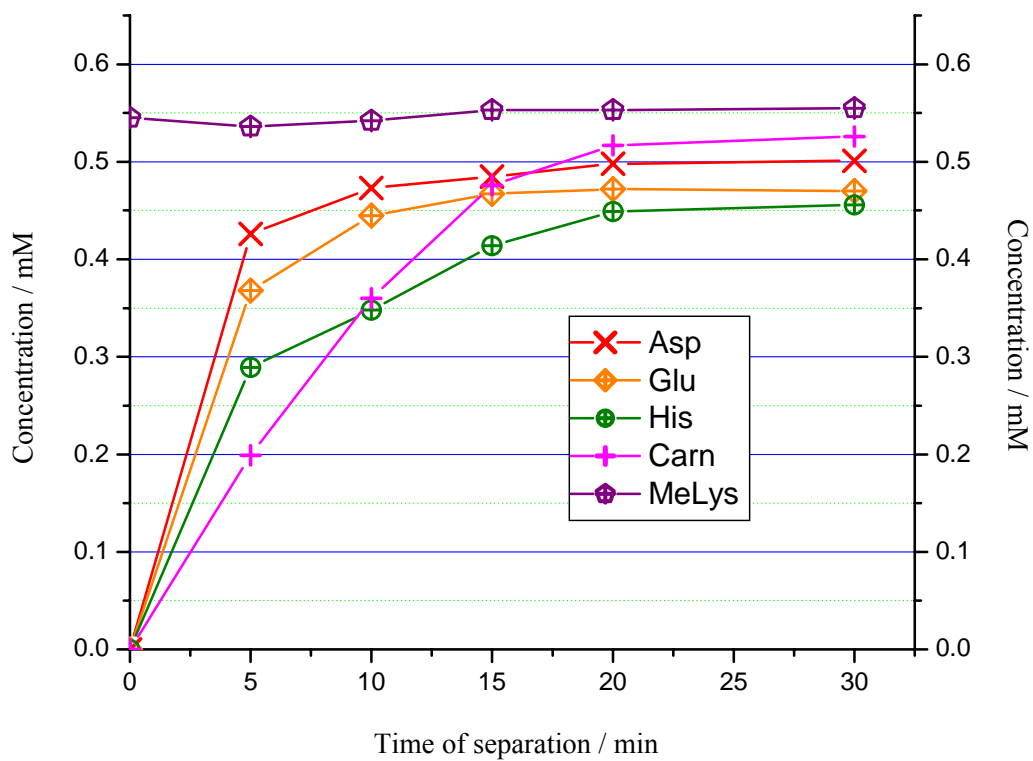
Figure 34. Concentration of the amino acids in their corresponding compartments as IET progresses.
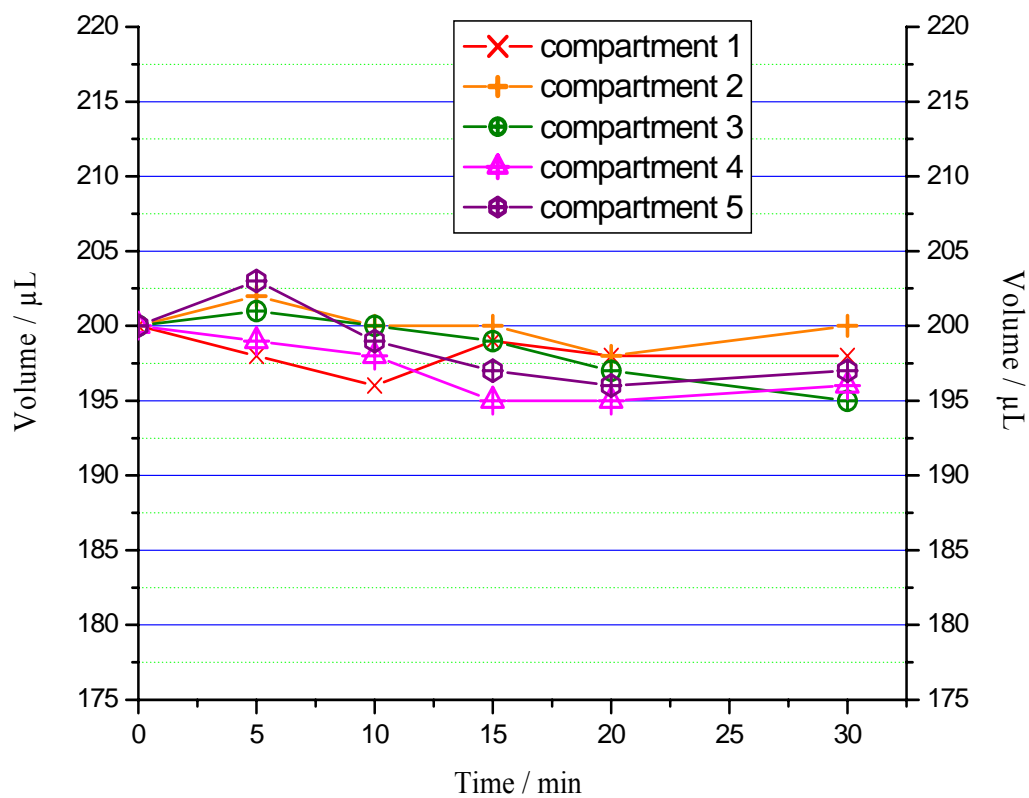
Figure 35. Solution volume in the compartments as a function of separation time.
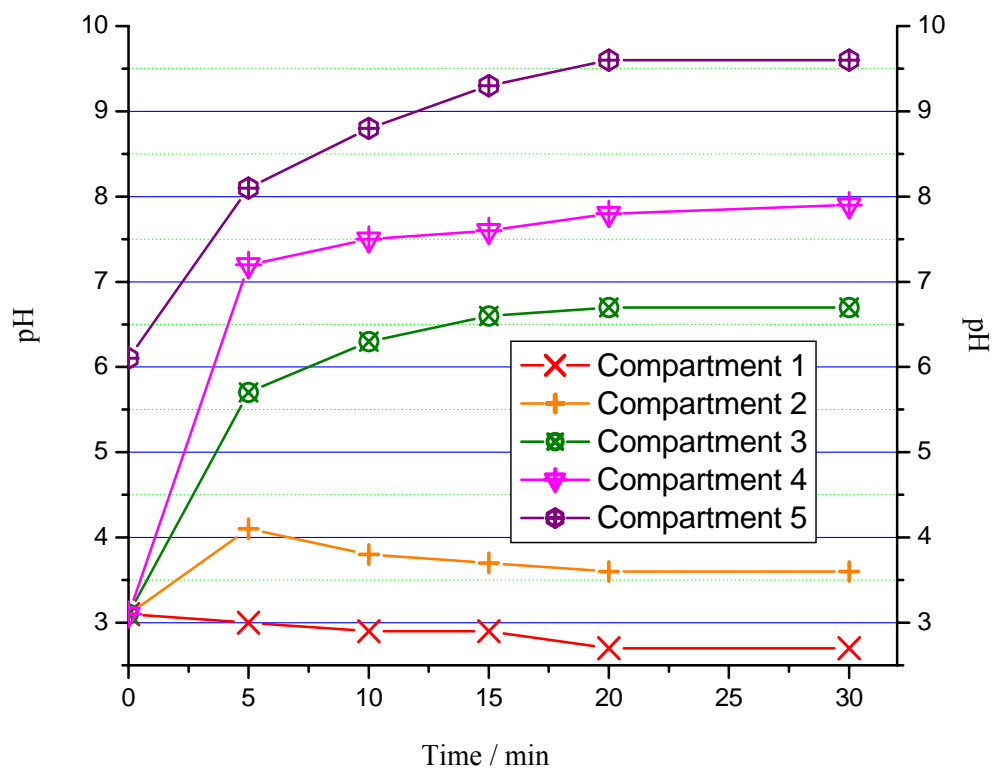
Figure 36. pH of the solution in the respective compartments as a function of separation time.
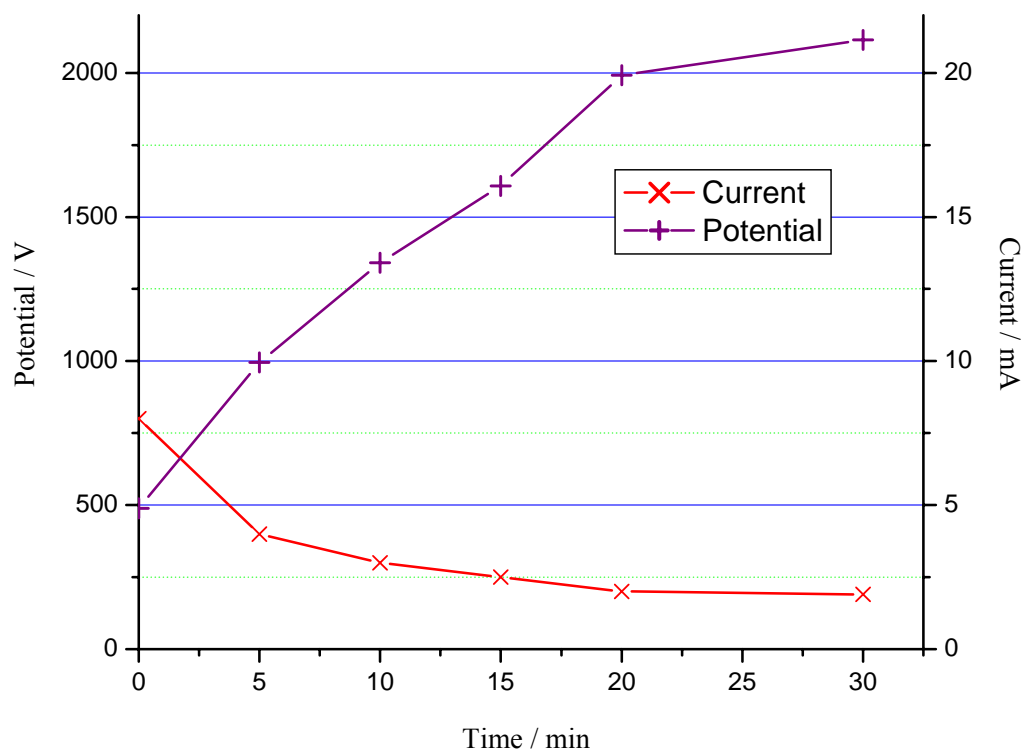
Figure 37. Current and voltage profiles during IET.

3.3 Purification of target components from a crude ampholytic sample

3.3.1. Background and objectives

Synthesis of UV-active isoelectric compounds to be used as pI markers during isoelectric focusing is of importance for IEF. In many cases, the reactants produce a series of compounds with different isoelectric points. Then, the products are subjected to several processing steps including solvent removal, precipitation and/or crystallization, which result in significant losses of the target before a pure compound suitable as an IEF standard is obtained. In a micro-scale synthesis, such losses cannot be tolerated. Thus, it was interesting to see if the MSWIFT could serve as an efficient purification method for crude ampholytic products obtained in micro-scale reactions. If yes, in order to maximize

production efficiency, it would be important to find out how large an electrical power load the MSWIFT could tolerate.

The purification of a reaction mixture containing 4-hydroxy-3-(morpholinomethyl)benzoic acid (HMMB, pI=5.8), 4-hydroxy-3,5-bis(morpholinomethyl)benzoic acid (HBMMB, pI=6.1) and other UV-active ampholytic products is detailed in this section.

3.3.2. Instrument set-up, materials, and method

The sample tested is a reaction mixture containing derivatives of HMMB. The MSWIFT setup was designed to isolate HMMB and HBMMB from the rest of the derivatives. Five compartments were used in the experimental setup: two were used as the electrode compartments, three as the separation compartments. The PVA-based buffering membranes separating the compartments were pH 2.0; 6.0; 6.3 and 10 and were arranged with their pH increasing from the anode to the cathode. The anode-to-cathode distance was 2 cm. The anode chamber was filled with a 30 mM MSA solution; the first separation chamber was filled with 200 µL of a 0.5 mM aspartic acid solution, the second separation chamber contained 200 µL of the sample mixture; the third separation chamber was filled with 200 µL of a 0.5 mM histidine solution; the cathode chamber was filled with a 100 mM sodium hydroxide solution. The schematic diagram of the MSWIFT set-up used for this experiment is shown in Figure 38. The separation was run with a constant power of 5 W, and the compartments were sampled every 5 minutes. The fractions were analyzed by CE, with the UV detector set at 280 nm. All CE runs were carried out in a 50 µm internal diameter fused silica capillary ($L_t = 26.5$ cm, $L_d = 19.5$

cm), at a potential of 25 KV, using a 20 mM TRIS, 10 mM MSA, pH 8.11 buffer as the

background electrolyte. The fractions were also analyzed by electrospray ionization mass

spectrometry (ESI-MS).
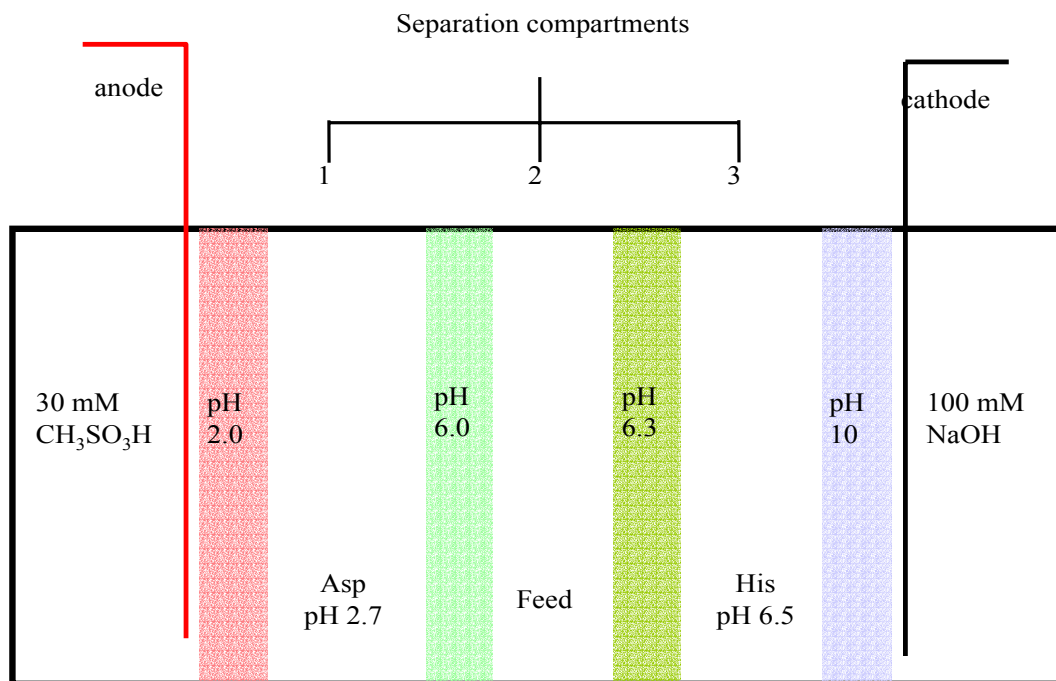
Figure 38. Schematic diagram of the MSWIFT setup. The crude sample is loaded at the middle compartment.

3.3.3. Results and discussion

A CE trace and the mass spectrum of the sample mixture is shown in Figure 39, revealing

numerous impurities in the reaction mixture. Previous work in our laboratory indicated

that most of these derivatives were ampholytic and had pI values greater than 6.3. CE

experiments revealed that the effective mobilities for HMMB and HBMMB were -

15.0×10^{-5} $cm^2V^{-1}s^{-1}$ and -9.7×10^{-5} $cm^2V^{-1}s^{-1}$, respectively, in a 20 mM TRIS-MSA, pH

8.1 buffer as the BE; and their corresponding pI values were 5.8 and 6.1. Thus, the

experimental setup was designed to trap these targets in compartments 1 and 2,

respectively. Figure 40 portrays the results of the CE analysis of the MSWIFT fractions after 20 minutes of separation. The fraction from compartment 1 contained only HMMB, with a μ^{eff} value of -15.0x10^{-5} cm^{2}V^{-1}s^{-1}, in agreement with previous analytical data. The
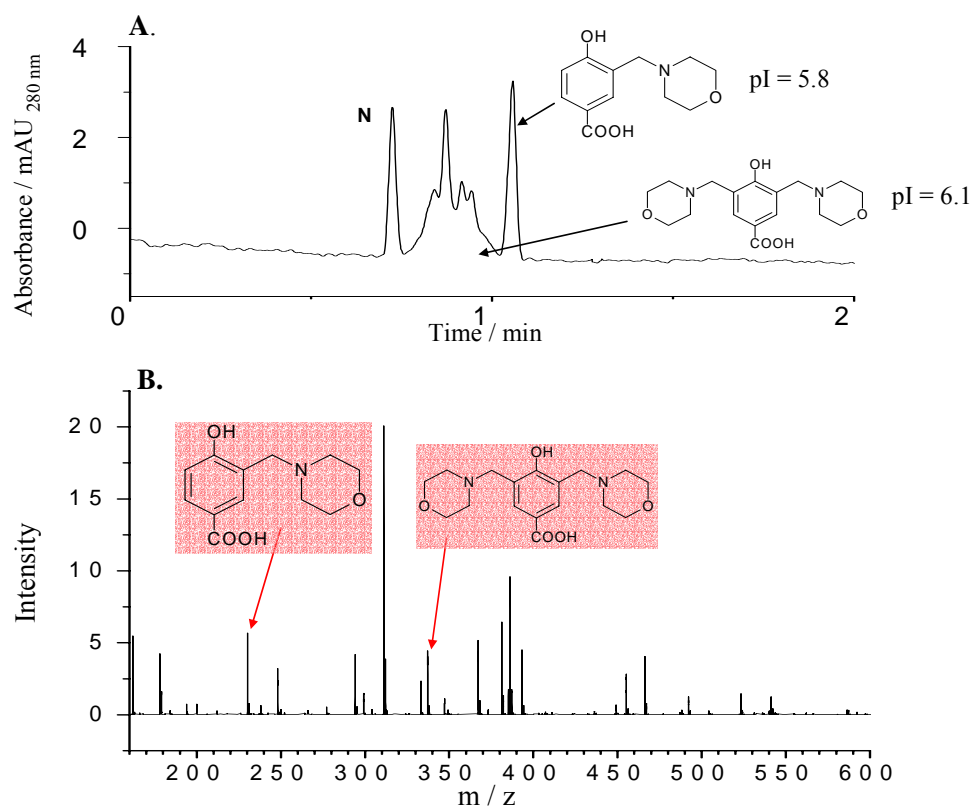
Figure 39. A. CE trace of a crude ampholytic sample. **B**. ESI-MS of the sample

fraction from the second separation compartment contained isolated HBMMB, with a μ^{eff} of -9.7x10^{-5} cm^{2}V^{-1}s^{-1}, consistent with the earlier CE results. ESI-MS data (Figure 41) provided additional confirmation of the purity of the fractions obtained from the MSWIFT. Each mass spectrum indicates the presence of a single component with mass-to-charge ratio (m/z) of 238.12 and 338.17 for HMMB and HBMMB, respectively. The m/z values are consistent with their calculated (M+H$^+$) values. This experiment has also shown that the MSWIFT was able to operate at a higher wattage effectively. Even at 6

watts, the sample solutions inside the separation compartments did not boil, though the aluminum heat sink began to feel warm. Thus, the IET was run repeated at constant 5 watts. The final corresponding current and potential values were 2.5 mA and 2025 V. With the anode-to-cathode distance at 2 cm, the operational field strength at the end of the run reached over 1000 Vcm^{-1}.
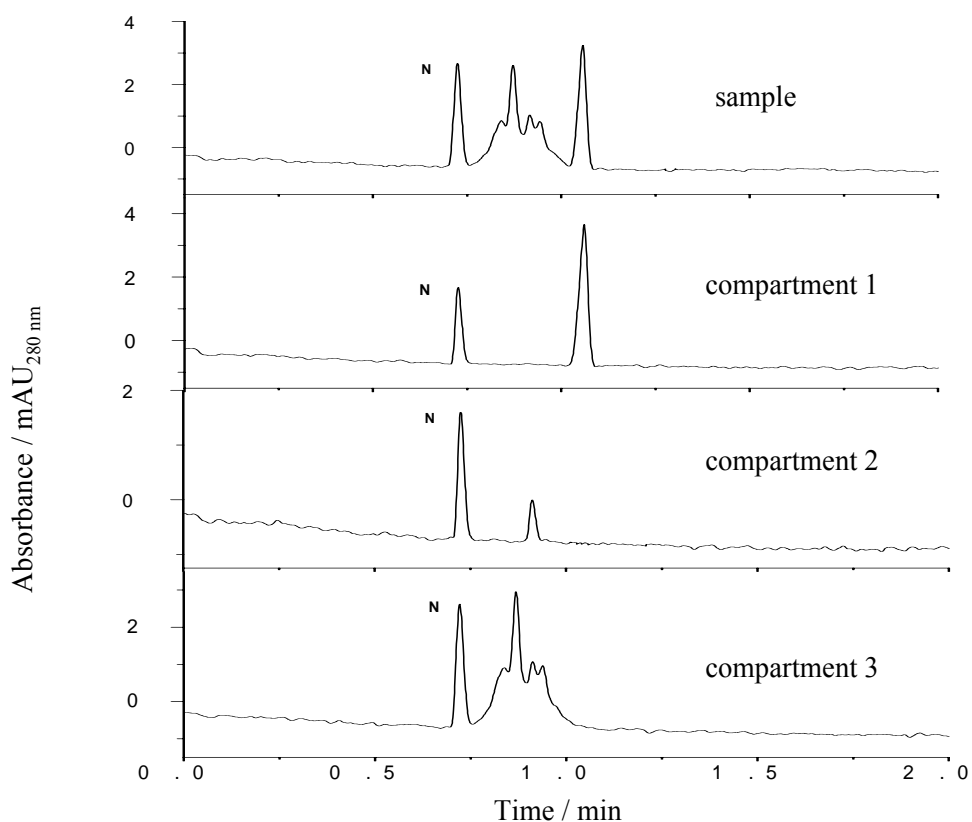
Figure 40. CE analysis of MSWIFT fractions after 20 minutes of electrophoresis.

3.4. Fractionation of proteins from egg white

3.4.1. Background and objectives

The most significant application of IET is protein fractionation. In protein analysis, desalting, fractionation, and preconcentration of biological samples are commonly required prior to downstream analyses such as capillary IEF, two-dimensional

electrophoresis (2DE), and mass spectrometry. One of the major advantages of an MCE device is that it can perform all these operations in a single run. The previous sections have demonstrated that the MSWIFT can desalt and fractionate ampholytic compounds. In this experiment, the MSWIFT was tested to see if it can also effectively enrich proteins. Fresh eggwhite was used as the sample, because its proteins have a wide pI range, water-soluble and it is readily available. The major proteins in egg white are ovalbumin (54 w/w%, pI 4.8), ovotransferrin (11 w/w%, pI 6.1), avidin (0.05 w/w%, pI 8.9) and other isoforms of ovalbumin (13 w/w%, pI 4.9-5.0) [65-67].
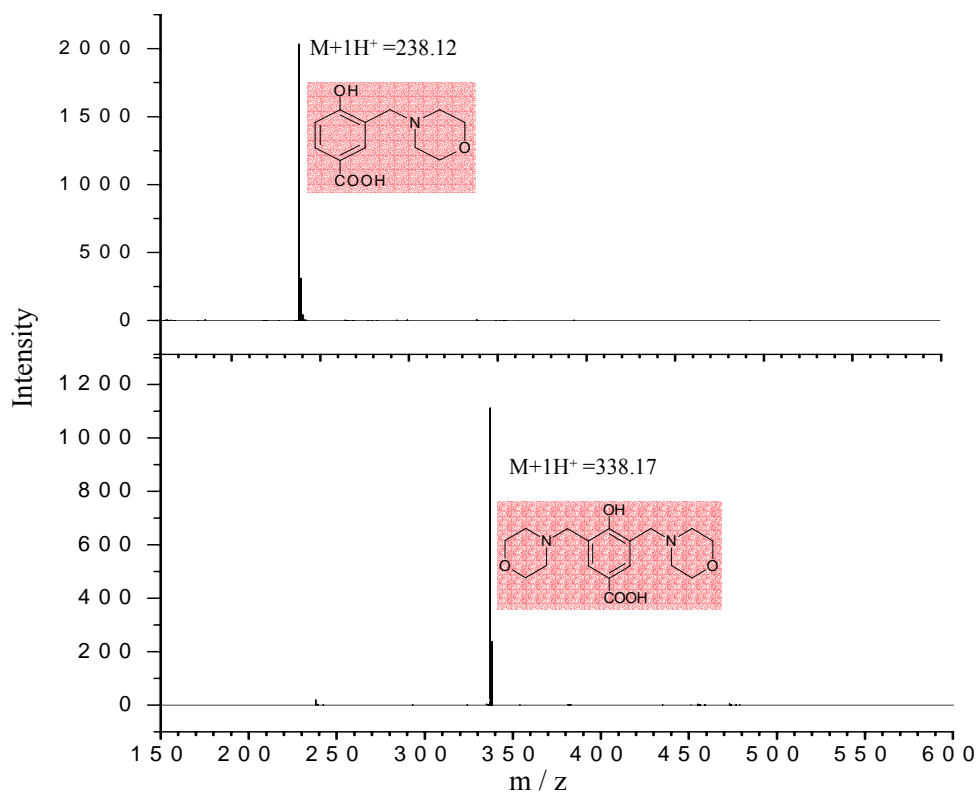
Figure 41. ESI-MS of fractions from compartments 1 and 2.

3.4.2. Instrument setup, materials, and method

A 10 mL stock solution of the sample was prepared by diluting eggwhite with deionized

water to a concentration of 25 mg protein/mL. Figure 42 illustrates the MSWIFT setup

employed in this experiment. A total of five compartments were used: two of them were

the electrode compartments, three of them the separation compartments. The PVA-based

buffering membranes used to separate these compartments were pH 3.0; 5.2; 8.2 and 10,
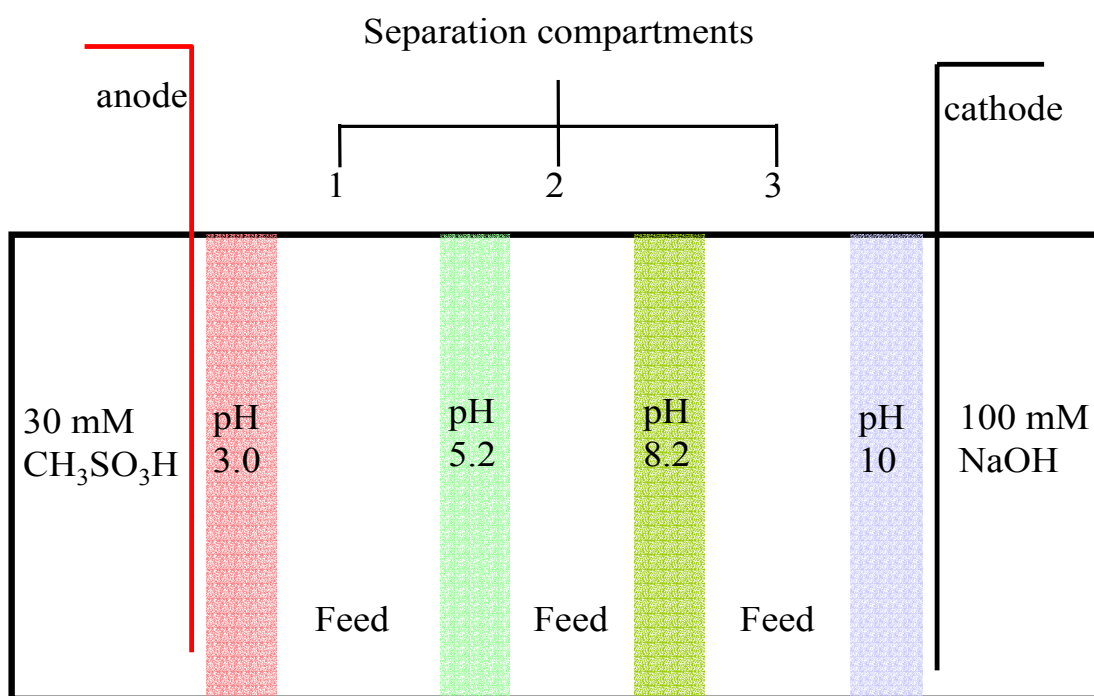
Figure 42. Schematic diagram of the MSWIFT setup for fractionation of egg white
proteins. The sample is loaded into all separation compartments.

their pH values increased from the anode to the cathode. The anode chamber was filled

with a 30 mM MSA solution. All three separation compartments were filled with 200 μL

of the sample solution. A total of 15 mg protein was loaded into the system. Glutamic

acid, 1,3-bis(4-morpholino)-2-*O*-sulfo-propane (BMSP, pI 5.6), 1,3-bis(*N,N*-dimethylamino)-2-*O*-sulfo-propane (BDMASP pI 7.7), were added to compartments 1, 2, and 3, respectively at a concentration of 2 mM. The cathode chamber was filled with a 100 mM sodium hydroxide solution. The separation was run with a constant power of 5 W. After 25 minutes, as the current leveled off at 2 mA, fractions were collected and analyzed by gel isoelectric focusing. Five sample wells of the IEF gel were used: three of them contained the MSWIFT fractions, one the sample feed the last one the protein pI standards. The gel IEF separation was initially run at constant 100 V for 45 minutes, then 250 V for 45 minutes and 500 V for another 30 minutes. After 2 hours of IEF, the gel was stained with Coomassie Brilliant Blue solution (Gradipore, French's Forest, NSW, Australia) and destained on a shaker bath according to the manufacturer's instructions. Finally, the gel was rinsed with DI water and photographed.

3.4.3. Results and discussion

The photograph of the IEF gel is shown in Figure 43. Lanes A, B, and C were used for the MSWIFT fractions from compartments 1, 2, and 3 respectively. The original sample was loaded in Lane D. The rightmost lane was used for the protein pI standards to characterize the pH gradient of the IEF gel. The results show that the MSWIFT could efficiently prefractionate a total of 15 mg of proteins in less than 30 minutes. This is 6 to 50 times faster than what is possible in the present, commercially available small-scale IET devices. The intensity of the protein bands in the fractions was slightly increased compared to the band intensity of the feed, proving that there was protein enrichment.

However, avidin (pI 8.9) which comprises only 0.05 w/w% of the total protein in eggwhite, was not detected.
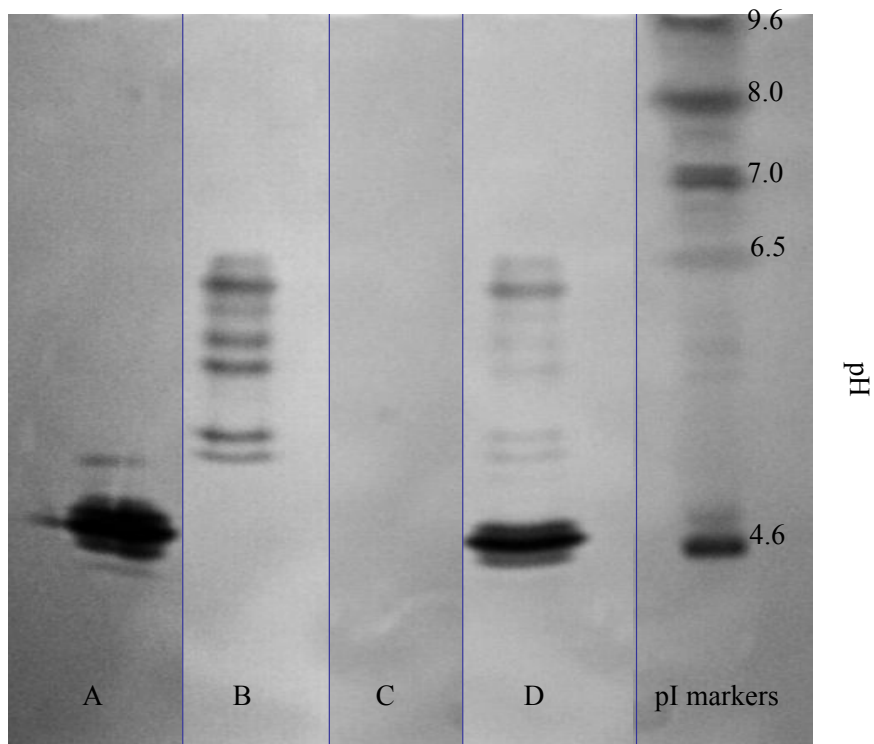
Figure 43. Photograph of the IEF gel used to characterize the MSWIFT fractions. Lanes A, B, and C were loaded with the 25-minute fractions from compartments 1, 2 and 3, respectively. Lane D was loaded with the feed and the rightmost lane was used for the protein pI standards.

3.5. Sample enrichment using the MSWIFT

3.5.1. Background and objectives

In a conventional MCE format, such as the MSWIFT, the separation compartments are arranged serially in between the electrodes. In principle, when equal amounts of sample are loaded into n separation compartments of equal volumes, the target component, focused into one compartment, can be enriched n-fold after the IET process. Moreover, if

the compartment where the sample is trapped has half the volume compared to the rest of the separation chambers, the concentration of the ampholytic sample can be potentially increased by a factor of $2n$-1. The protein enrichment described in Section 3.4 was obvious, but not quantitative. The aim of this experiment was to quantitatively measure the enrichment of aspartic acid one can obtain using the MSWIFT.

3.5.2. Instrument setup, materials, and method

The MSWIFT was set up to have 7 compartments. The first and last compartments were used as the electrode compartments. Five separation compartments were placed in between the electrode chambers. The separation compartment next to the anode had a shorter length than the other separation compartments: it held 100 μL of volume, while the rest of the separation compartments held 200 μL of volume (Figure 44). All wells were separated by PVA-based buffering membranes of pH 2.0; 3.0; 4.9; 6.0; 7.8 and 10.0. 200-μL volumes of a 0.016 mM aspartic acid solution were loaded into separation compartments 2 to 5. pH biasers with pIs 4.2; 5.7; 7.7 and 8.4 were also added into separation compartments 2 to 5, respectively, such that the final concentrations of the isoelectric buffers were 0.5 mM. The pH biasers used did not contain primary amine functional groups [68]. The collected fractions were treated with NDA, and then analyzed by CE, with the UV detector set at 280 nm. All CE runs were carried out in a 50 μm internal diameter fused silica capillary (L_t = 46.5 cm; L_d = 39.5 cm), with a potential of 25 KV, using a 30 mM piperidine/ 10 mM HEPES, pH 10.9 buffer as the background electrolyte. The polarity used was plus-to-minus.

0.16 mM Asp
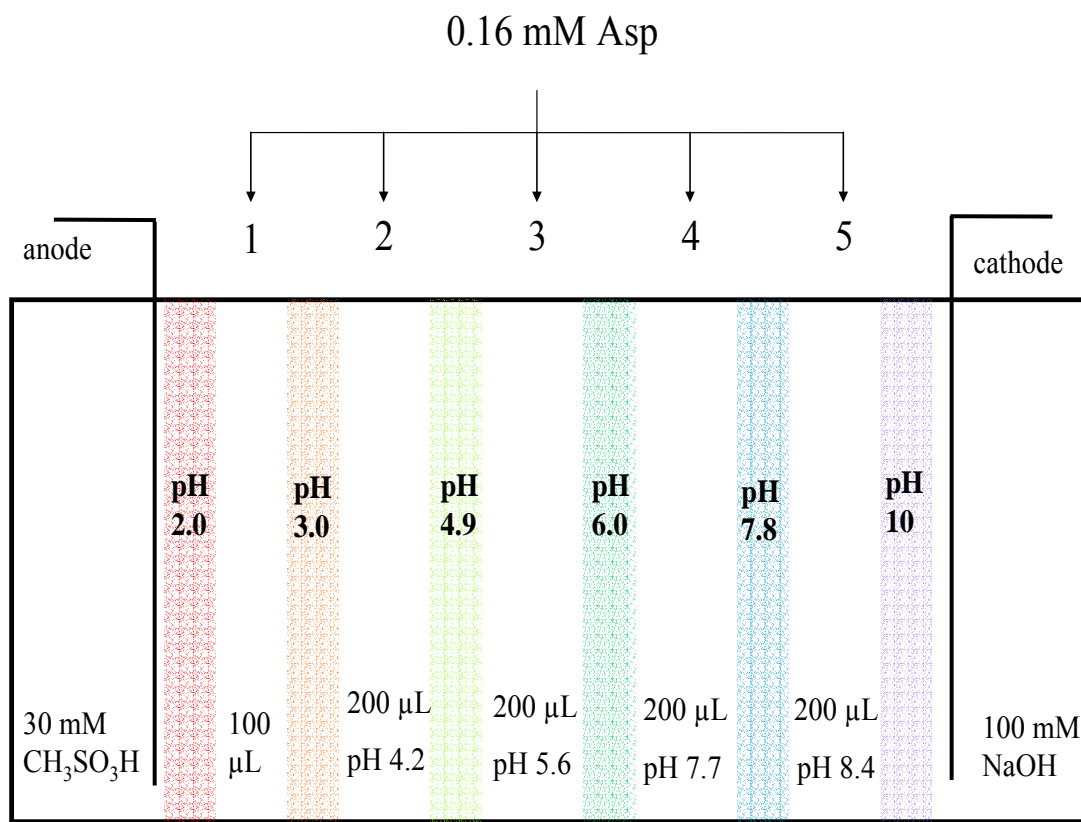
Figure 44. Schematic diagram of the MSWIFT setup for concentration of aspartic acid into compartment 1.

3.5.3. Results and discussion

In this experiment, nine-fold enrichment was expected after IET (the MSWIFT was set up according to the (2*n*-1)-fold enrichment pattern, where, *n* = 5). The CE traces of the fractions obtained from the 100-μL compartments are shown in Figure 45 and the concentration of Asp accumulating in compartment 1 as a function of time is shown in Figure 46. The concentration step was completed in 20 minutes and a 9-fold enrichment of aspartic acid was indeed observed. If higher enrichment of a sample component is required (*e.g.*, low abundance proteins) using this MCE format, two things can be done:

(i) increase the number of separation compartments, n; and/or (ii) decrease the volume of the compartment where the sample is trapped. Both solutions are plagued by physical limitations. When n is increased, the anode-to-cathode distance increases, which leads to the same problems that plague the present-day commercial IET devices. Hence, there is a practical limit for the value for n (commercially available small-scale IET devices such as the ZOOM™ and the IQ^2 have $n_{max} = 7$). Decreasing the compartment volume is also limited due to the available micro-machining techniques and experimental concerns (evaporation during IET).
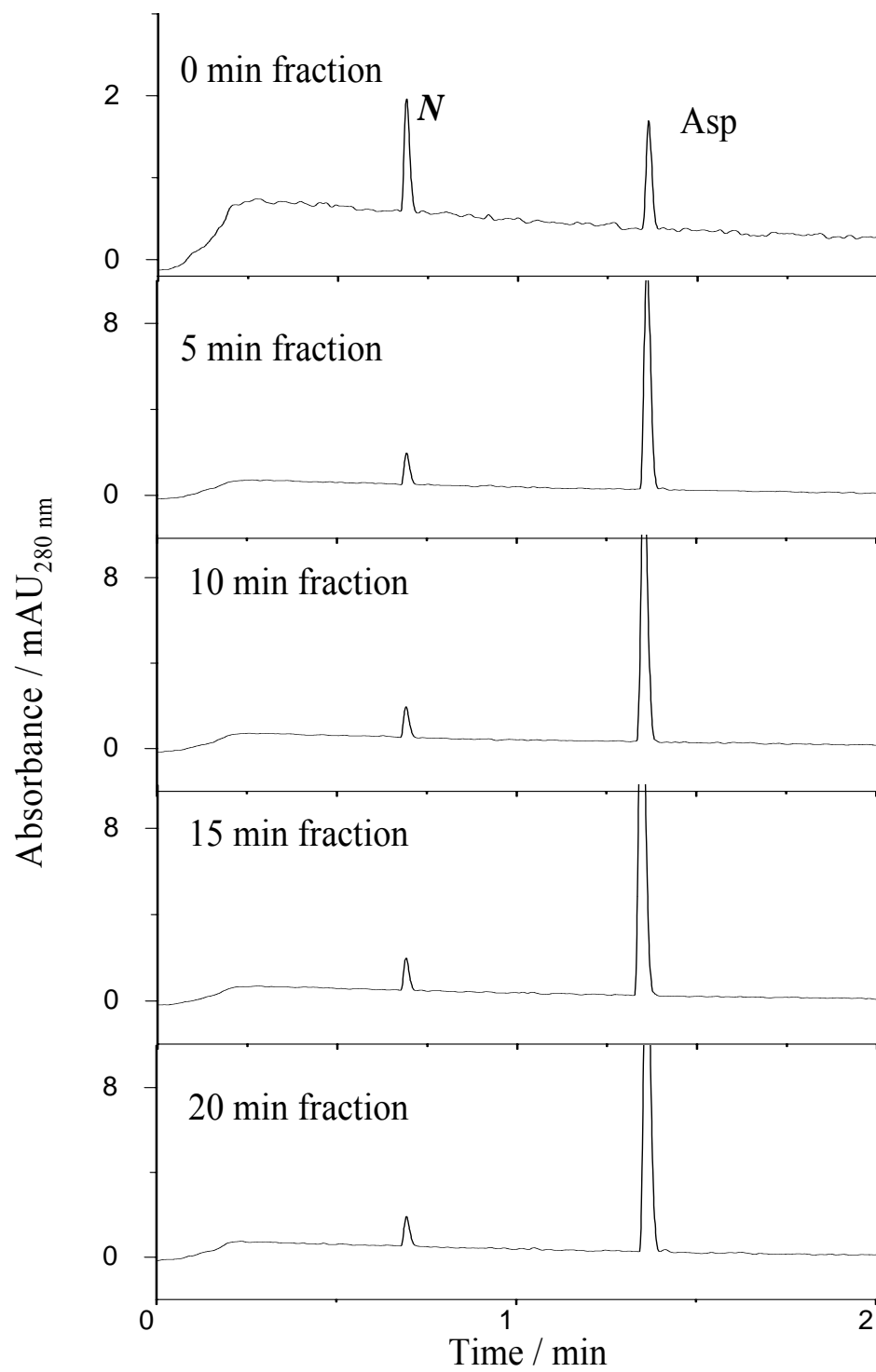
Figure 45. CE analysis of compartment 1 as a function of the separation time.
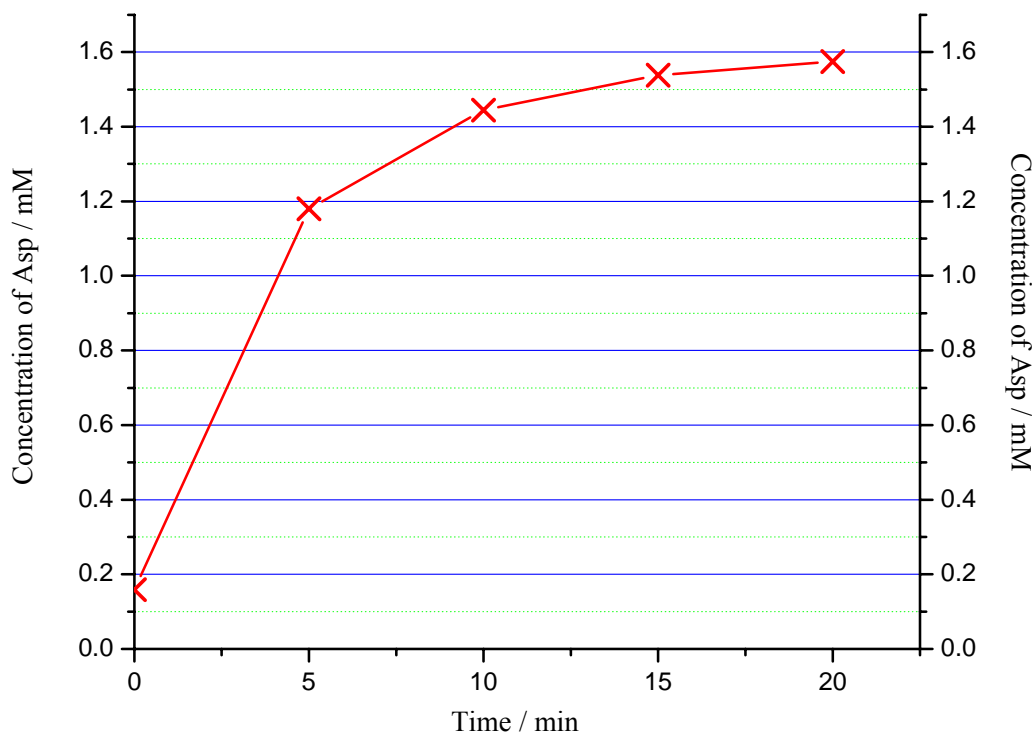
Figure 46. Concentration of Asp as a function of separation time. Aspartic acid was enriched 9-fold in 20 minutes.

3.6. Concluding remarks

Evidently, the MSWIFT provides a solution to the heat dissipation problems that plague the commercially available MCEs. The thin compartments minimize the anode-to-cathode distance and maximize the field strength (up to 1000 Vcm^{-1} has been used in the experiments). The narrow grooves of the compartment provided a 1-mm long heat conduction path from the center to the wall. The high thermal conductivity and high specific heat of alumina (the structural material of the compartments) helped to efficiently dissipate the Joule-heat created by 3 to 5 watts of power in all the experiments. Overall, the MSWIFT presented a fast way to desalt ampholytic samples, fractionate amino acids and peptides, purify isoelectric compounds from a crude sample, and

prefractionate a complex protein sample. However, the design of the device is limited in two important aspects: (i) the number of the fractions (also equal to n) that could be obtained; (ii) only one order of magnitude enrichment could be realized with this system.

4. CONCENTRATION-FRACTIONATION (CONFRAC) DEVICE: IMPROVING THE DETECTION OF LOW ABUNDANCE PROTEINS

4.1. Construction principles

Thus far, no analytical-scale IET system provided a practical solution that sufficiently improved the detection limits for low abundance proteins. The investigation of low abundance proteins including many regulatory proteins and enzymes, is vital in proteomics. While certain groups [69-75] reported protein enrichment using chromatographic methods, they created other problems including large amounts of salts introduced during elution, and protein loss due to adsorption on the chromatographic stationary phase. Additional desalting steps were required for these fractions before performing 2DE and MS experiments and dilution brought about by these extra processes defeated the purpose of preconcentration. In prospect, conventional chromatographic techniques can selectively enrich a particular group of proteins, but do not provide a global collection of the proteome of an organism. A month ago, Righetti *et al*. published an affinity chromatographic method that might provide global protein enrichment [76].

A possible solution to the problem of detecting low abundance proteins could come from the creation of an IET system that can: (i) process a sufficiently large volume of sample; (ii) isolate, trap and concentrate the minor components of the sample into a small-volume collection compartment (*e.g.*, if the target component from a 10 mL sample is isolated into a 0.1-mL collection chamber, the component is enriched 100-fold). Therefore, in this system, the magnitude of enrichment depends on the volume of the available sample. In

principle, as long as there is a sufficiently large volume of sample, the proposed system can concentrate a component until its solubility limit is reached.

Such a system can be realized by modifying the MSWIFT. By replacing one or more of the open separation compartments of MSWIFT by closed compartments that have an inlet and an outlet to facilitate the flow (or recirculation) of a sample solution from an external reservoir through the compartments, and having one small volume reservoir (*e.g.*, 100-µL) where the liquid is stagnant, one could trap and enrich a target ampholyte in the small-volume chamber. The drawback of this format is that the number of fractions that can be collected, *n*, is limited, unless the penalties associated with a large anode-to-cathode distance are accepted. However, if a system were created in which: (i) the sample is allowed to flow through two channels; (ii) *n* sample collection compartments are placed side by side and positioned in-between and orthogonal to the flow-through channels; and (iii) the electrode compartments are placed outward, adjacent to each of the flow-through channels, then the anode-to-cathode distance could be kept small and it would be independent of *n*. The collection compartments and the flow-through channels would be separated by buffering membranes, just as in other IET systems (Figure 47). This design could eliminate the limitations of the present-day IET devices.

4.2. A thought-experiment using a hypothetical ConFrac system

In Figure 47, a hypothetical ConFrac system is shown. A feed solution of volume *V* is placed in a sample reservoir. The two flow-through channels are labeled lower and upper flow-through channels. In between them there are four collection compartments (*n* = 4),

each compartment holding a volume of m, such that $V/m \geq 50$. The collection

compartments are physically isolated from each other, and are interfaced to the flow-

through channels by buffering membranes of selected pH values. The outer electrode
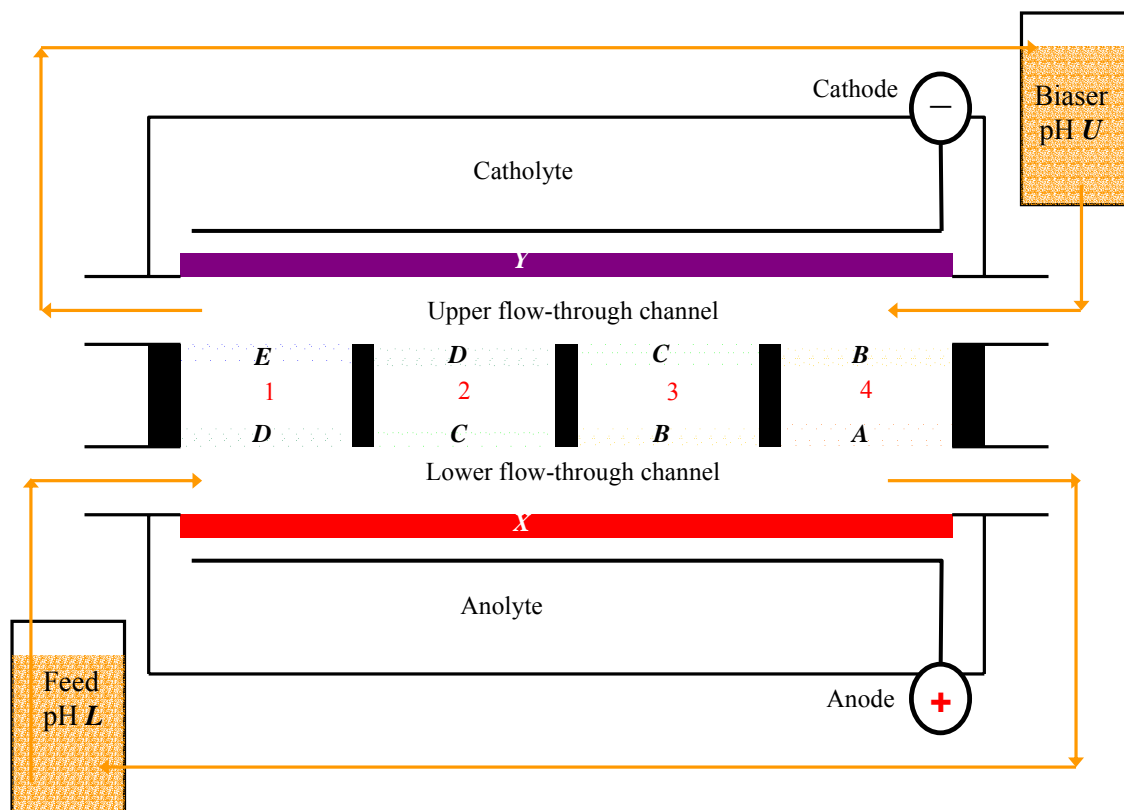
Figure 47. A hypothetical ConFrac setup. Individual collection compartments are labeled 1, 2, 3 and 4.

compartments are also separated from the flow-through channels by buffering

membranes. The buffering membranes used to separate the 4 collection compartments

from the lower flow-through channel buffer at pH A, B, C, and D, where, $D > C > B > A$.

The membranes are arranged in the order of decreasing pH from left to right. The

buffering membranes interfacing the collection compartments and the upper flow-through

channel have pH values of E, D, C, and B, where $E > D$. These buffering membranes are

also arranged in the order of decreasing pH from left to right, such that each collection

compartment is bracketed by lower-side/upper-side buffering membranes with pH values

of: D/E, C/D, B/C, and A/B. The anode compartment is separated from the lower flow-

through channel by a buffering membrane of pH X, where $X < A$. The cathode

compartment is separated from the upper flow-through channel by a buffering membrane

of pH Y, where $Y > E$. To provide initial conductivity, a salt solution with a very low

concentration is loaded into each collection compartment. The sample solution contains

an isoelectric buffer setting the pH to a value of L, where $A > L > X$, and is flowed

through the lower channel from left to right, and recirculated back to its reservoir. An

isoelectric buffer solution with a pH value of U, where $Y > U > E$, is flowed through the

upper channel and recirculated back to its respective reservoir: the direction of its flow is

opposite to that of the flow in the lower flow-through channel. The anolyte and catholyte

are placed into the anode and cathode compartments and the respective reservoirs, and

are recirculated. When an electric potential is applied, separation takes place in two pH

gradients: the first pH gradient is perpendicular to the electric field; the second pH

gradient is parallel to the electric field. In the early stages of IET, the salt components

migrate into the respective electrode compartments, then the trapping and concentration

of the ampholytic sample components begin. At the end of the run, components with pI

values between X and A, remain in the lower feed stream; components with pI values

between E and Y become trapped in the upper stream. Components with pI values

between A and E, are fractionated, trapped and enriched (V/m)-fold into compartments 1,

2, 3 and 4, respectively. In practical terms, if $X = 2$ and $Y = 12$, then all proteins with pI

values $2 < pI < 12$ can be trapped. If the volume of the sample is 100 mL, and the volume

of each collection chamber is 0.1 mL, $A = 3$, and $E = 11$, then all proteins with pI values between 3 and 11 are trapped and enriched 1000-fold. If the same volume of sample is fed through both the upper and lower flow-through channels (one buffered at a pH between 11 and 12, the other buffered at a pH between 2 and 3), then the enrichment factor becomes 2000-fold. Moreover, if a larger number of fractions with narrower pI ranges are required; n can be increased without increasing the anode-to-cathode distance or reducing the electric field strength.

4.3. Design and manufacture of ConFrac

The concentration and fractionation (ConFrac) device was developed to simultaneously fractionate and enrich ampholytic samples. The next sections describe the structural components that were designed and manufactured to build the ConFrac system.

4.3.1. Flow-through channels, collection compartments and electrode compartments

All elements were designed in ACAD software. Conventional machining was used for each part of the device. Due to limitations of our Machine Shop, the flow-through channels and electrode compartments of the prototype ConFrac were made of poly(vinyl chloride) (PVC), the collection compartments were made of Macor (16% alumina, 45% borosilicate, magnesium oxide and potassium oxide). Macor has a thermal conductivity of 2 $Wm^{-1}K^{-1}$, an order of magnitude better than plastics. The buffering membrane sealing system was the same as in the MSWIFT. 0.080"-wide by 0.60"-long oval windows were created in the middle of the silicon pouches to expose a 0.31 cm^2 area of the buffering membrane to the electric field. To create seals easily, a common housing

accommodated a shared cathode compartment and four individual, parallel sets of electrolyzers (each consisting of a cathode membrane, upper flow-through channel, upper buffering membrane, collection compartment, lower buffering membrane, lower flow-through channel, anode membrane, and anode compartment).
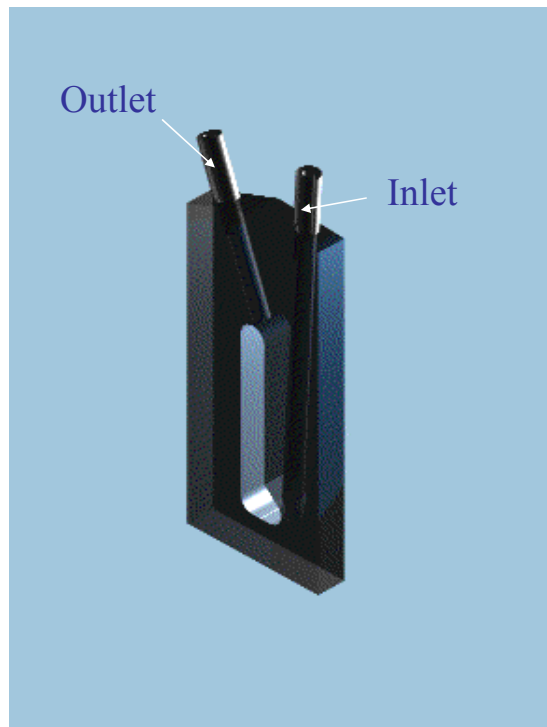
Figure 48. ACAD generated diagram of a microchannel.

Figure 48 shows the ACAD generated model of a flow-through channel. Made of PVC, it is 1.186" high, 0.500" wide and 0.100" thick. It contains an inlet tube with an internal diameter of 1 mm: the tube starts 0.20" above the main structure and goes through the bottom of the oval window at an angle of 5° with respect to the vertical axis. In this configuration, the liquid entering the channel fills up the compartment from the bottom up, which prevents bubble trapping. An outlet tube of 1 mm internal diameter starts at the

top of the oval window and ends 0.15" above the main structure of the channel. The

outlet tube is oriented at an angle of 20º with respect to the inlet tube. Half of the top

surface of the flow-through channel was milled at an angle normal to the inlet tube, the

other half was milled normal to the outlet tube. A total of 8 flow-through channels were

made.
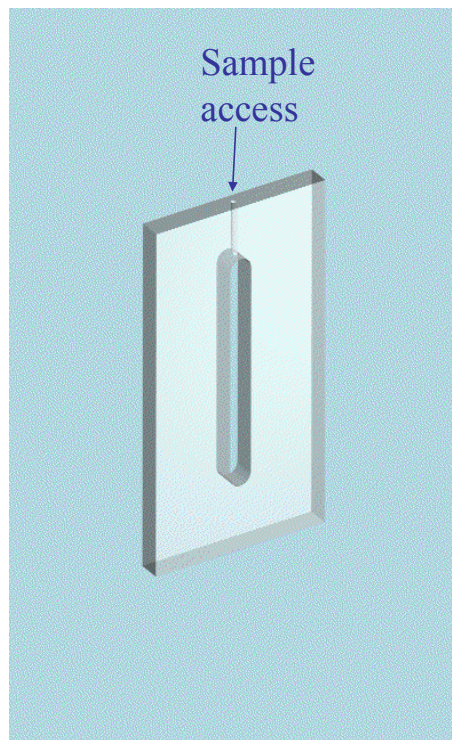
Figure 49. An ACAD model of a collection compartment.

The length, width and window of the Macor collection compartments were machined to

match the dimensions of the silicone pouches. A 0.050"-diameter pinhole was drilled at

the top of the collection compartment to provide access for sample introduction and

collection. An ACAD model for the collection compartment is shown in Figure 49. Four

collection compartments were manufactured.

Figure 50 depicts an ACAD drawing of an anode compartment. The anode compartment

also has a threaded inlet and an outlet hole to accommodate barbed tube connectors with

an internal diameter of 0.100", providing a circulation path for the anolyte. It also has an

anode socket into which a platinum wire was installed. The outlet hole is positioned right

above the anode so that gas formed at the electrode during electrophoresis can be easily

swept out of the compartment. Four anode compartments were fabricated.
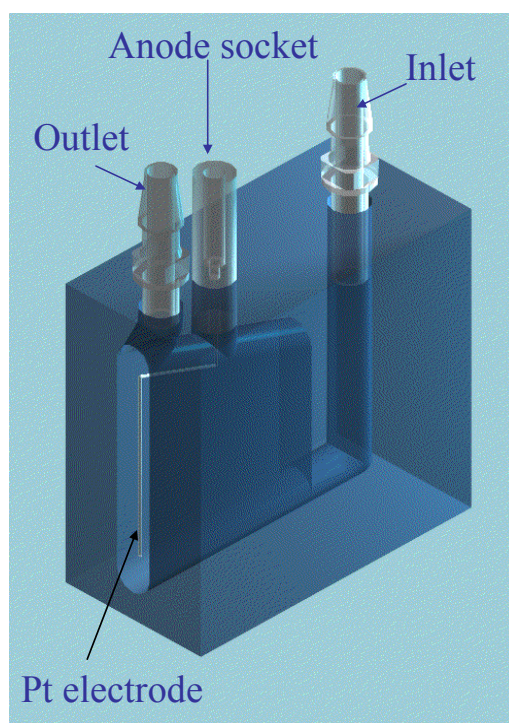
Figure 50. An ACAD generated schematic diagram of an anode compartment used in the
ConFrac.

A common cathode compartment containing a cathode socket, catholyte inlet and outlet

(ID = 0.200") was machined from PVC. It has a sturdy construction to facilitate the

forming of the compression seals.

4.3.2. Main holder

A holder was fabricated to contain the electrode compartments, flow-through channels, collection compartments and membrane-loaded pouches. The main body was precision machined to insure good alignment of the neighboring compartments. Four 0.500" wide and 1.000" deep grooves were milled along a pre-cut 1.500"-long, 4.000"-wide, and 1.375" high, PVC block. All 4 grooves were parallel to each other, and each was separated by a distance of 0.400". The block was reversed such that the grooves opened to the bottom. Then, 1.250" long, 0.500" wide rectangular windows were machined directly above the inverted grooves to provide access for placing the collection compartments, the flow-through channels, membrane-loaded pouches, and, ultimately, the sample. A 0.375"-thick, 3"-long and 4"-wide aluminum plate was machined to serve as the heat sink for the device. It was installed at the bottom of the main holder. To prevent electric current leaks and short circuits, a 1 mm-thick, 1.500"-long, and 4.000"-wide alumina plate was placed in between the main holder and the aluminum base. The anode compartments were used as the end compression pieces to create water-tight seals in the system. Efficient sealing was achieved with the help of four 1.5"-long 0.25"-diameter bolts threaded into to a 4.00" wide, 0.50" long aluminum block that was fixed onto the aluminum base. Figure 51 shows a photograph of an assembled ConFrac.
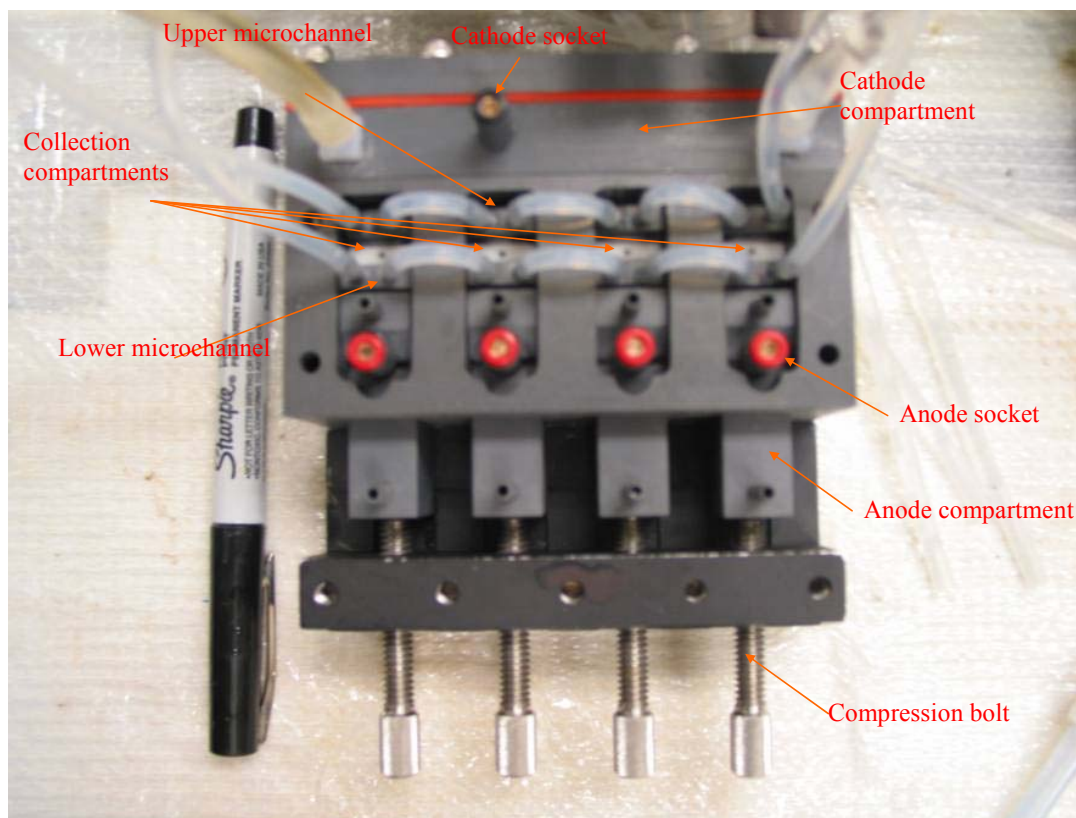
Figure 51. A photograph of the assembled ConFrac components.

The outlet of each flow-through channel was linked to the inlet of the adjacent flow-through channel with a 1 mm-ID silicone tubing. The anolyte, catholyte and the sample streams were recirculated using a peristaltic pump through temperature-controlled, jacketed glass reservoirs custom-made from graduated cylinders to keep all solutions at 5 °C. A digital picture of the whole ConFrac system is shown in Figure 52. Chapter 5 discusses the optimization and characterization of this novel device.
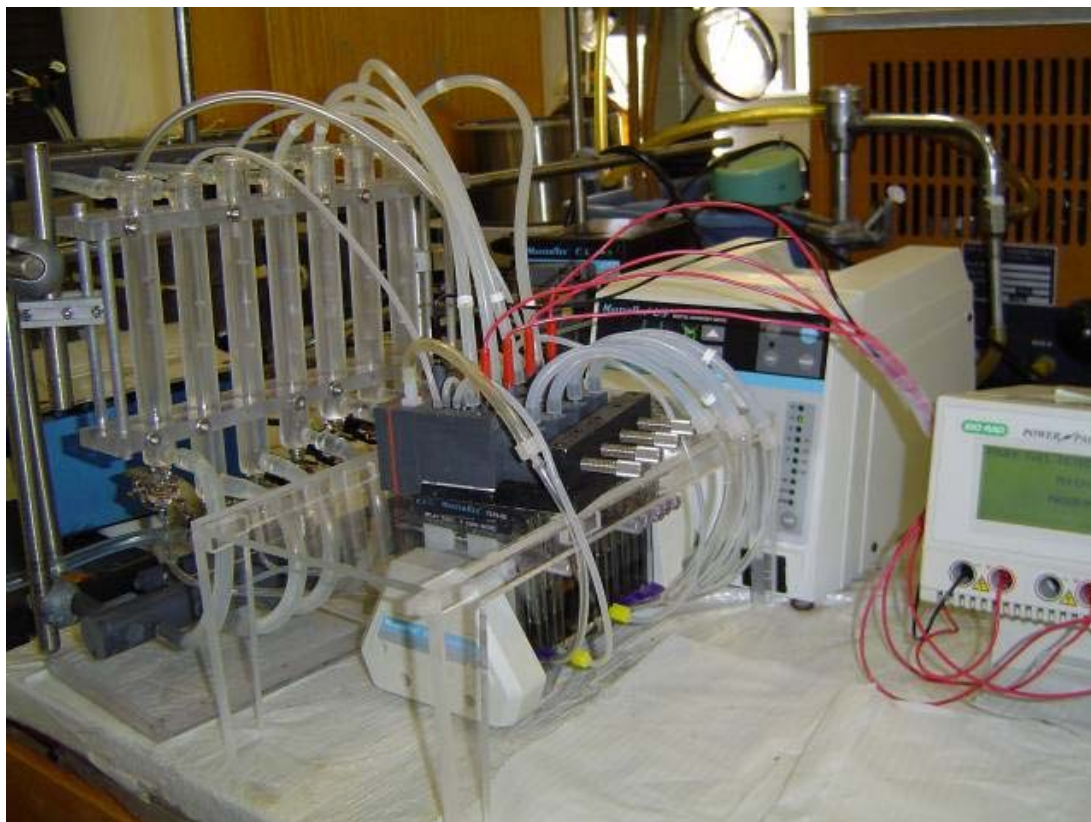
Figure 52. A photograph of ConFrac system.

5. PROBING THE CONFRAC: OPTIMIZATION, CHARACTERIZATION AND APPLICATIONS

5.1. Asymmetrical sample introduction

5.1.1. Background and objectives

The goal of the first experiment was to answer the question: Would the ConFrac operate according to the thought-experiment discussed in Section 4.2? Or would unforeseen events happen during the experiment? Since amino acids served well as test substances for the quantitative characterization of the performance of MSWIFT, they were selected as sample components for the ConFrac as well. The experimental set-up was simple: a measured volume of sample solution was loaded into one of the flow-through channels, the ConFrac was operated in recirculating mode, the components were trapped into different 100-µL collection chambers, and the concentration increases were observed.

5.1.2. Instrument setup, materials, and method

Figure 53 shows a schematic diagram of the ConFrac setup. Four 100-µL collection compartments (labeled 1, 2, 3, and 4, respectively, in the diagram) were used. The anode compartments and the lower flow-through microchannel were interfaced by pH 2-buffering membranes. Collection compartments 1, 2, 3, and 4 were bounded by pairs of buffering membranes with the following pH values: 2.6/3.0, 3.0/4.9, 4.9/7.8, and 7.8/8.2, respectively; the higher pH membrane in each pair faced the upper flow-through microchannel. The upper microchannel and the cathode compartment were separated by a pH 10-buffering membrane. A 100-mL sample stock solution containing 25 µM of Asp, Glu, His, and Carn was prepared. 26.6 mg of iminodiacetic acid was added to the stock

solution (resulting in an IDA concentration of 2 mM) to set the pH at 2.5. A 15 mL

portion of a 30 mM solution of CH_3SO_3H was recirculated through each anode

compartment at a flow rate of 32 mL/min. A 5-mL aliquot was taken from the sample
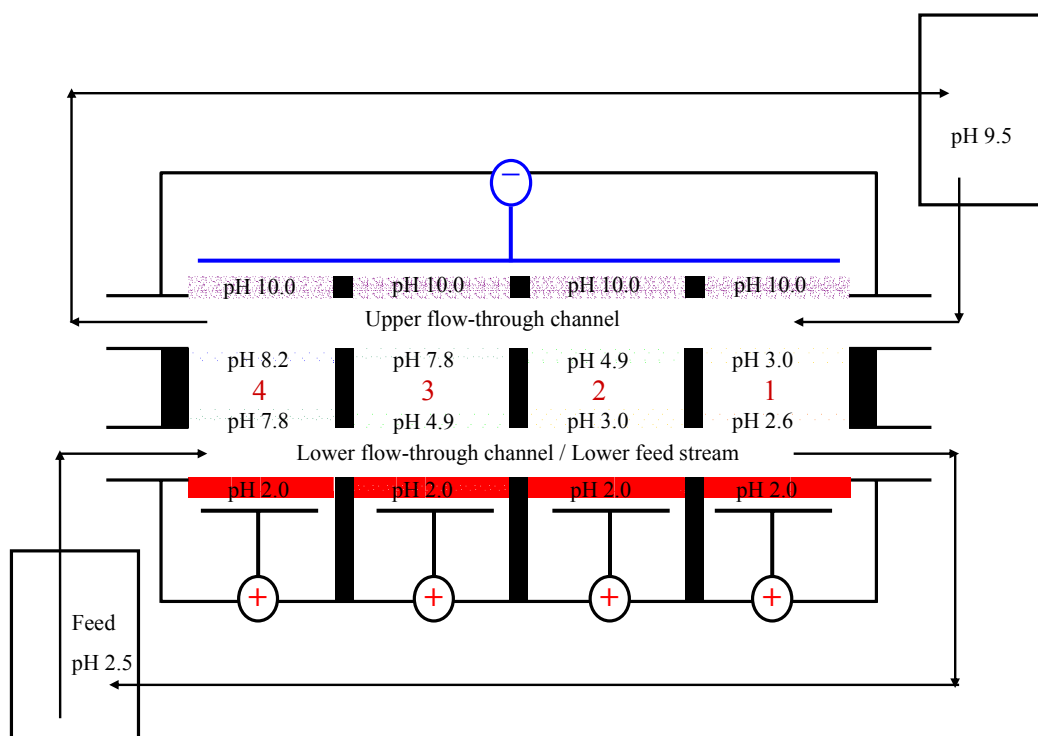
Figure 53. Schematic diagram of the first ConFrac experimental setup. Sample was loaded into the lower flow-through channel.

stock solution, placed into the sample reservoir connected to the lower flow-through

microchannel and recirculated at a flow rate of 8 mL/min. A 2-mL portion of a 1 mM

solution of MeLys (pH 9.5) was filled into the upper flow-through microchannel and its

reservoir, and recirculated at a flow rate of 8 mL/min. A 60 mL portion of a 100 mM

solution of NaOH was recirculated through the cathode compartment at a flow rate of 120

mL/min. The reservoirs were maintained at 10 ºC. A 100 μL portion of a 10 μM solution

of NaCl was loaded in all collection compartments to provide initial conductivity. The separation was run at a constant 2 watts power load for 20 minutes. The compartments were sampled every 5 minutes. The fractions were derivatized with NDA using the procedure described in Section 3.2.2. The NDA-treated fractions were analyzed by CE, with the UV detector wavelength set at 280 nm. All CE runs were carried out in a 50 μm internal diameter fused silica capillary (L_t = 46.5 cm; L_d = 39.5 cm), with a potential of 25 KV, using a 30 mM piperidine / 10 mM HEPES, pH 10.9 buffer as the background electrolyte. The polarity was plus-to-minus.

The procedure described in Section 3.1.2 was used to collect the fractions, except that the NaCl solution, rather than the pH biaser solution was used to fill the collection compartments.

5.1.3. Results and discussion

In the ConFrac, the anode-to-cathode distance was only 2 cm. The sample solution was biased with IDA at a pH of 2.5 to keep the net charge of the sample components in the feed stream positive at all times and insure their ready migration toward the cathode. The CE traces of the fractions obtained from the lower flow-through microchannel (feed stream) are shown in Figure 54. The top panel is the electropherogram of the original sample solution. The 5-minute fraction (second panel) indicated that Carn had completely migrated out of the feed stream; the rest of the components were still detectable, and the depletion rate of Asp was the slowest. The reason for this was that the cathode-bound Carn had four chances to leave the feed stream through the four membranes with pH

values lower than the pI value of Carn. Asp, however, had only one chance to leave the feed stream, because only one membrane had a low enough pH (pH 2.6) to allow its passage toward the cathode. The depletion of the sample components continued until no detectable amounts of amino acids were found in the feed stream resulting, typically, in 20-minutes of runtime. The concentrations of the sample components in the feed stream are plotted as a function of the separation time in Figure 55.
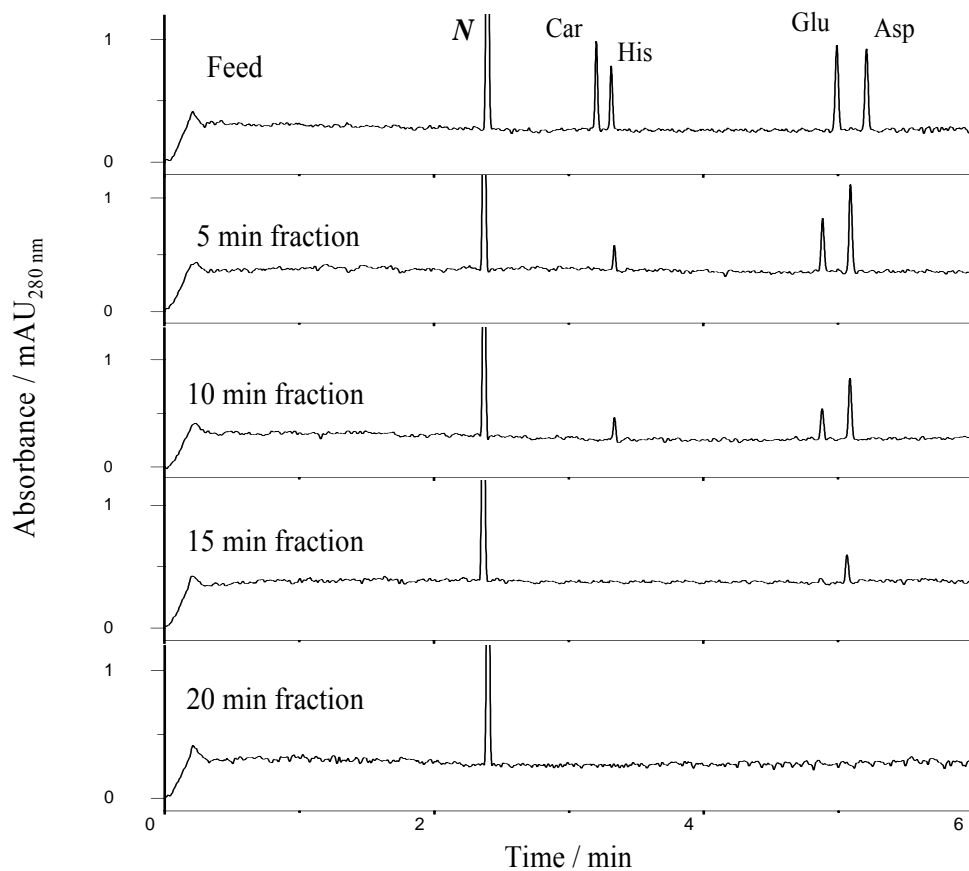
Figure 54. CE analysis of the feed stream.
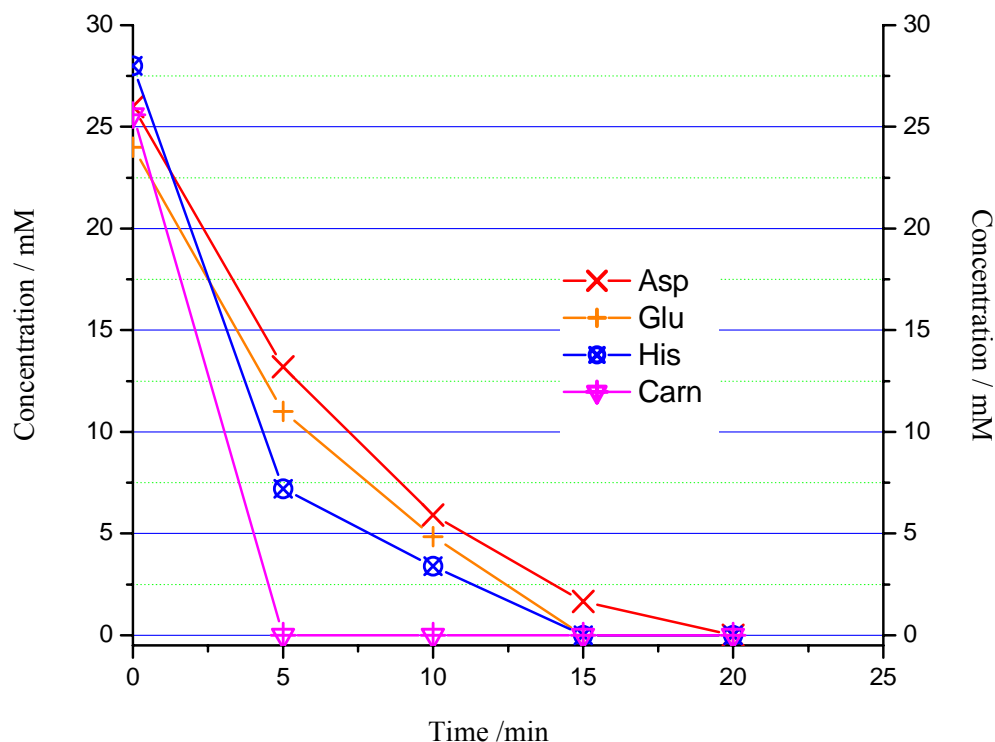
Figure 55. Concentration profile of the sample components in the feed stream.

The experiment was designed to trap Asp, Glu, His, and Carn in collection compartments 1, 2, 3, and 4, respectively. The electropherograms of the fractions collected from compartment 1 are shown in Figure 56. The 5-, 10-, and 15-minute fractions indicated that Asp was indeed concentrated in compartment 1. Transient peaks of glutamic acid were also detected in these fractions. Histidine was found in this compartment only in the 5-minute fraction. The transient peaks confirmed that these amino acids had access to compartment 1 as they were moving toward the cathode during the early stages of IET. The 20-minute fraction shows that only aspartic acid was present in the first collection compartment. At the same time, Glu, His, and Carn were also accumulating in compartments 2, 3, and 4, respectively. Figures 57, 58, and 59 show the respective sets of

CE traces. The concentrations of the separated components were plotted as a function of time in Figure 60. Clearly, simultaneous separation and 50-fold enrichment were observed for the amino acids.

Fractions taken from the solution flowing in the upper microchannel were also investigated. Transient peaks of Glu, His, and Carn were seen in the early stages of electrophoresis. Since the solution in the upper microchannel was buffered at pH 9.5, all sample components that reached the channel became negatively charged and were attracted toward the anode. The amino acids, now recirculating in the upper stream and flowing in the opposite direction with respect to the feed stream, had another opportunity to become trapped in their respective collection compartments. Figure 61 illustrates the events that occurred in the upper stream.
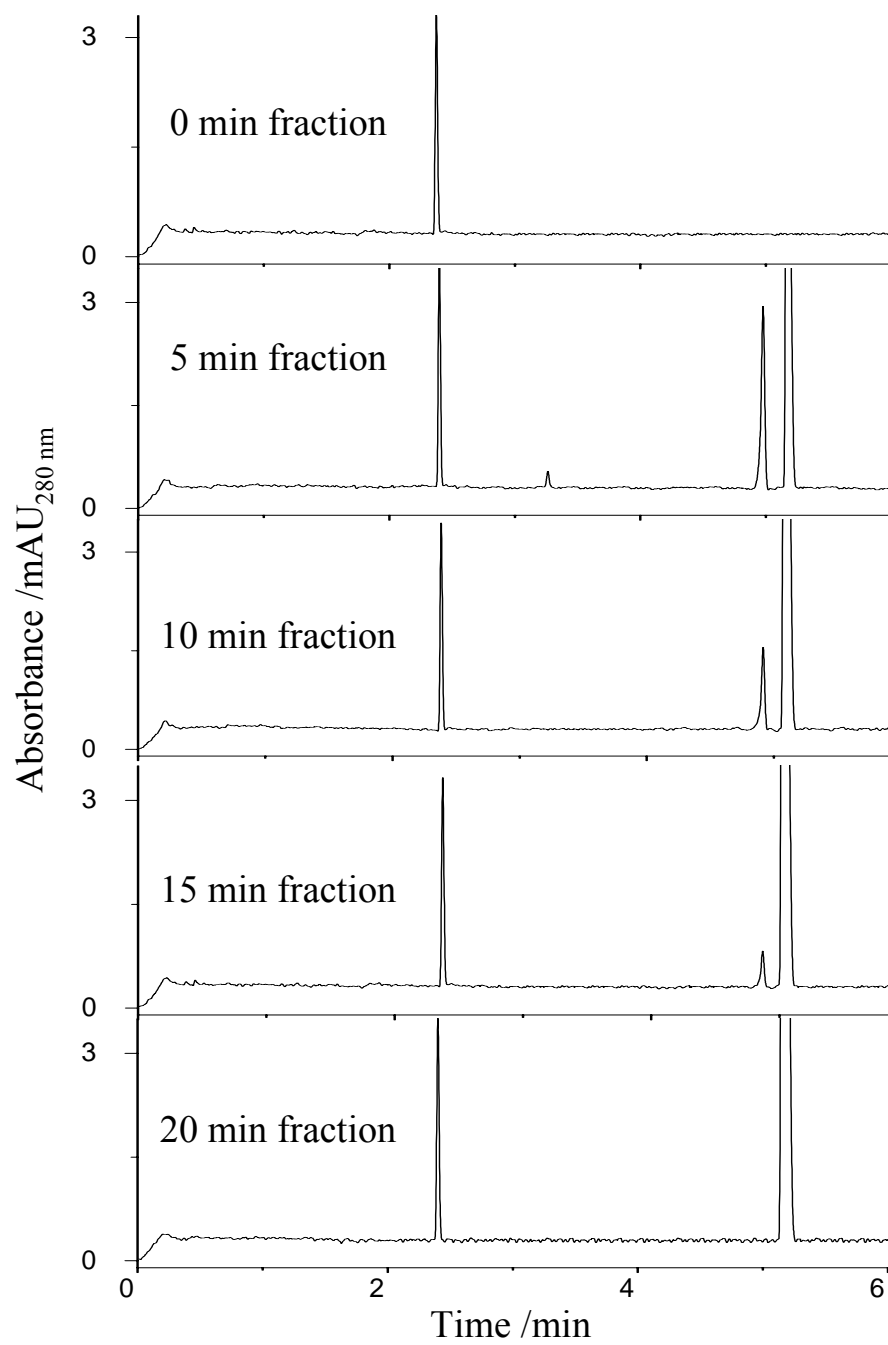
Figure 56. CE analysis of the fractions from collection compartment 1.
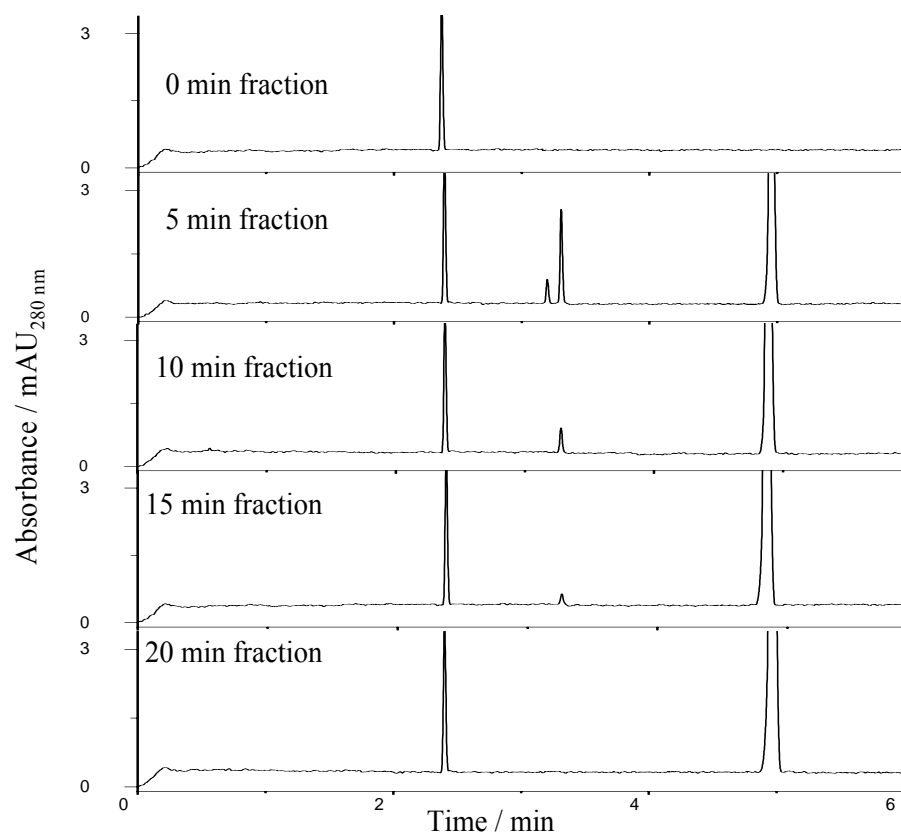
Figure 57. CE analysis of the fractions from collection compartment 2.
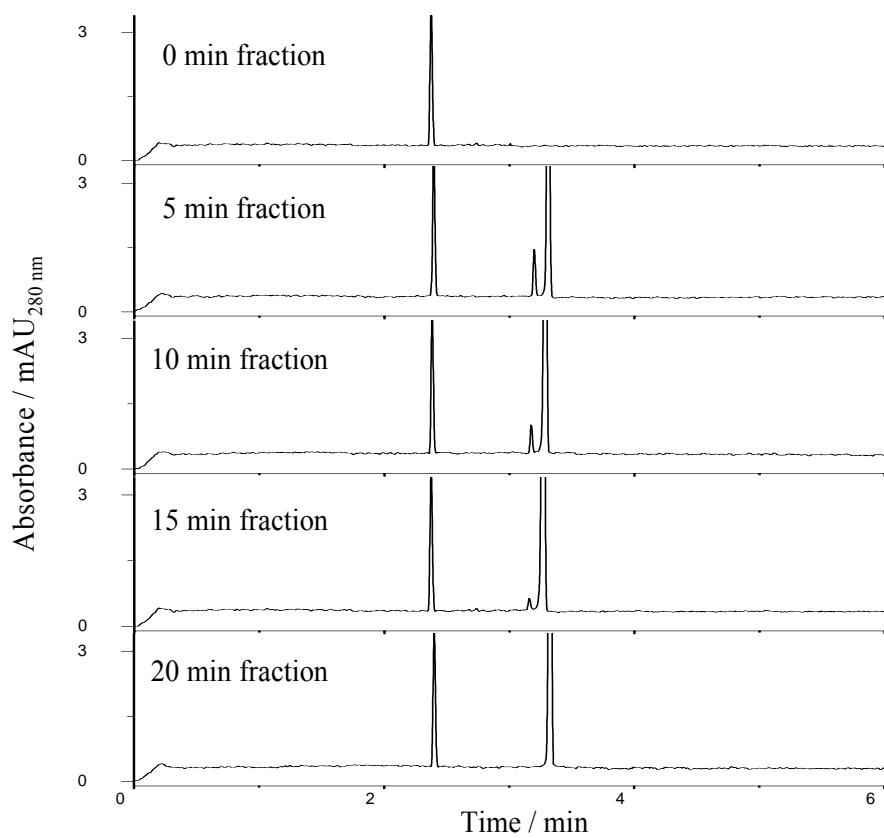
Figure 58. CE analysis of the fractions from collection compartment 3.
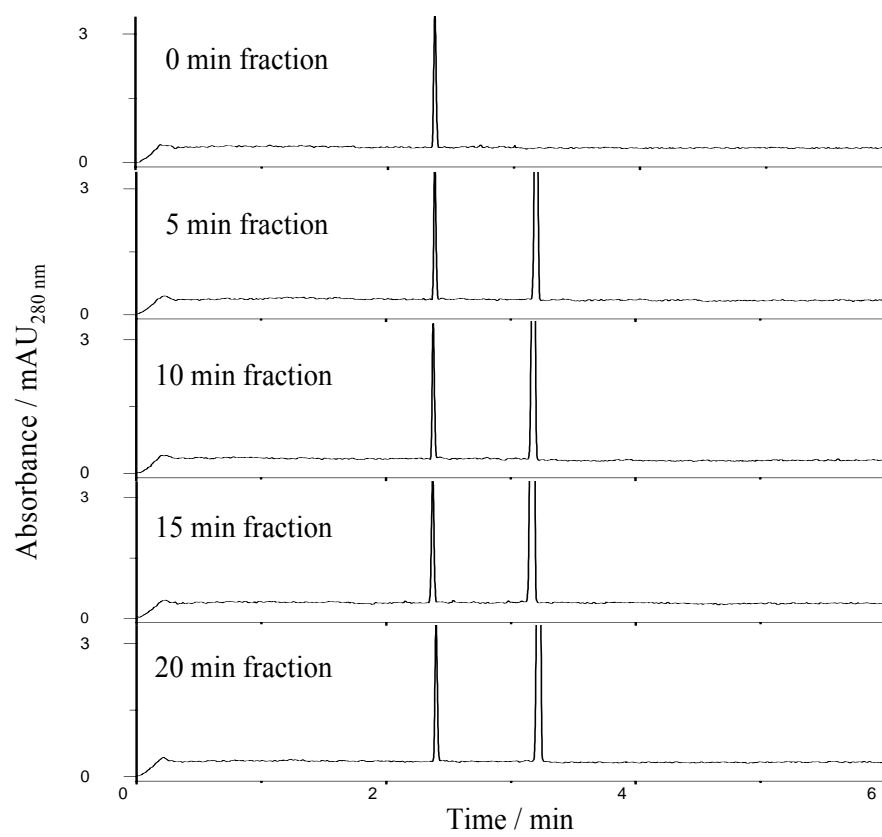
Figure 59. CE analysis of the fractions from collection compartment 4.
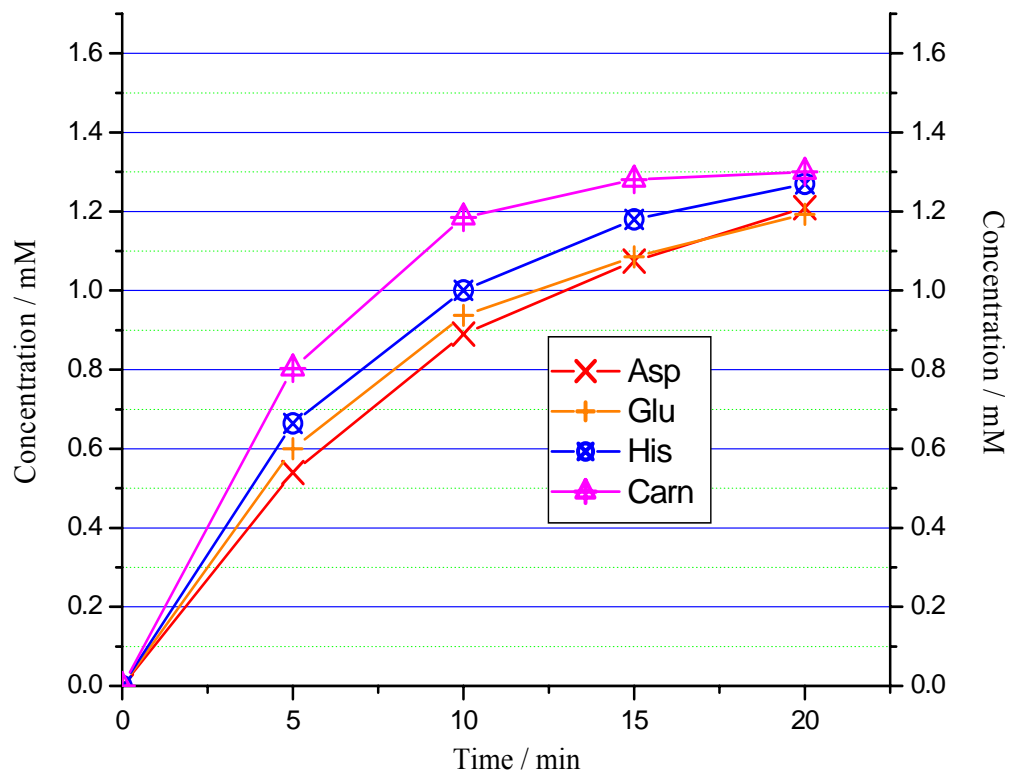
Figure 60. Concentration profile of each sample component in the compartment where they were trapped.
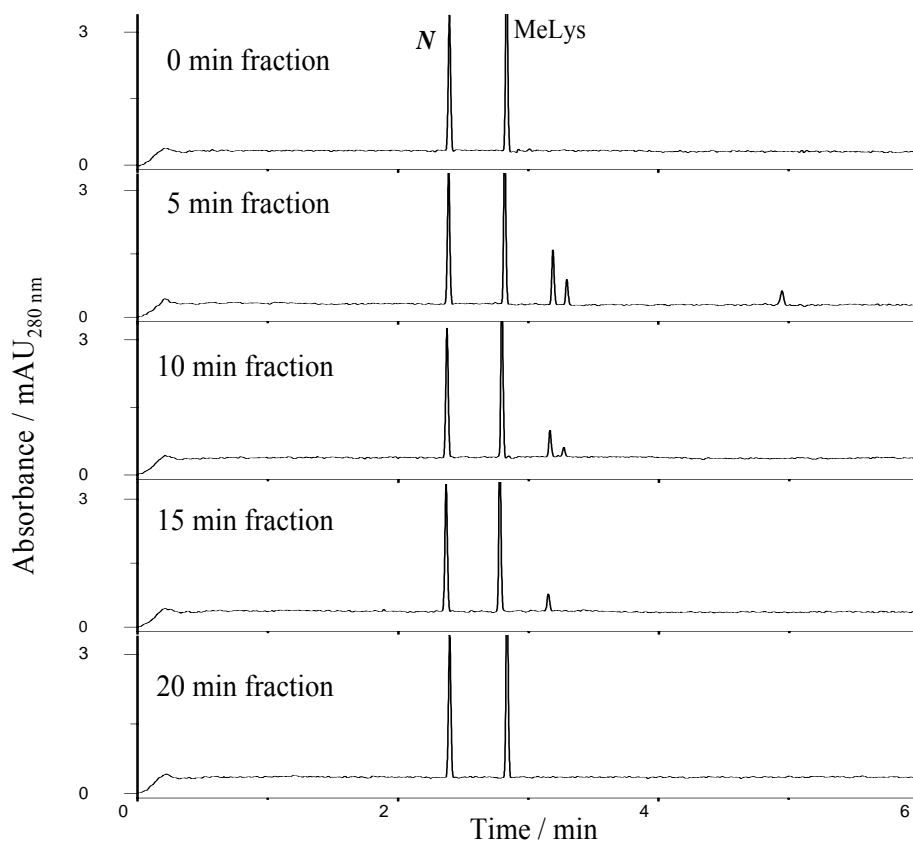
Figure 61. CE analysis of the upper stream.

5.2. Symmetrical sample introduction

5.2.1. Background and objectives

The asymmetric loading of the sample in the previous experiment proved the ability of

the ConFrac to achieve simultaneous separation and concentration. It was interesting to

see if loading the sample in both flow-through channels would enhance the rate of

enrichment. If the rate was increased, then sample introduction in the future should be

done symmetrically.
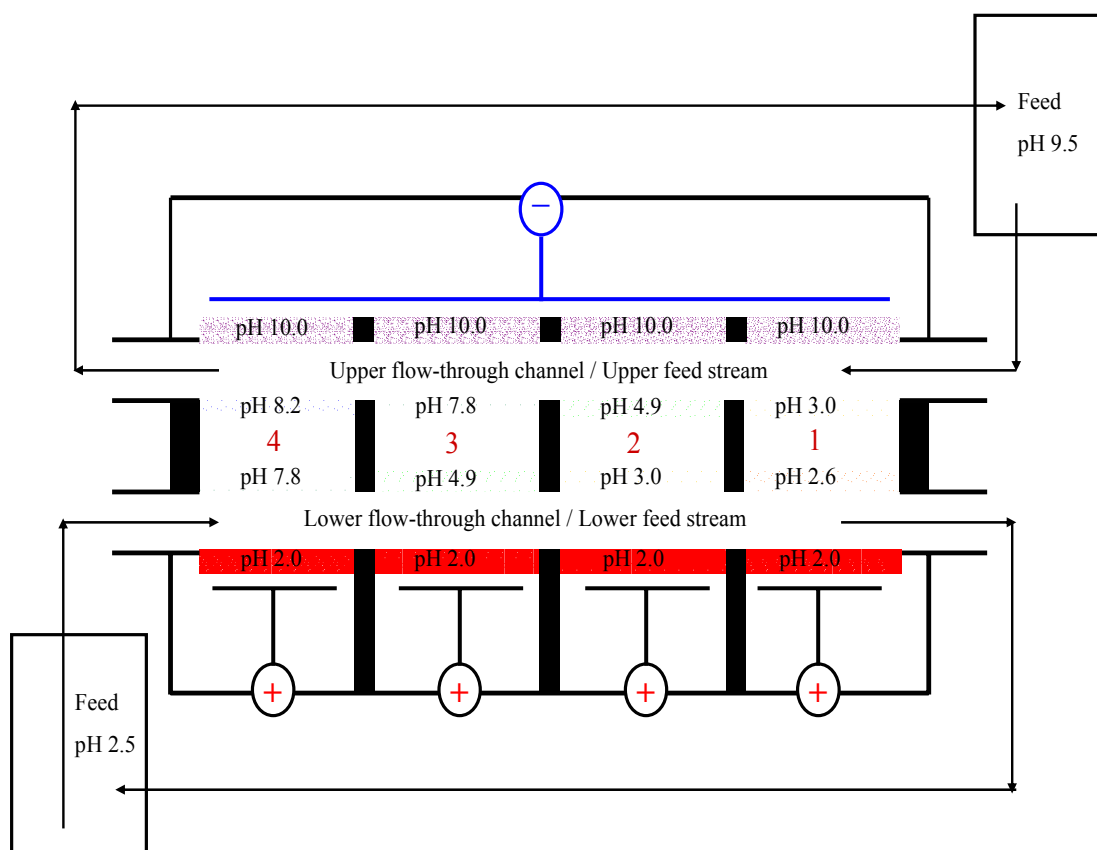
Figure 62. Schematic diagram of the ConFrac experimental setup. Sample was loaded into both the lower and upper channels.

5.2.2. Instrument setup, materials, and method

Figure 62 portrays the schematic diagram of the ConFrac setup. The experimental setup used was the same as in Section 5.1.2, except that two 100-mL sample stock solutions were prepared. The concentrations of the sample components (Asp, Glu, His and Carn) were 15 µM each. A 26.6 mg portion of IDA was added to the first stock solution to buffer it at pH 2.5. A 5 mL aliquot of this stock solution was recirculated in the lower microchannel at a flow rate of 8 mL/min. A 16 mg portion of MeLys was added to the second stock solution to set its pH at 9.5. A 5 mL aliquot of this stock solution was

recirculated through the upper microchannel at a flow rate of 8 mL/min. While the total

sample volume used now was 10 mL, the total amount of sample components remained

the same as in the previous experiment. The running conditions of the ConFrac, the

fraction collection methods, and the characterization of the fractions were the same as

described in Section 5.1.2.

5.2.3. Results and discussion

The CE traces (Figure 63) of the fractions taken from the lower flow-through

microchannel indicated that all sample components have left the feed stream in 15

minutes, 5 minutes shorter than in the previous experiment. Once again, the basic

ampholytes left the lower flow-through microchannel faster than the acidic ampholytes

and Asp remained the slowest component to clear the channel. The time course of the

separation is illustrated in Figure 64 by plotting the concentration of each sample

component as a function of IET time
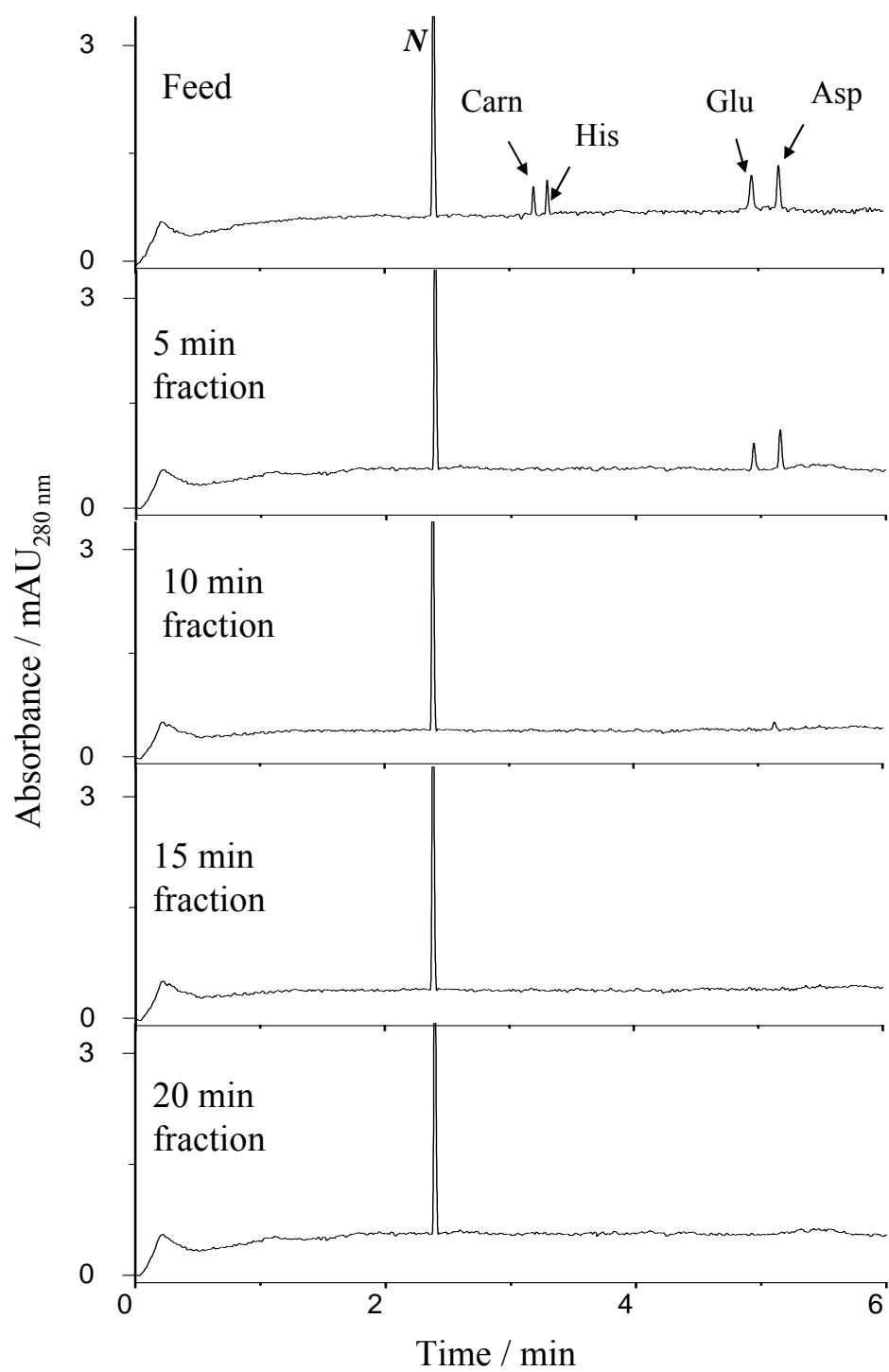
Figure 63. CE analysis of the lower feed stream.

.
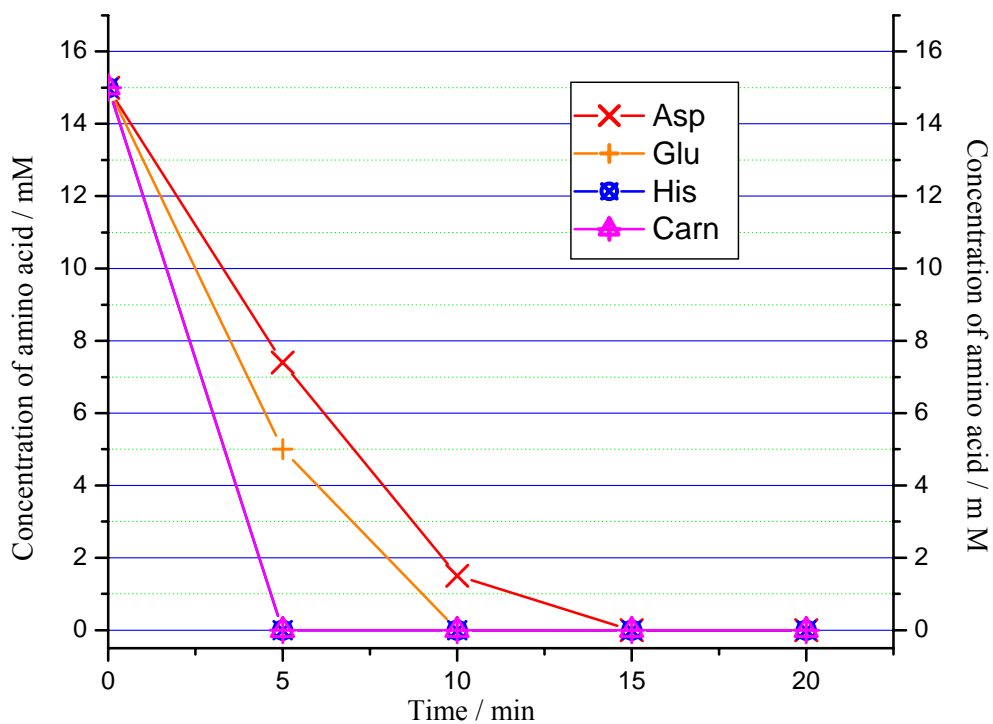
Figure 64. Concentration of each amino acid in the lower feed stream as a function of separation time.

In the upper channel, all sample components were negatively charged (pH was maintained at 9.5). A comparable scenario took place in the upper feed stream, except that this time around, anode-bound Asp had four chances to leave the upper feed stream, because it was exposed to 4 membranes with pH values higher than its pI value. Carn now had the lowest number of opportunities to leave the feed stream, because only one membrane (pH 8.2) allowed its passage toward the anode. Figure 65 shows the CE results and Figure 66 describes the concentration profile for each sample component in the upper microchannel.
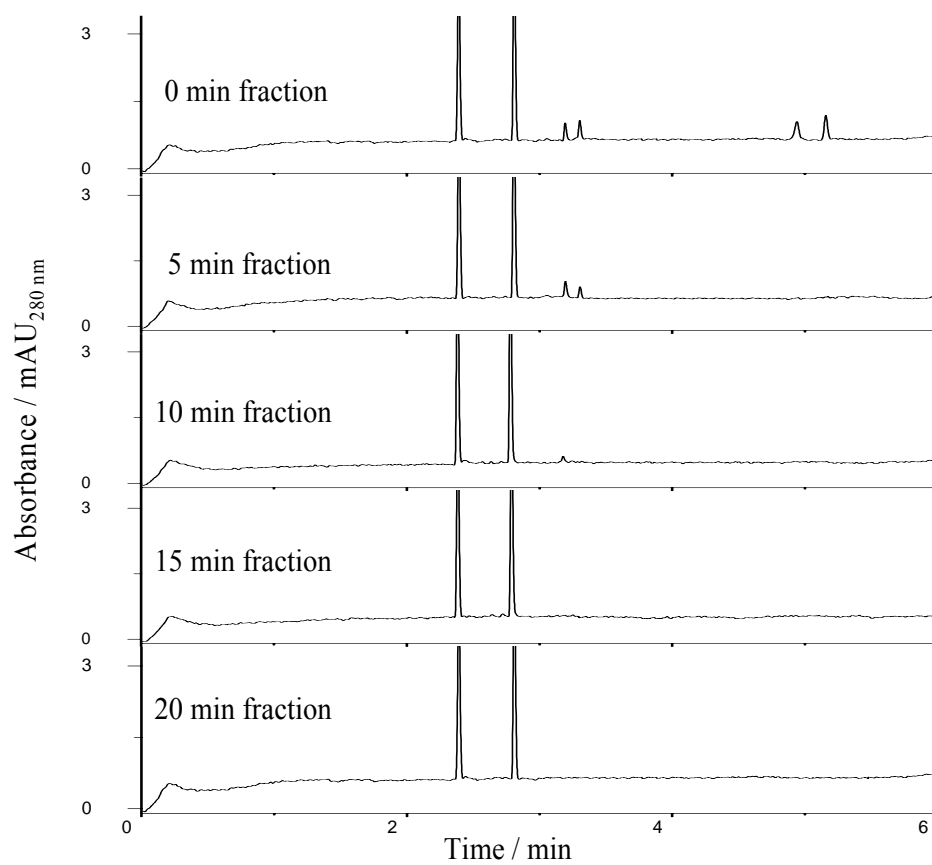
Figure 65. CE analysis of the fractions from the upper feed stream.
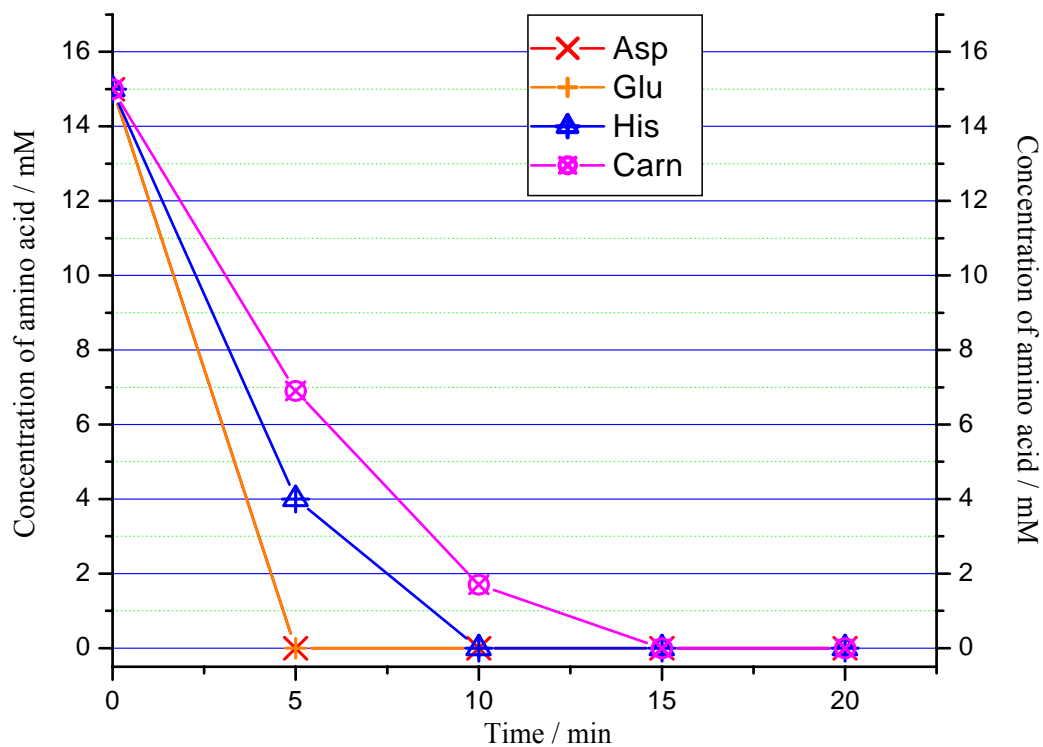
Figure 66. Concentration of each amino acid in the upper feed stream as a function of the separation time.

The CE traces of the fractions obtained from compartments 1, 2, 3, and 4 are shown in Figures 67, 68, 69 and 70, respectively. The rate of trapping for each amino acid is shown in Figure 71. This mode of sample introduction gave similar opportunities to each sample component to focus into the respective collection compartments, thus the rate of trapping for each sample component was almost identical. At 15 minutes, about 100-fold enrichment was observed for each sample component.
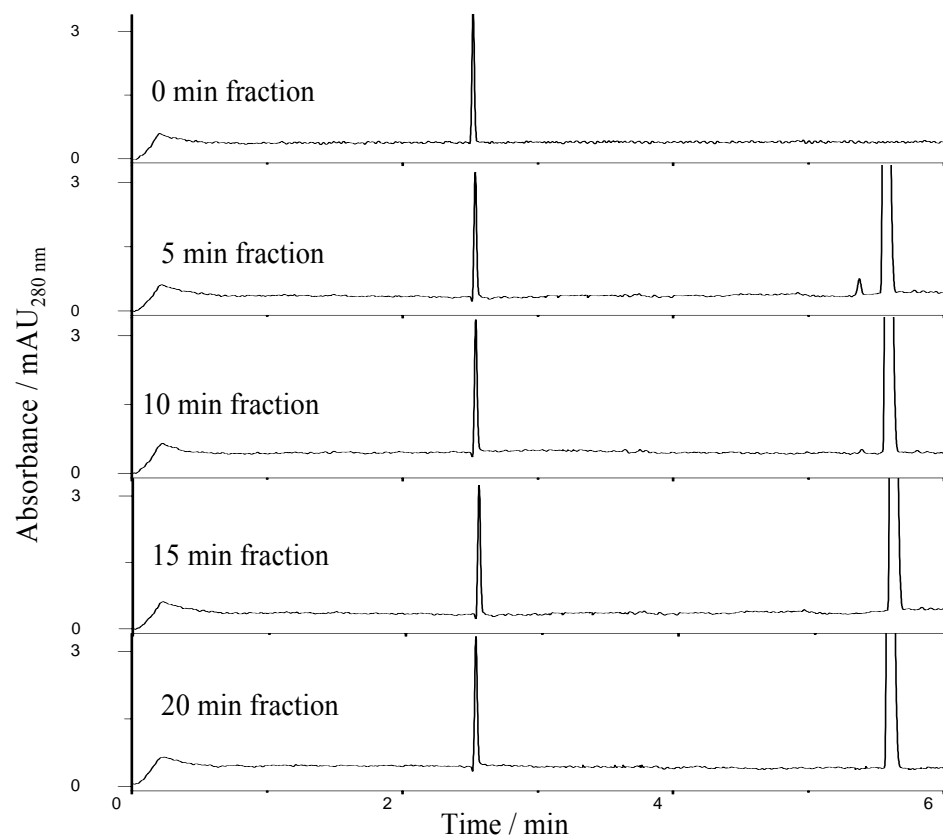
Figure 67. CE analysis of the fractions from collection compartment 1.
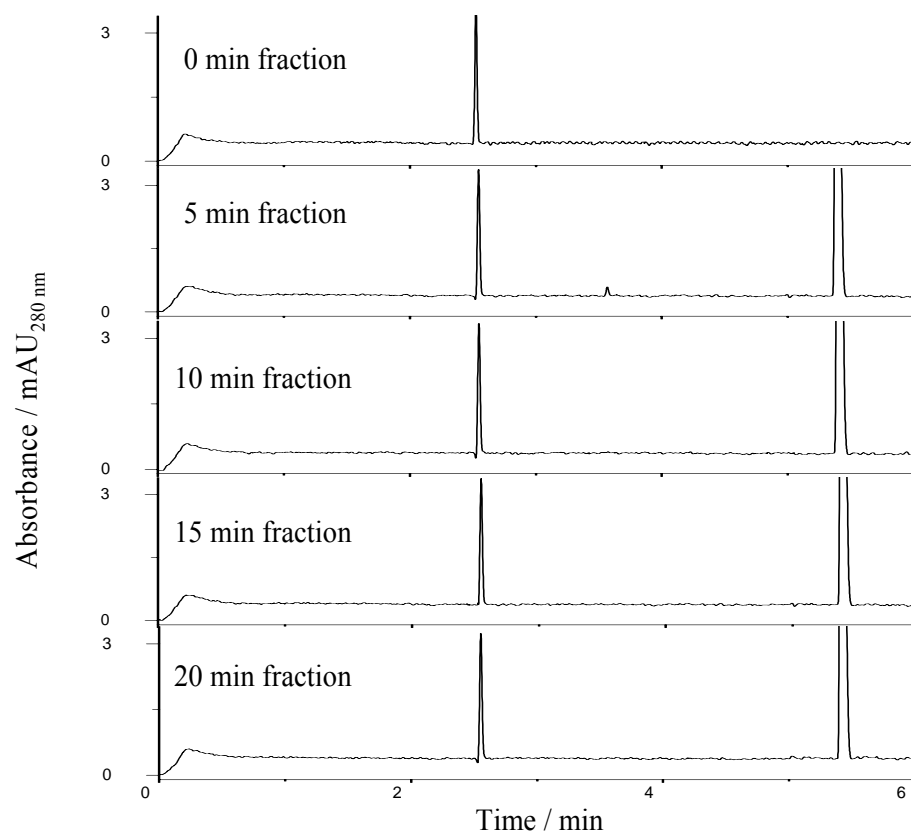
Figure 68. CE analysis of the fractions from collection compartment 2.
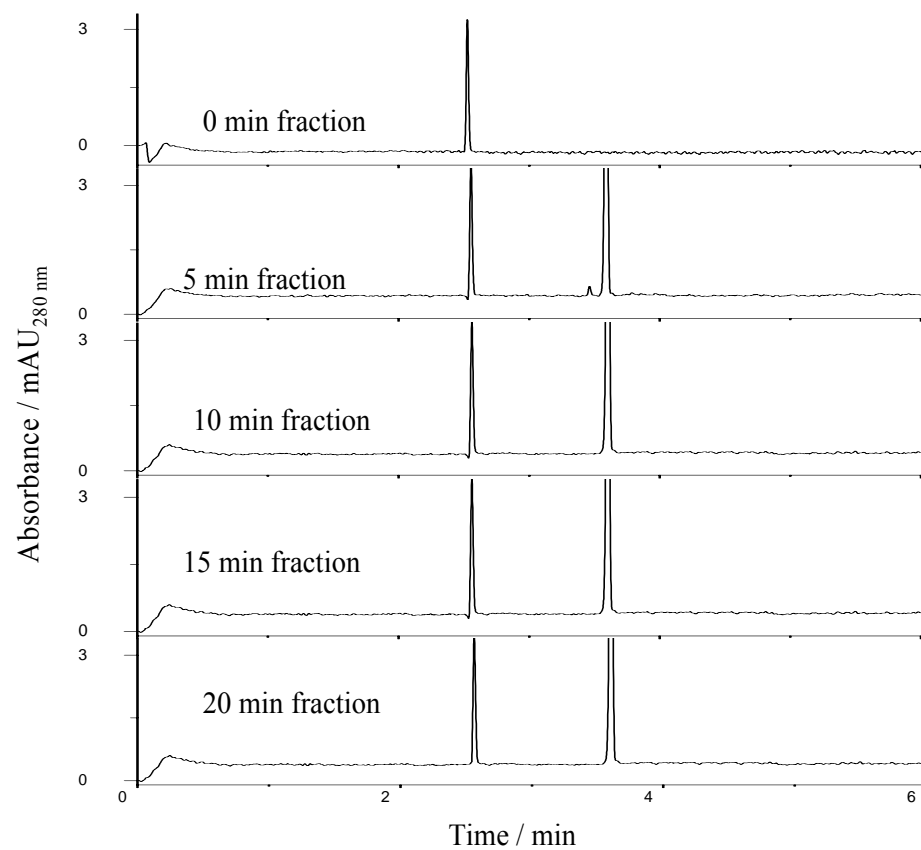
Figure 69. CE analysis of the fractions from collection compartment 3.
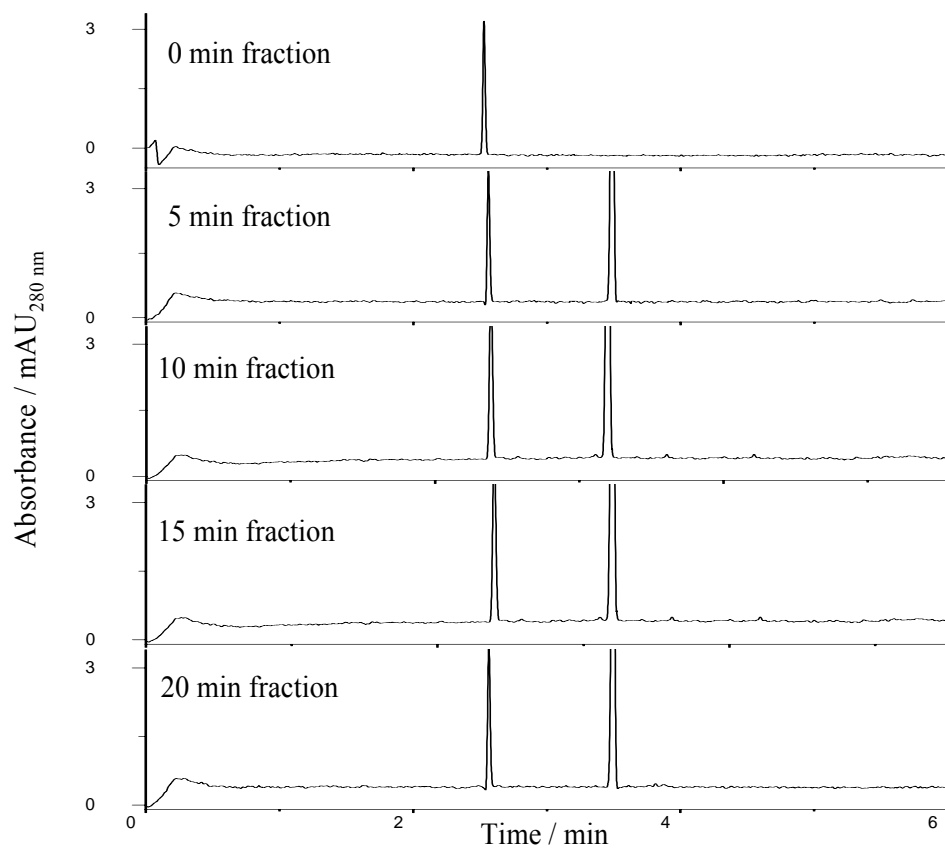
Figure 70. CE analysis of the fractions from collection compartment 4.
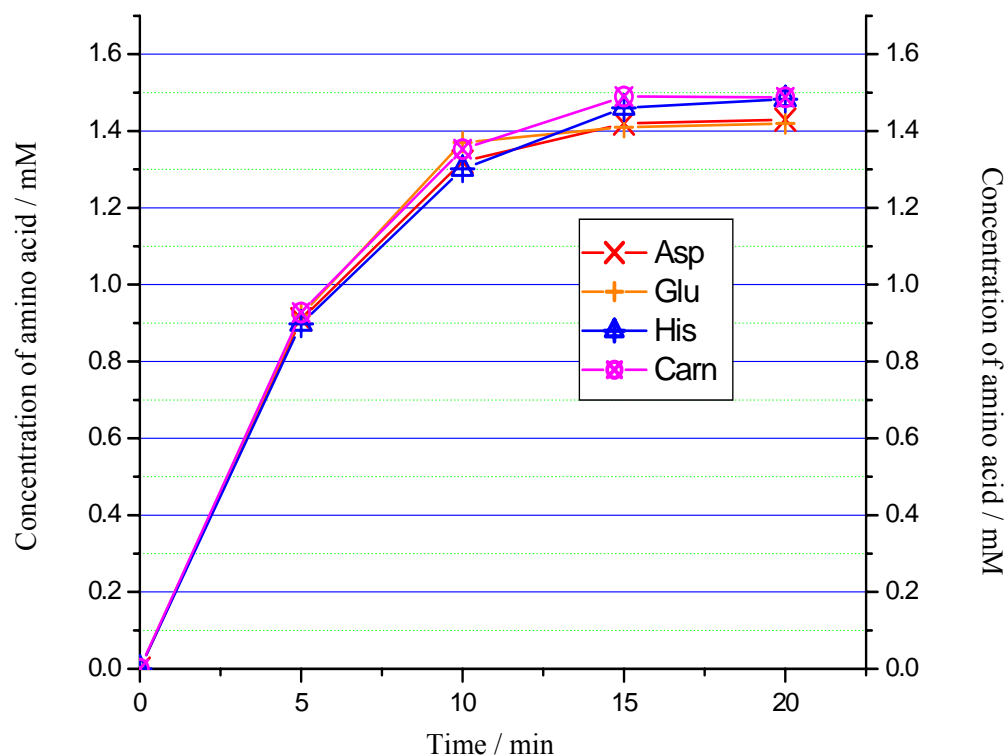
Figure 71. Concentration of the sample components trapped in the respective collection compartments as a function of separation time.

5.3. Flow rate optimization: fine tuning the residence time

5.3.1. Background and objectives

So far, all ConFrac experiments were done with a sample feed flow rate of 8 mL/min. At this flow rate, the temperature of the effluent leaving the electrophoresis compartment was 17 °C. It was interesting to see if the rate of trapping could be further optimized by increasing the residence time for each sample component in the electric field. This can be done by decreasing the feed flow rate, but there is a penalty: the longer the sample solution stays in the electric field, the higher its temperature becomes. The objective of

this experiment was to find the optimum flow rate, a compromise between processing speed and temperature rise.

5.3.2. Instrument setup, materials, and method

The experimental setup described in Section 5.2.2 was used here as well, except that the flow rate was 6 mL/min in the first, 5 mL/min in the second, 4 mL/min in the third and 2 mL/min in the fourth experiment. The analytical procedure described in Section 5.2.2 was used to characterize the collected fractions.

5.3.3. Results and discussion

Effluent temperatures were 30 ºC and 39 ºC, respectively, when the flow rates were 4 mL/min and 2 mL/min. Since the effluent was collected 3 and 6 seconds after it has left the electric field (the effluent tube was 26 cm long, with an internal diameter of 1 mm), the measured effluent temperature values were lower than the actual temperature of the solution in the electric field. Since the pK_a values of the sample components and the buffering species attached to the membranes are temperature dependent, irreproducible results would be obtained. Using 6 mL/min and 5 mL/min flow rates, the effluent temperatures decreased to 22 and 25 ºC, respectively.

The concentration of Asp in the lower feed stream at different flow rates was plotted as a function of electrophoresis time (Figure 72). After 5 minutes of IET, at 5 mL/min flow rate, only 2.5 μM of Asp was left in the feed stream. At 6 mL/min, 4.5 μM of Asp remained, and at 8 mL/min, 7.3 μM of Asp was found in the 5-minute fraction. After 10

minutes of IET, Asp was completely removed from the lower feed stream both at 5- and

6- mL/min.
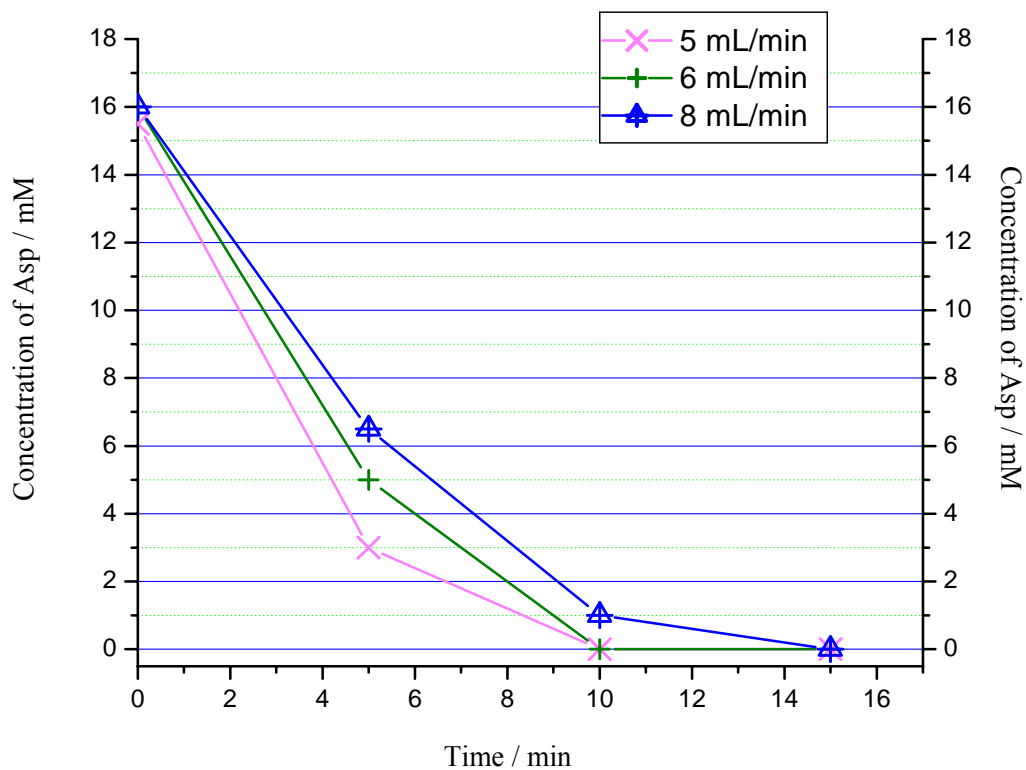
Figure 72. Asp concentration in the lower feed stream at different flow rates.

The trend was the same for Carn in the upper feed stream. The 5-minute fractions showed

that 2 µM, 3.8 µM and 6 µM of Carn was left using the 5, 6, and 8 mL/min feed flow

rates, respectively. Figure 73 shows the graph of the concentration of Carn at different

feed flow rates as a function of the separation time. The results indicate that the 5

mL/min feed flow rate is the best compromise; consequently, the rest of the experiments

were carried out at that flow rate.
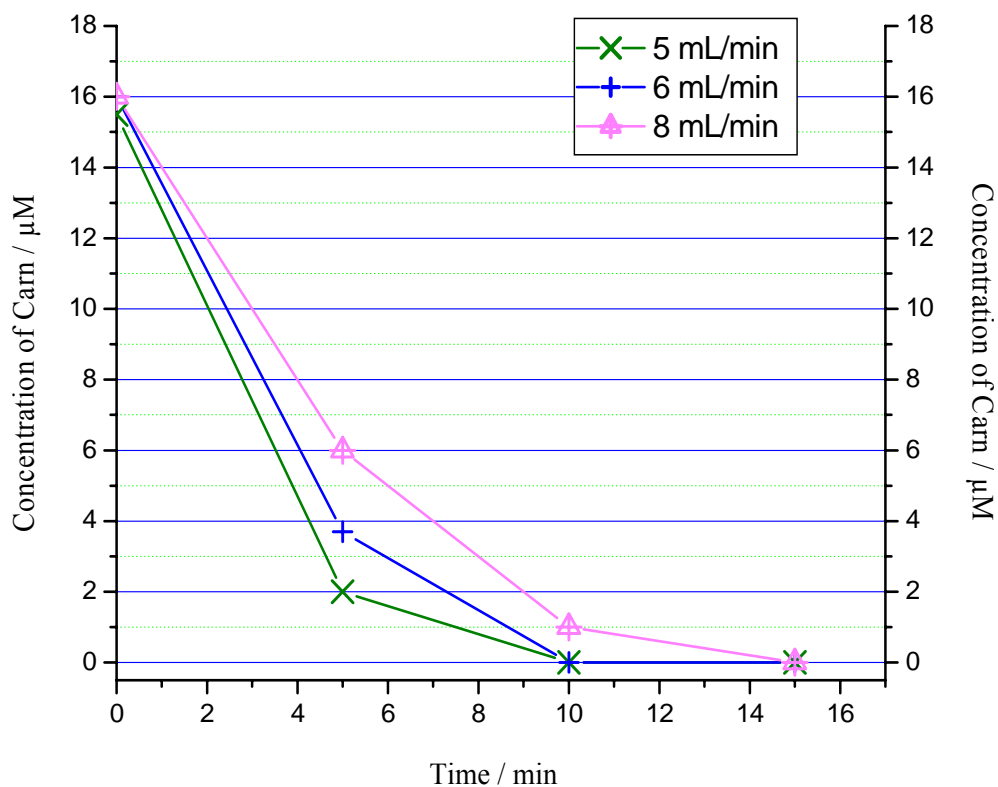
Figure 73. Concentration of Carn in the upper feed stream at different flow rates.

5.4. Pass-by-pass separation

5.4.1. Background and objectives

To this point, all separations were done by recirculating the sample solution. However, the ConFrac can also be operated in the pass-by-pass mode. In this mode, the entire sample volume in the feed reservoirs is pumped through the microchannels and collected in external reservoirs (this constitutes a single pass). After each pass, the effluent can be sampled and characterized. The passes are then repeated until the IET process is deemed complete. The rate of disappearance of the components from the feed solution and their

rate of enrichment in the collection compartments can then be represented by plotting the sample concentration as a function of the number of passes.
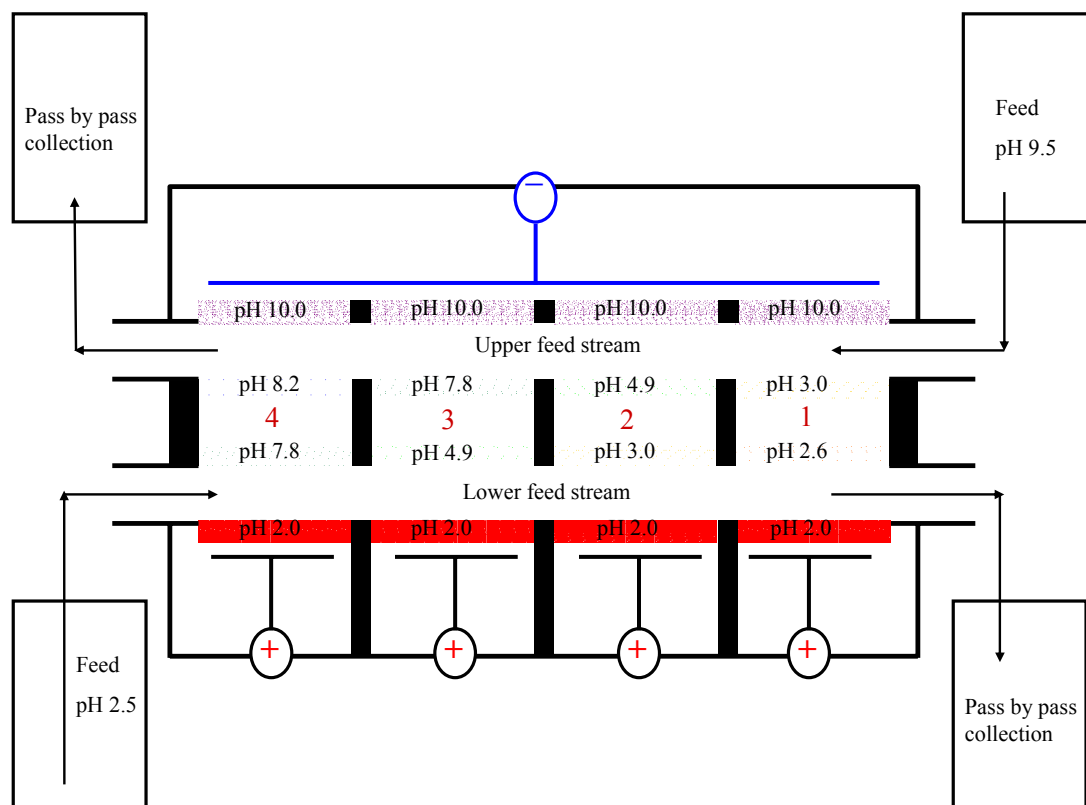
Figure 74. Schematic diagram of the ConFrac experimental setup using the pass-by-pass mode.

5.4.2. Instrument setup, materials, and method

The setup for the pass-by-pass mode IET experiment is depicted in Figure 74. The same amounts of aliquots from the sample stock solutions prepared in Section 5.2.2 were used. However, instead of recirculating the feed solutions, they were pumped through the microchannels at a flow rate of 5 mL/min and directly collected in different external reservoirs after each pass. Each pass took one minute to complete. After each pass, the

collected fractions were derivatized with NDA and analyzed by CE. The pH of the

effluents was also monitored after each pass.
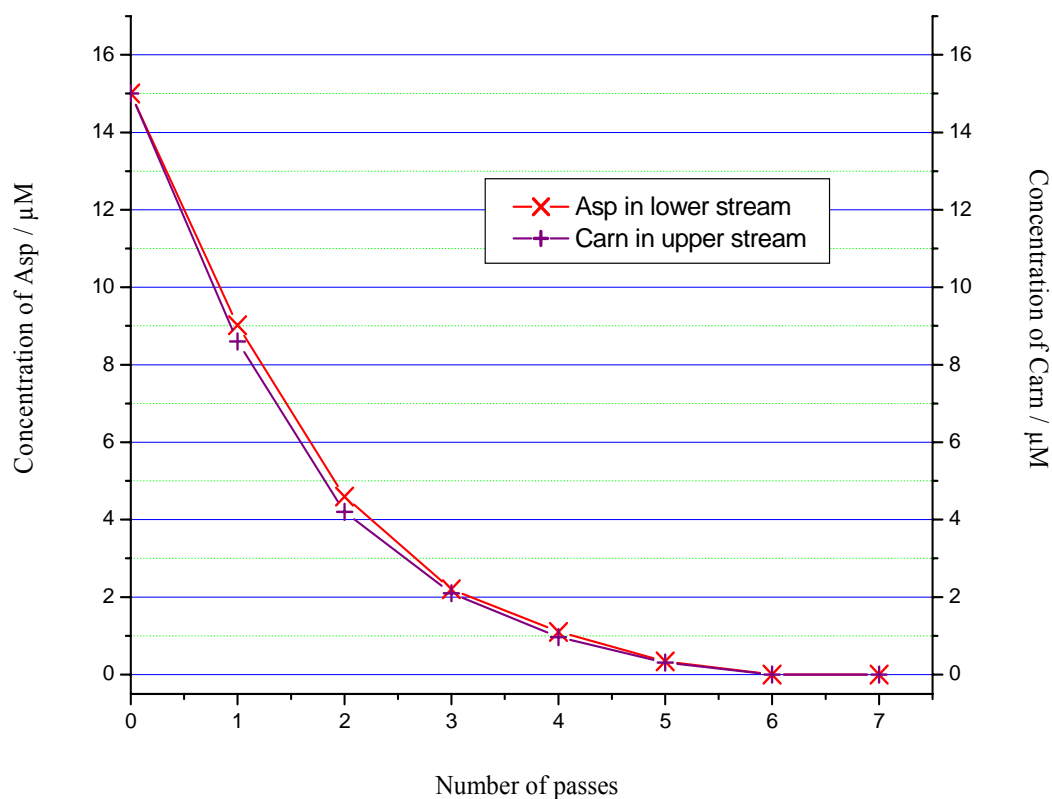
Figure 75. Concentration profile of aspartic acid and carnosine as they leave the lower and upper feed streams, respectively.

5.4.3. Results and discussion

The sample components were completely removed from both the lower and the upper

feed streams by the 6th pass. The concentrations of Asp and Carn in the lower and upper

microchannels were plotted as a function of the number of passes in Figure 75. The pH

profiles of the lower and upper feed streams are shown in Figure 76: the pH values

gradually approached the pI values of the respective isoelectric buffer present in the feed

streams. Figure 77 shows that each sample component was completely trapped by the 6th pass and each concentration was increased to about a factor of 100.
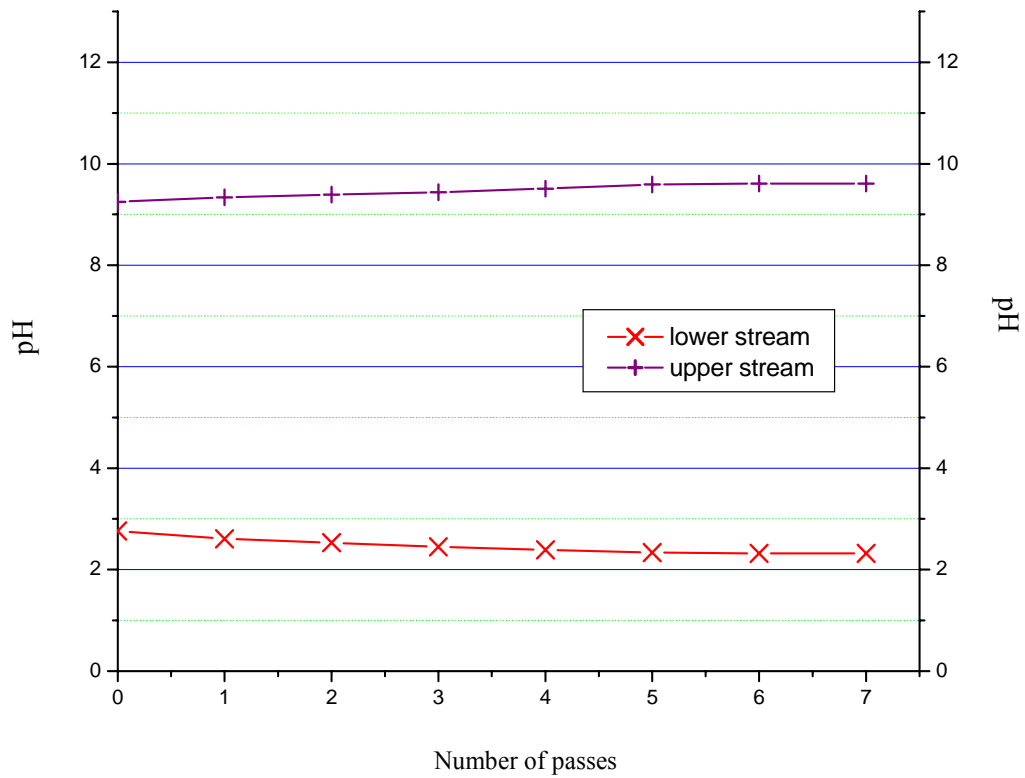
Figure 76. pH in the lower and upper feed streams as a function of the pass number.
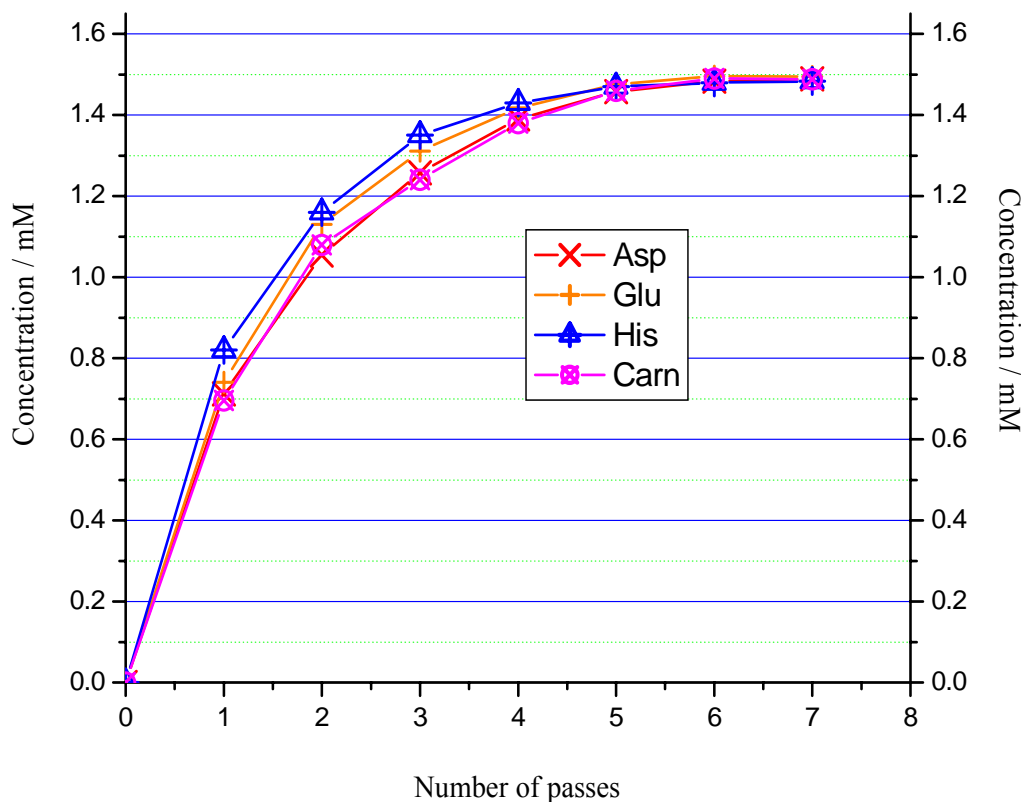
Figure 77. Concentration profile of ampholytes versus the number of passes as it is trapped in their compartment.

5.5. Desalting experiments using ConFrac

5.5.1. Background and objectives

It is also important to know whether the ConFrac has the same desalting capabilities as the MSWIFT. The electric resistance in the ConFrac is much lower than in the MSWIFT, because the membrane surface areas exposed to the electric field are 4 times larger and the anode-to-cathode distances are shorter. Thus, the objective here was to examine if the power supply could handle the rapid resistance change that would accompany efficient salt removal in the ConFrac. If needed, the ConFrac could be operated in one of two ways: (i) without diluting the sample, a constant low current could be applied initially,

and the current could be gradually increased until the power supply could run the process at a constant power of 2 watts; or (ii) the sample could be diluted gradually until 2 watts could be applied to the system at the beginning of the run. A UV-absorbing salt was used in the experiments to easily track salt removal.

5.5.2. Instrument setup, materials, and method

The experimental setup described in Section 5.2.2 was used. The anode compartments and the lower flow-through microchannel were interfaced by pH 2 buffering membranes. Collection compartments 1, 2, 3, and 4 were bounded by pairs of buffering membranes with the following pH values: 2.6/3.0, 3.0/4.9, 4.9/7.8, and 7.8/8.2, respectively; the higher pH membrane in each pair faced the upper flow-through microchannel. The upper microchannel and the cathode compartment were separated by a pH 10 buffering membrane. The UV-absorbing salt was prepared by titrating benzyltrimethylammonium hydroxide (BzTMAOH) with p-toluenesulfonic acid (PTSA), until the pH of the solution was 7.0. To prepare the lower feed solution (Solution 1XA), IDA, Asp, Glu, His, and Carn were added to100 mL of the UV absorbing salt solution to obtain a 150 mM salt, 3 mM IDA and 15 μM individual amino acid concentrations. The same mixture was prepared for the upper microchannel feed solution (1XB) except that 3 mM IDA was replaced by 1 mM MeLys. For the first experiment, 5 mL aliquots of solution 1XA and 1XB were recirculated through the lower and upper microchannels at a flow rate of 5 mL/min, respectively. A constant current of 1 mA was initially applied for 10 minutes, followed by constant 2 mA for the next 10 minutes. Then, 2 watts of power was applied for an additional of 40 minutes of IET.

In the second experiment, 5 mL aliquots of solutions 1XA and 1XB were independently diluted 2, 5, and 10 times to make lower/upper feed solutions 2XA/2XB, 5XA/5XB, and 10XA/10XB, respectively. The entire diluted sample solution volumes were introduced into their respective ConFrac channels, recirculated, and 2 watts of power was applied. In both experiments, fractions were collected every 10 minutes. The pH of each fraction was measured before the addition of the naphthalene dialdehyde derivatization solution. The NDA-treated fractions were then analyzed by CE.
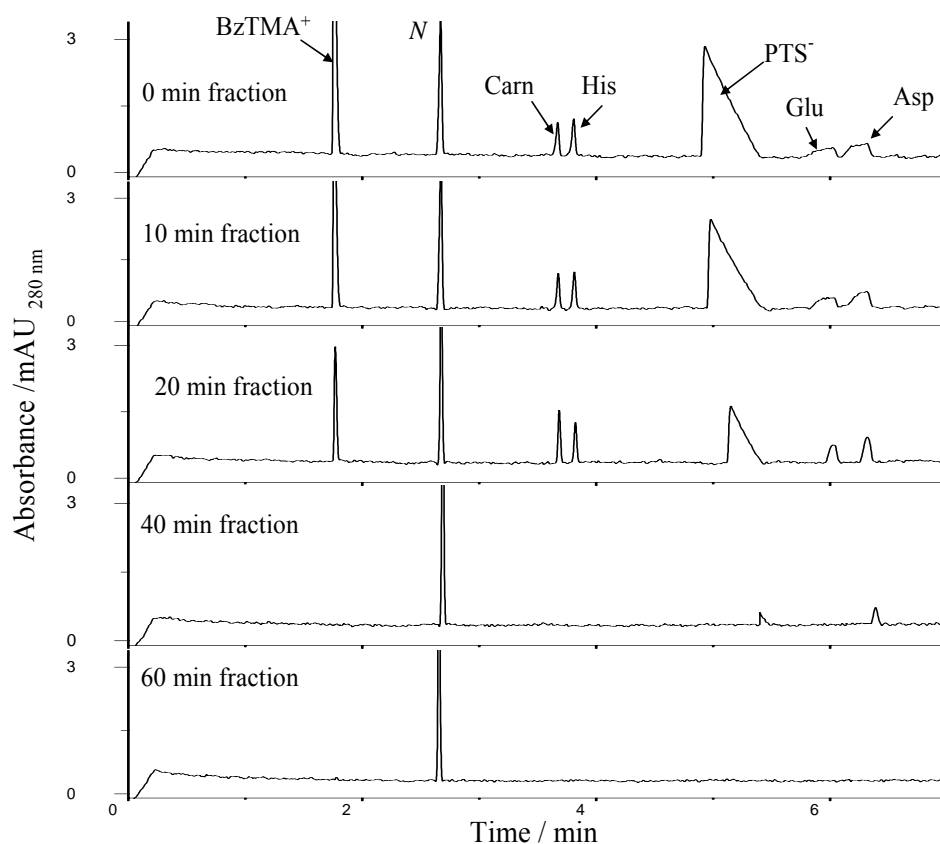
Figure 78. CE analysis of the lower feed stream during desalting.
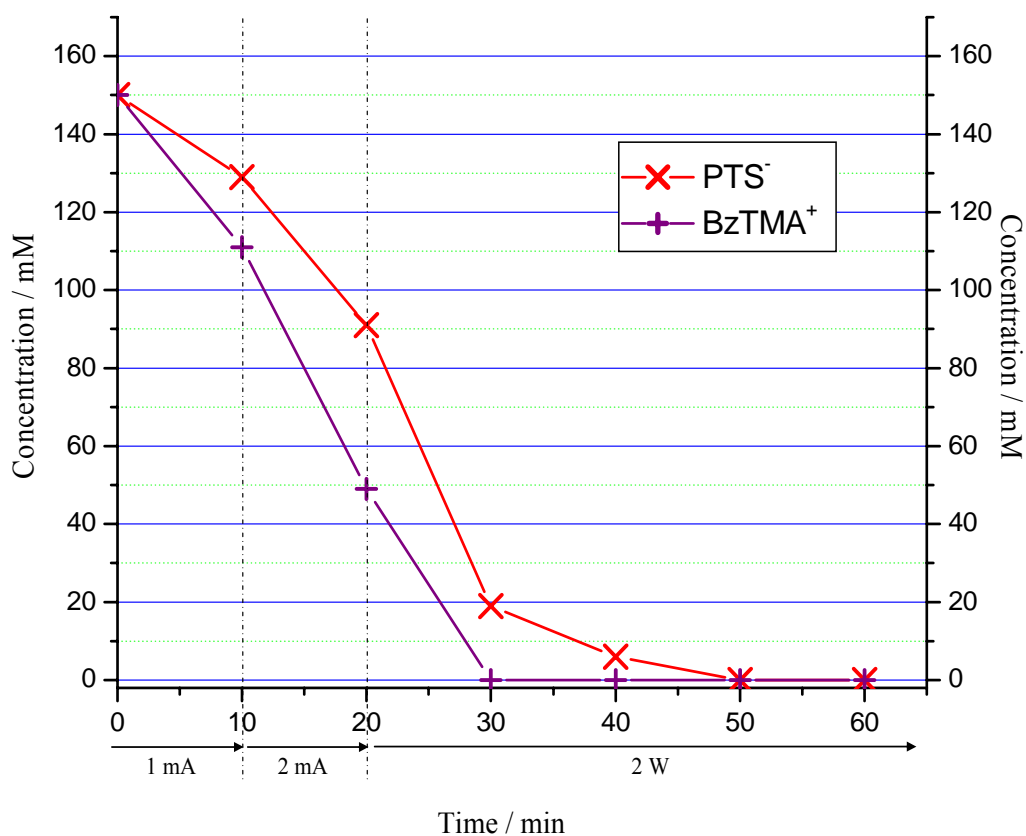
Figure 79. Concentration of BzTMA$^+$ and PTS$^-$ in lower feed stream.

5.5.3. Results and discussion

In the first desalting experiment, the power supply signaled an error due to the rapid

change of resistance when 1 watt of power (minimum power that can be set on the

controller of power supply) was applied initially. The power supply could only be

operated when a constant current of 1 mA (minimum current that can be set on the

controller of the power supply) was used to run the IET experiment. Figures 78 and 79

illustrate the disappearance of the salt from the lower feed stream. The rate of salt

removal increased as the current passing through the system was increased in the

successive segments of the experiment. The rate further increased when 2 watts of power

(corresponding to a current and voltage setting of 4 mA and 516 V) was applied.

BzTMA$^+$ was removed from the lower stream faster than PTS$^-$, because the difference between the pH of the separation membrane and pH 7 was smaller than the difference between the pH of the anodic membrane and pH 7, (non-symmetrical Donnan potentials [77]). Once the majority of the strong electrolyte ions were removed (after 30 minutes of IET), electrophoretic transport of the ampholytic sample components began. The pH of the lower stream is shown in Figure 80 as a function of time. A considerable drop in pH
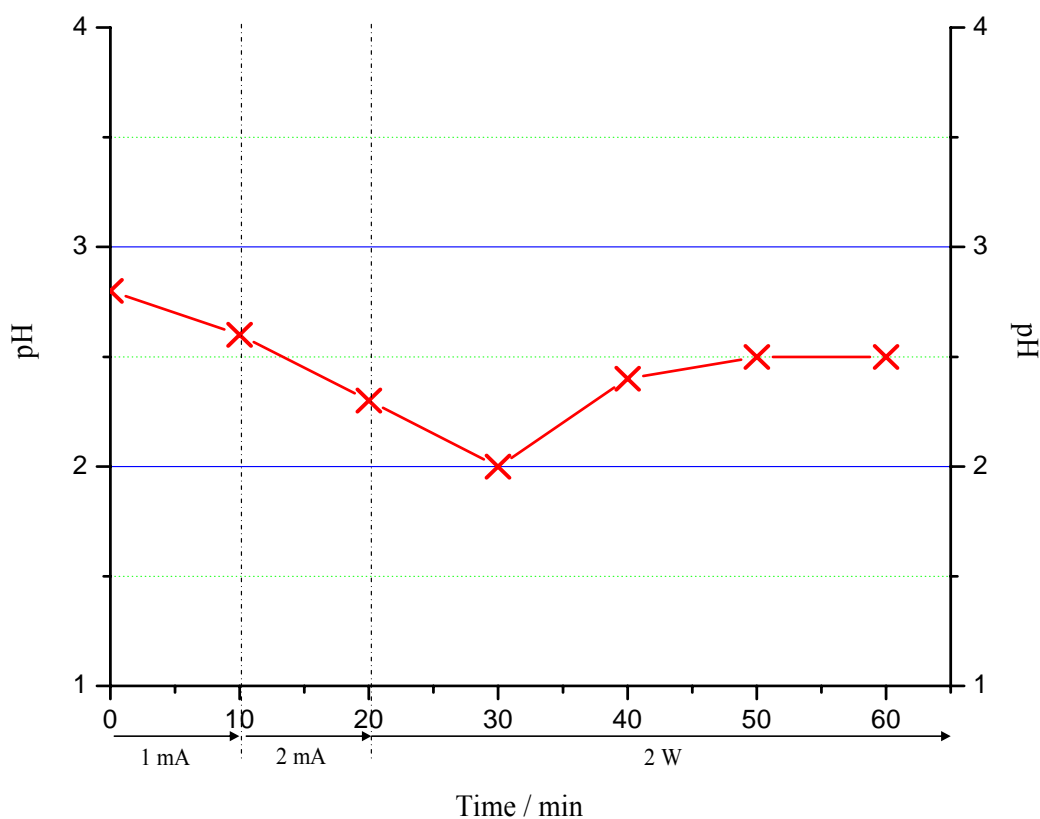
Figure 80. Acidic pH transient in the lower feed stream.

occurred in the first 30 minutes of the run, especially when the current was ramped up to 4 mA (2 watts), in agreement with previous results [76], as hydronium ions (H$_3$O$^+$)

replaced BzTMA$^+$ in the lower feed stream as counter-ions of PTS$^-$. After all PTS$^-$ was removed, the pH returned to the expected value.
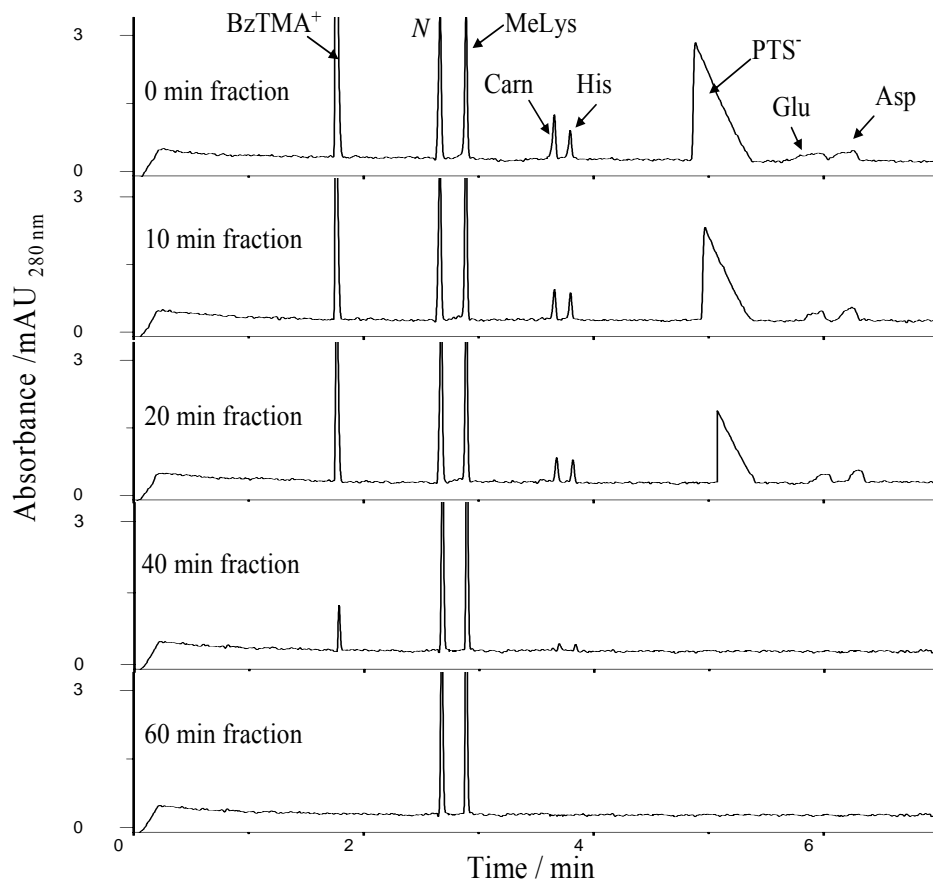
Figure 81. CE analysis of the upper feed stream during desalting.

Comparable rapid removal of salt was also observed in the upper channel as shown in Figures 81 and 82. This time around, PTS$^-$ was lost faster, causing a basic pH transient as OH$^-$ ions from the catholyte replaced PTS$^-$ as the counter-ions for the lingering BzTMA$^+$ ions [76]. The pH profile in the upper feed stream is shown in Figure 83.
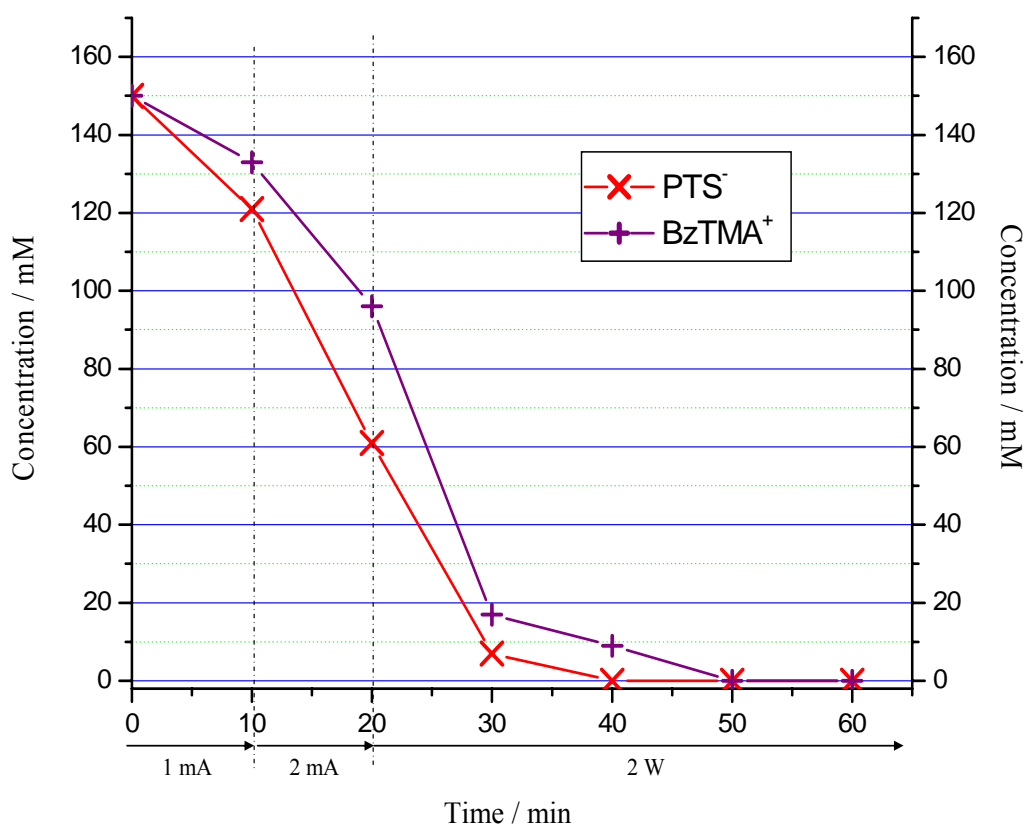
Figure 82. Concentration of BzTMA$^+$ and PTS$^-$ in upper feed stream.

In the second desalting experiment, 2 watts of power (causing an initial current of 9 mA and voltage of 219 V) could only be maintained with the 10-fold diluted feed solutions (10XA and 10XB). The total volume of each feed solution was 50 mL (15 mM salt concentration). Figures 84 and 85 portray depletion of the salt from the channels. Salt removal took about the same time as in the first experiment. A plot of the pH as a function of time is shown in Figure 86. The pH drop was more noticeable in the first 10 minutes of IET. It was at this point in time that the maximum currents were observed. A comparable scenario was observed in the upper feed stream. Salt removal from the upper

microchannel is depicted in Figures 87 and 88, indicating the presence of a basic pH

transient (Figure 89).
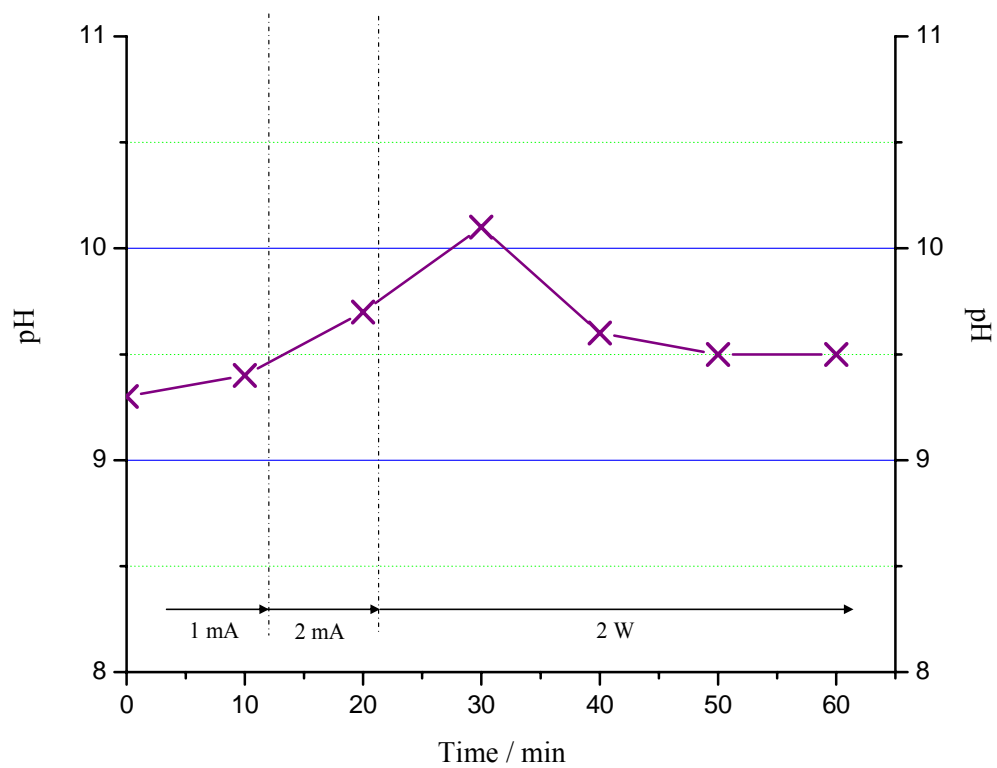
Figure 83. Basic pH transient in the upper feed stream.
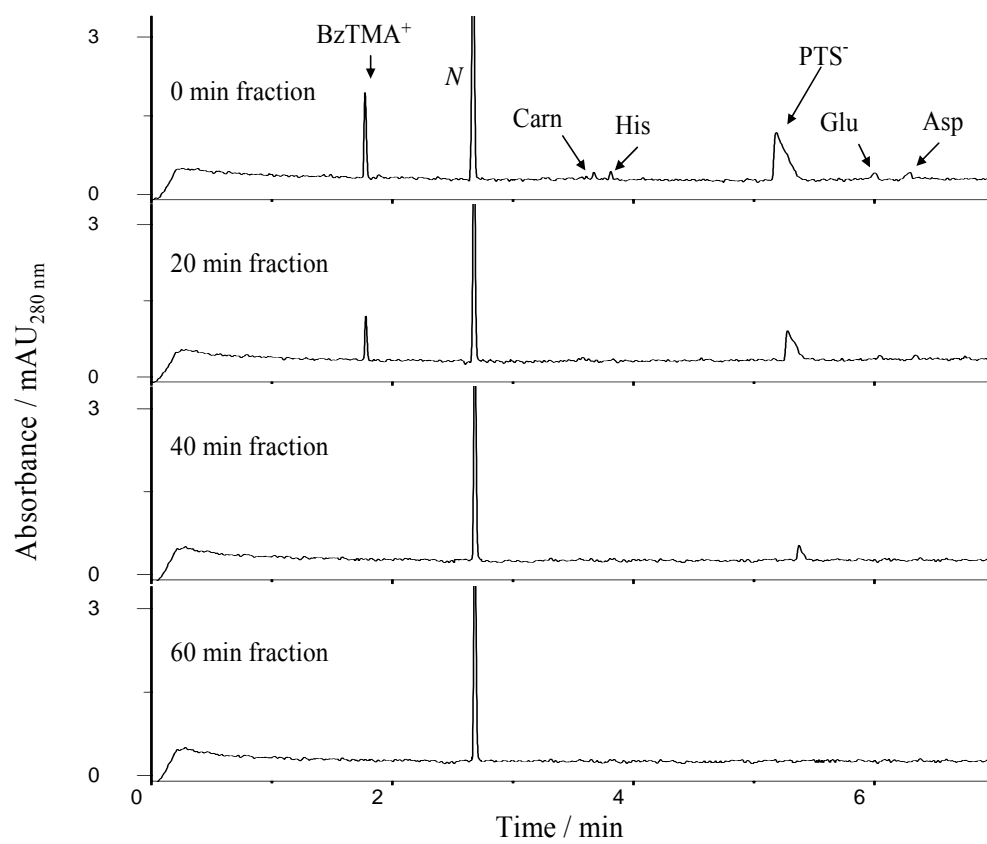
Figure 84. CE analysis of the lower feed stream during the second desalting experiment.
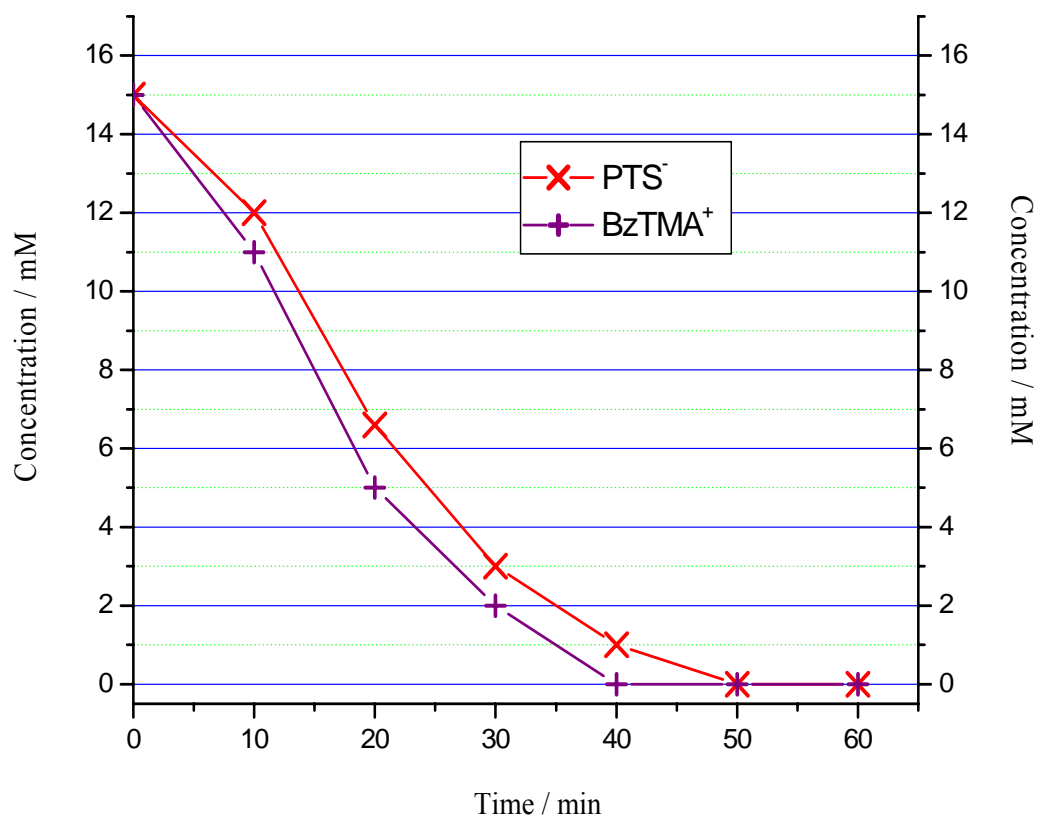
Figure 85. Concentration of BzTMA+ and PTS- in lower feed stream during the second desalting experiment.
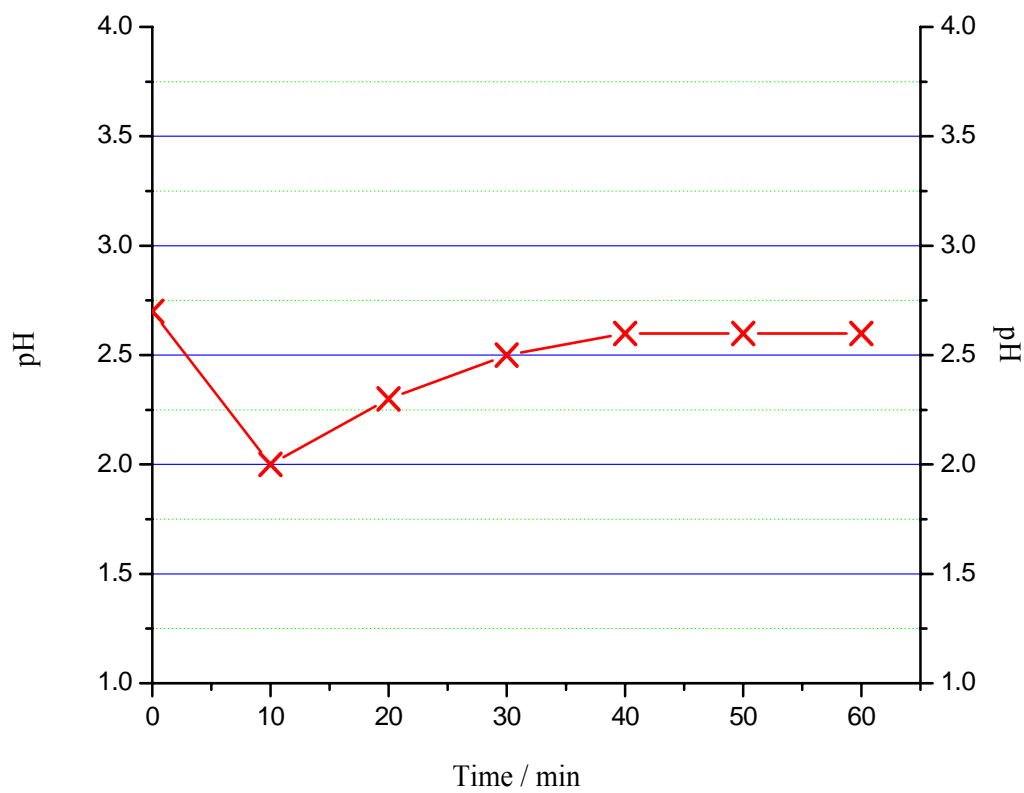
Figure 86. Acidic pH transient in the lower feed stream during the second desalting experiment.
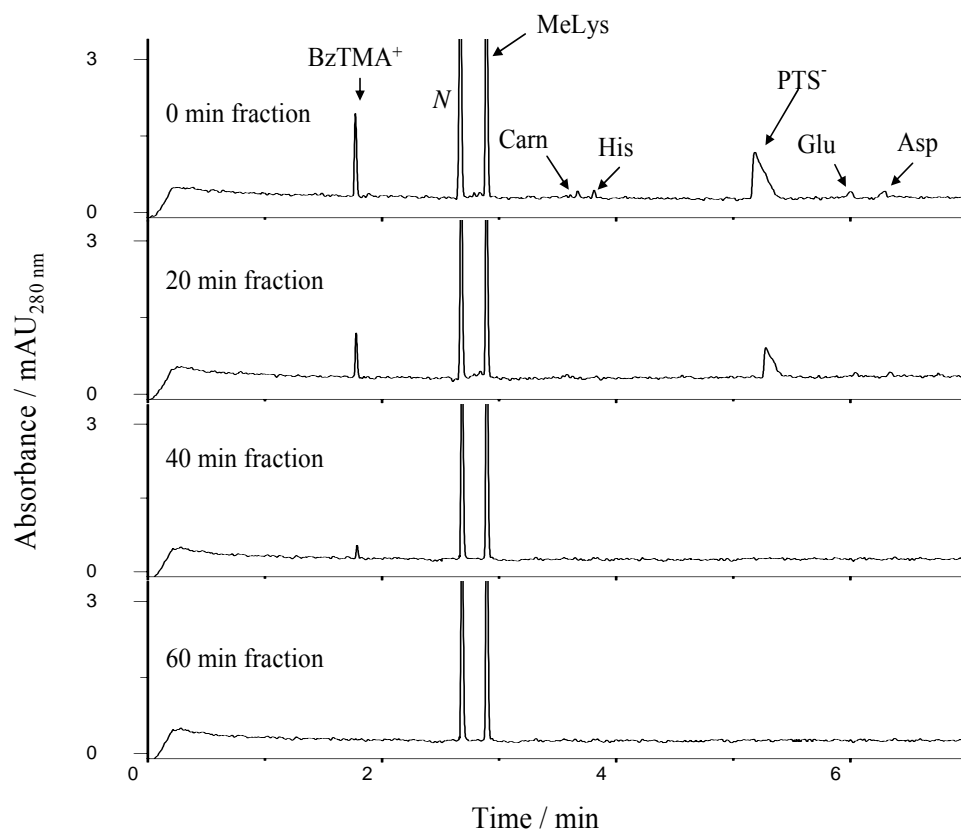
Figure 87. CE analysis of the upper feed stream during the second desalting experiment.
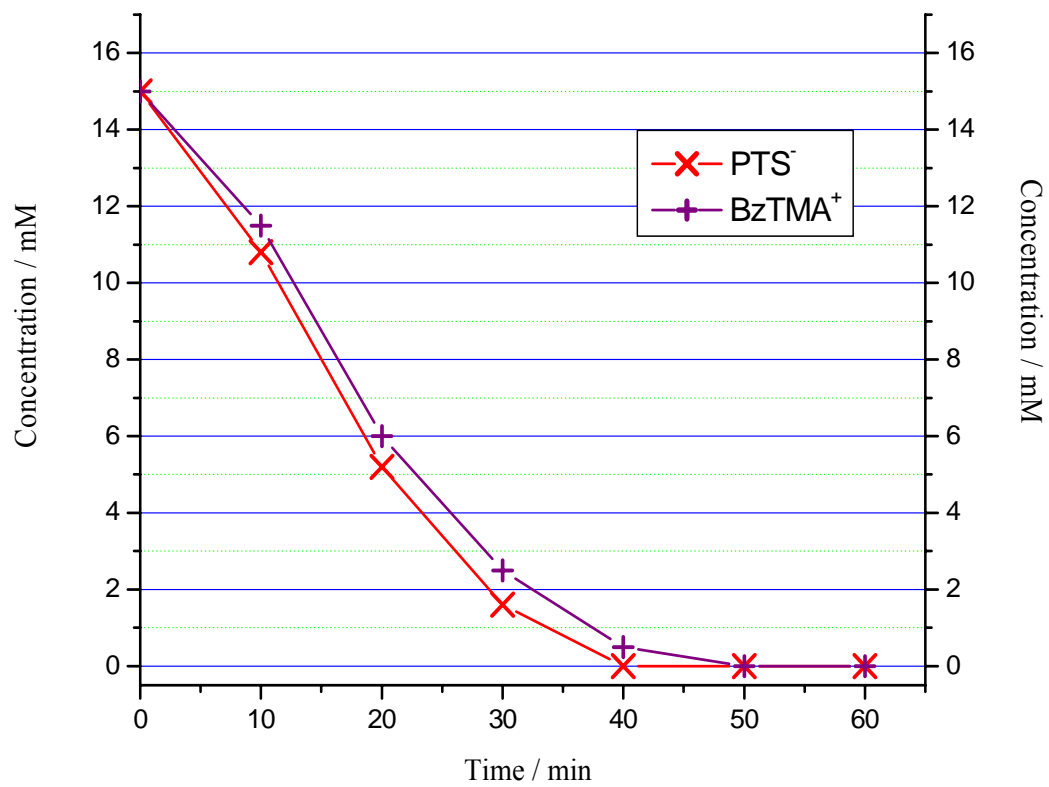
Figure 88. Concentration of BzTMA$^+$ and PTS$^-$ in the upper feed stream during the second desalting experiment.
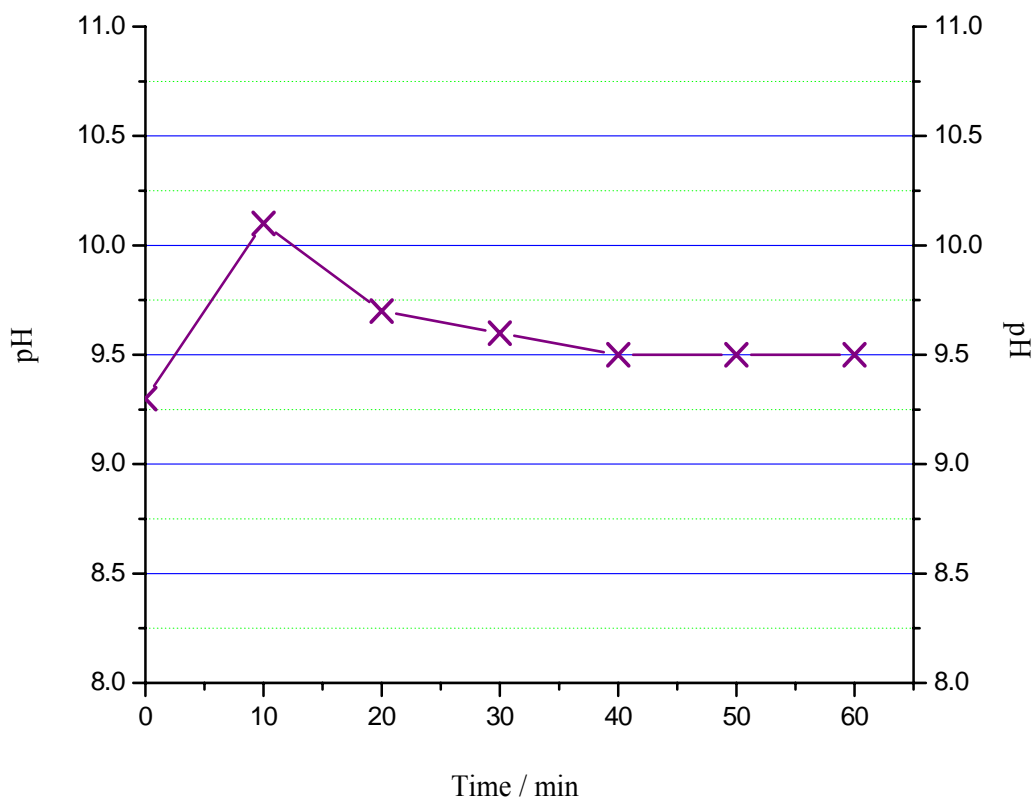
Figure 89. Basic pH transient in the upper feed stream during the second desalting experiment.

5.6. Isolation and enrichment of minor components from a 60% ovalbumin solution

5.6.1. Background and objectives

Aside from a large amount of strong electrolytes, biological samples also contain some proteins in large quantities (*e.g.*, blood serum contains about 60 w/w% of albumin) and some proteins of interest in very small quantities (*e.g.*, disease markers, regulatory proteins). It is essential to know how fast the ConFrac would be able to isolate and concentrate the minor components into the collection chambers and keep the major proteins in the feed stream. Unlike the salts, the major ampholytic components remain trapped in the feed stream and carry the majority of the current, thus the minor

components would have a low transference number. To test this aspect of the ConFrac

quantitatively, a model sample mimicking blood serum was used.

5.6.2. Instrument setup, materials, and method

The setup used in this experiment is shown in Figure 90. A 100 mL portion of a model

sample solution containing 30 mg/mL ovalbumin, 1mM of IDA and 15 µM of His and
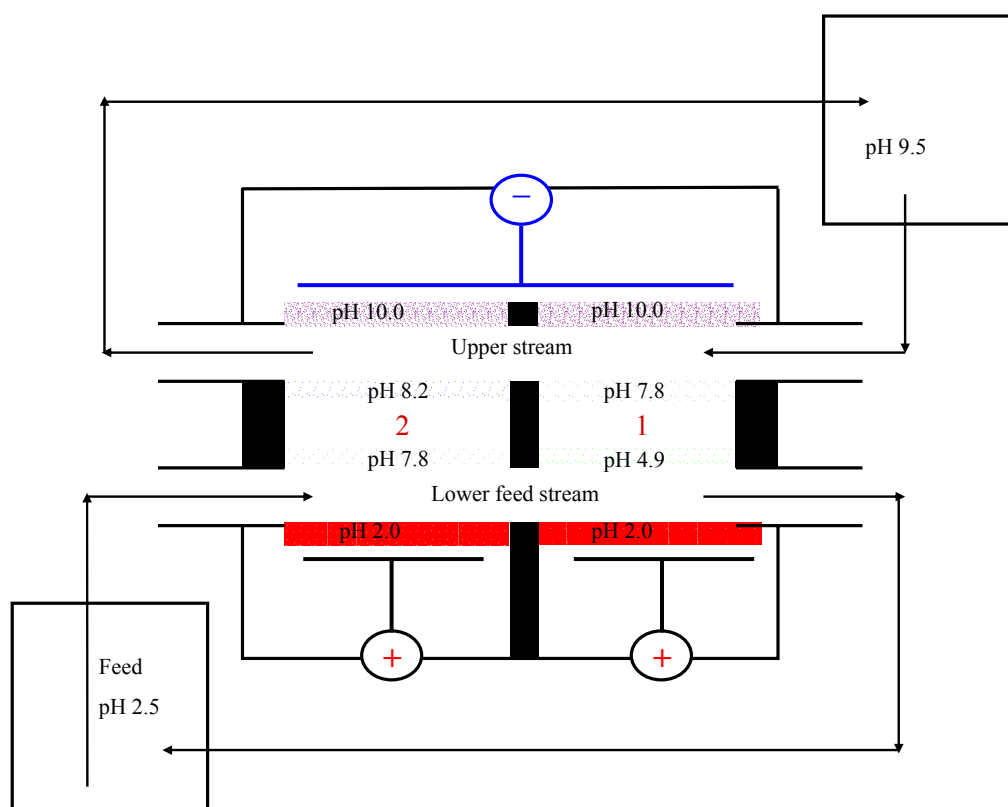
Figure 90. Schematic diagram of the ConFrac experimental setup. Sample was loaded
into the lower channel.

Carn was prepared. 10 mL of the sample was fed into the lower microchannel and

recirculated. 5 mL of a 1 mM MeLys solution was pumped through the upper

microchannel and recirculated. Only 2 collection compartments were used to isolate the

two minor components (His and Carn). The anolyte and catholyte systems used were the same as in Section 5.1.2. The IET separation was run at a constant power of 2 watts for 30 minutes. The fractions were collected every 5 minutes. The fractions from the lower feed stream were directly analyzed by CE using UV detection at 200-nm. The fractions obtained from the upper channel, compartments 1 and 2 were treated with NDA and analyzed by CE using UV detection at 280-nm.
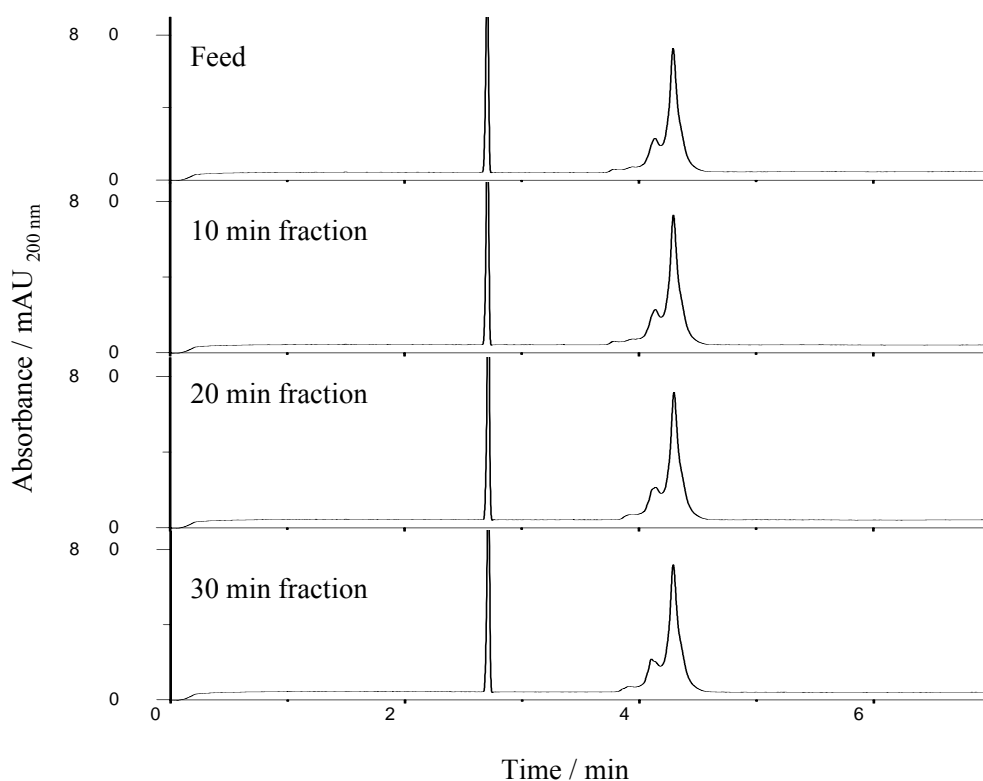
Figure 91. CE analysis of the lower feed stream.

5.6.3. Results and discussion

The fractions collected from the lower microchannel (Figure 91) indicated that ovalbumin was indeed retained in the lower microchannel. This fraction was not treated with NDA because ovalbumin would produce multiple NDA derivatives. The minor

components were quantitatively monitored in the fractions taken from compartments 1 and 2 and the upper channel (Figures 92 and 93). Rapid isolation and concentration was
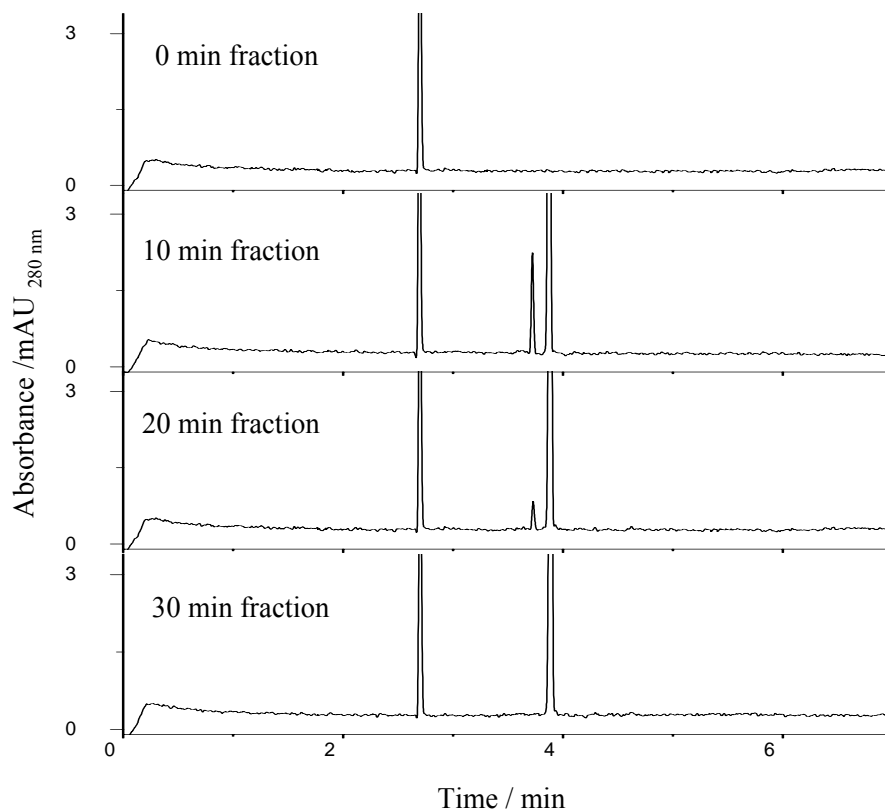
Figure 92. CE analysis of the fractions from compartment 1.

observed in the collection chambers. Figure 94 depicts the concentration profiles of ovalbumin in the feed stream, that of His in compartment 1, and Carn in compartment 2. Evidently, all of ovalbumin was kept in the feed stream and a 100-fold enrichment for each minor component was observed at the end of the 30-minute long run. The CE analysis results of the fractions collected from the upper microchannel are shown in Figure 95 where transient peaks of the minor components were once again observed.
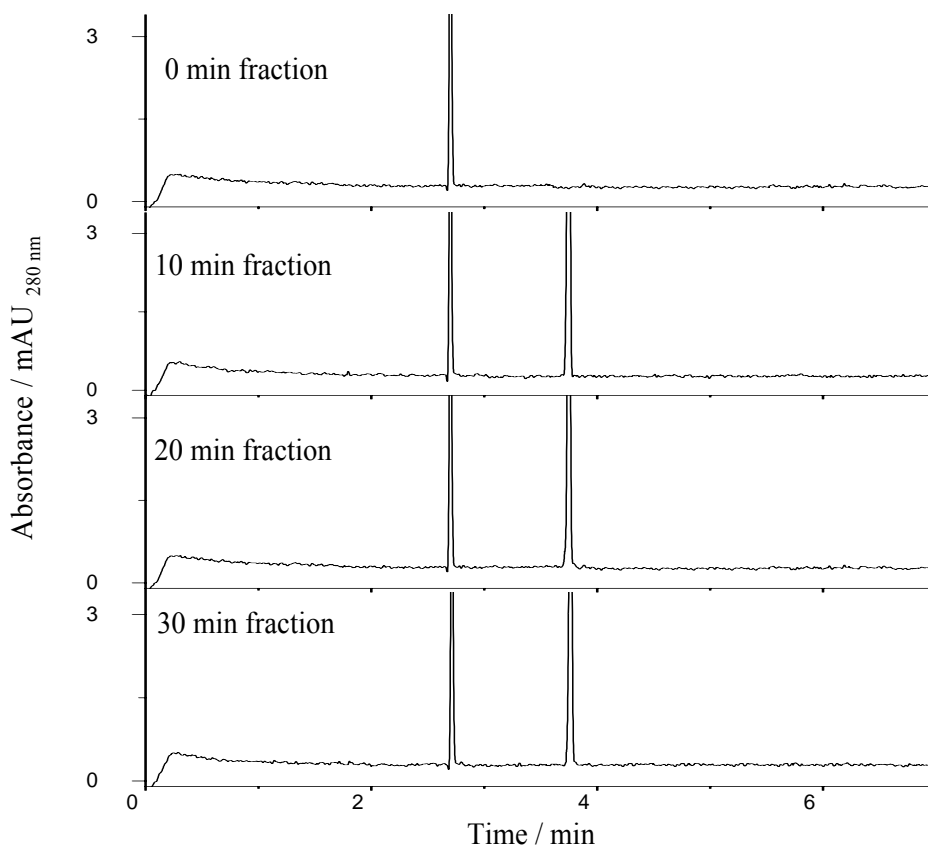
Figure 93. CE analysis of the fractions from compartment 2.

5.7. Concluding remarks

Optimization of the ConFrac system revealed interesting results. The sample can be

loaded either asymmetrically (only loaded into one microchannel) or symmetrically

(loaded into both microchannels). If the components to be trapped are the same in both

feed streams, their trapping rates are similar. If the solution reservoirs are kept at 10 ºC, a

5 mL/min feed flow rate represents the best compromise between processing rate and

temperature rise of the effluent. The ConFrac can also be operated in a pass-by-pass

mode. This mode provides a more thorough way of monitoring the transfer rate of the

sample components. The ConFrac was able to rapidly (i) remove salts, (ii) isolate and

enrich minor components into the collection chambers, and (iii) keep the major protein

component in the feed stream.
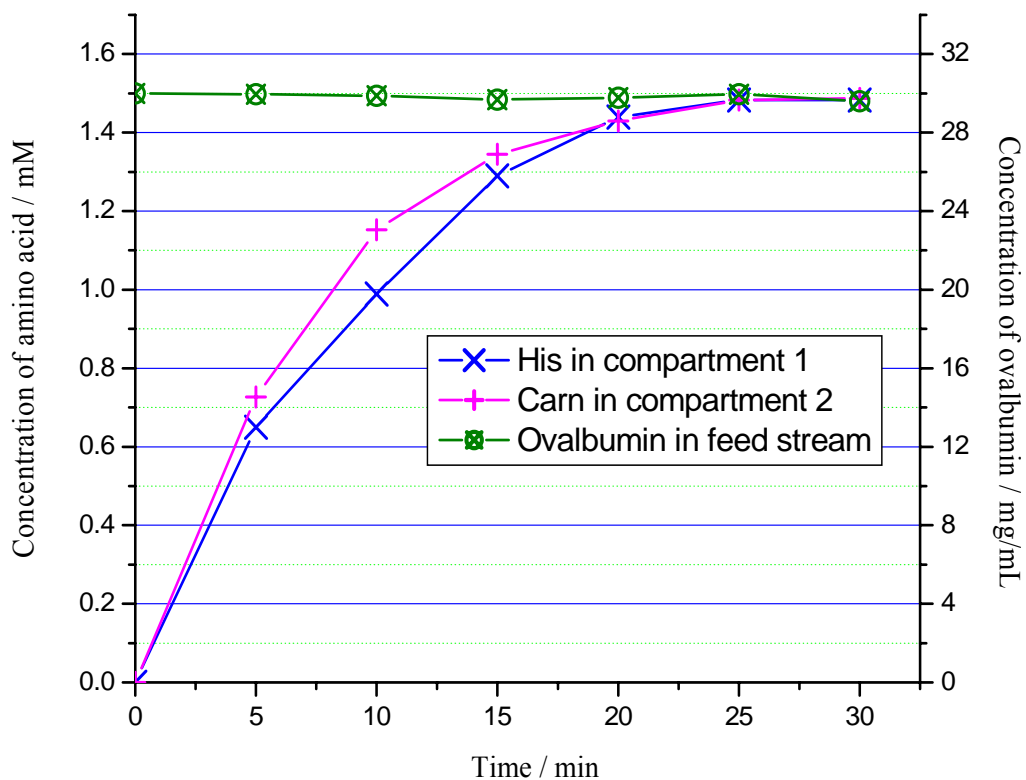
Figure 94. Isolation and enrichment of the minor components into their respective collection compartments and trapping of ovalbumin in the feed stream.
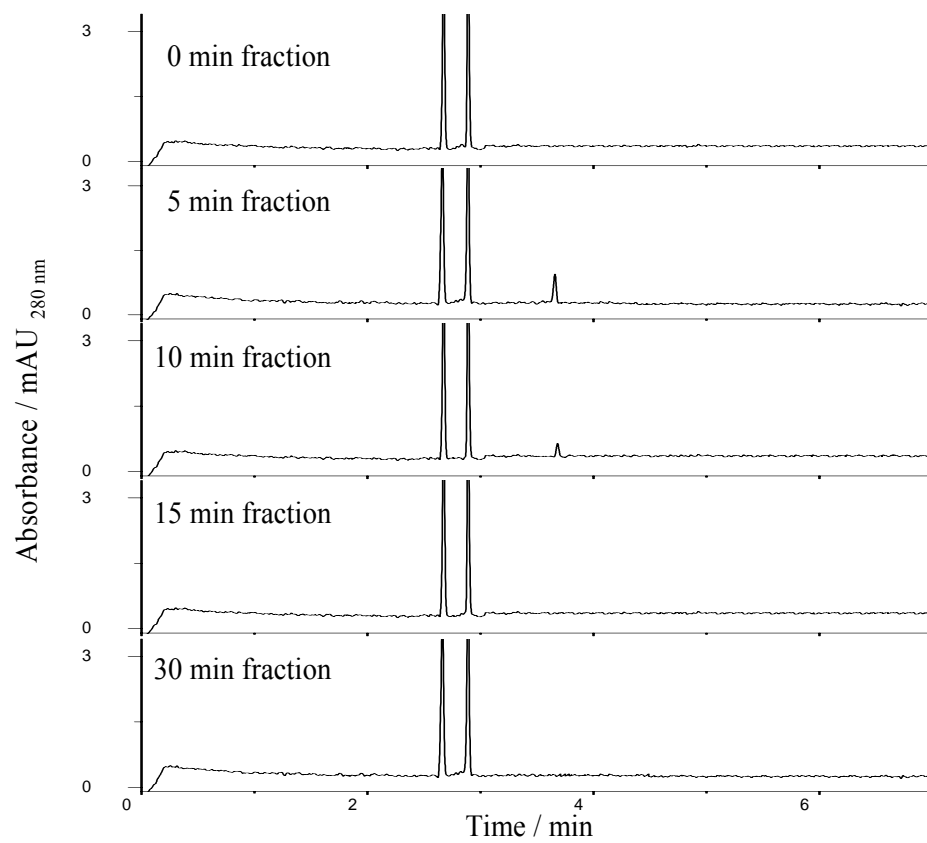
Figure 95. CE analysis of the upper channel.

6. CONCLUSIONS

6.1. Membrane-separated wells for isoelectric focusing and trapping (MSWIFT)

Small-scale isoelectric trapping separations have been carried out in multi-compartmental electrolyzers where the compartments were arranged serially and interfaced by buffering membranes. Typically, a protein sample is loaded into the compartments and electrophoresed to separate into fractions which are localized in the individual compartments bounded by buffering membranes whose pH values bracket the pI of the sample components. The narrowness of the pI range of the fractions depends on the buffering membranes selected. The commercially available small-scale IET instruments use long, cylindrical sample compartments which are made of plastics. Joule-heat created during electrophoresis dissipates poorly in these devices, because the center-to-wall heat conduction paths are long, and the thermal conductivity of the structural material (plastic) is low. Due to the excessive length of the compartments, the distance the sample components have to migrate in the commercially available devices before they get separated by the membranes is long, and the resulting electric field strength is low. These interrelated factors have led to long separation times.

A new device, the MSWIFT has been developed using the serial MCE format to achieve fast, small-volume IET separations. High-purity, nonporous aluminum oxide, which has a thermal conductivity of 30 W/mK (150 times better than that of the plastics), was used as the structural material for the sample compartments. Narrow channels were created in thin alumina blocks: each block can hold 100 to 200 μL of sample volume to provide (i) a center-to-wall heat dissipation path of only 1 mm; (ii) a short inter-membrane distance

(1/16 to ¼ ") (iii) a short anode-to-cathode distance (1/2 to 2 ") that leads to high field strengths. The system is able to dissipate up to 5 watts of power, which is 5 times better than what is possible in the commercially available devices. Separations of mixtures of ampholytes, both small molecules and proteins, have been achieved in the MSWIFT in less than 30 minutes. The MSWIFT proved to be a convenient device for the removal of salts, trapping of microgram to milligram quantities of proteins from microliter volumes of samples, and quantitative isolation of target compounds from complex reaction mixtures to facilitate further analysis.

The MSWIFT can be used as a tool to prefractionate complex protein samples and as an efficient alternative to scaled-up capillary isoelectric focusing methods when analyte fractions are to be collected for further downstream experiments.

6.2 Concentration-Fractionation (ConFrac) device

The drawback of the serial IET devices such as the MSWIFT is that the practical limit for the number of fractions that can be obtained is about 10 to 20 (*i.e.*, the device contains 10 to 20 serially connected sample compartments), unless the penalties associated with complex sealing systems and long anode-to-cathode distances are accepted. Thus, only an order of magnitude enrichment can be realized in these systems, which may not be enough to detect low abundance proteins.

The ConFrac device has been developed to eliminate the limitations of the serial MCE devices. During IET, the sample components are separated into small-volume

compartments that are arranged parallel to each other and orthogonal to the electric field. Simultaneous separation and enrichment are achieved in the ConFrac device by pumping a large, variable volume of sample through the flow-through channels. A ConFrac system containing four ceramic compartments was designed and manufactured. Easy to machine PVC was used to make the electrolyte and flow-through compartments. Each of the plastic chambers was provided with an inlet and outlet for the thermostated solutions to flow in and out.

Characterization and optimization experiments lead to simultaneous separation and concentration of ampholytic components with 100-fold and greater enrichment, in 30 to 60 minutes of IET. In addition, desalting, separation and concentration were achieved in one step. The ConFrac can be used to isolate and enrich low abundance proteins and keep the major protein components in the large reservoirs. In the ConFrac, the number of fractions that can be collected can be increased without concomitant increase in the separation time.

REFERENCES

[1] Mosher, R. A.; Saville, D. A.; Thormann, W. *The Dynamics of Electrophoresis*; VCH: Weinheim, Germany, 1992.

[2] Nisbet, A. D., Saundry, R. H., Moir, A. J. G., Fothergill, L. A., Fothergill, J. E., *Eur. J. Biochem.* 1981, *115*, 335-345.

[3] Peters, T., *All About Albumin: Biochemistry, Genetics, and Medical Applications*, Academic Press, San Diego, CA 1996, pp. 24-54.

[4] Kolin, A. *Journal of Chemical Physics* 1954, *22*, 1628-1629.

[5] Svensson, H. *Acta Chemica Scandinavica* 1961, *15*, 325-341.

[6] Liu, X., Sosic, Z., Krull, I.S., *J. Chromatography A*, 1996; *735*, 165.

[7] Righetti, P. G., Hjerten, S., *J. Biochem. Biophys. Methods* 1981, *5*, 259-272.

[8] Vingradov, S. N., Lowenkron, S., Andonian, H. R., Bagashaw, J., Felegenhauer, K., Pak, S. J., *Biochem. Biophys. Res. Commun.* 1973, *54*, 501-506.

[9] Righetti, P. G., Pagani, M., Gianazza, E., *J. Chromatogr.*1975, *109*, 341-356.

[10] Charlionet, R., Martin, J. P., Sesboue, R., Madec, P. J., Lefebvre, F., *J. Chromatogr.* 1979, *176*, 89-101.

[11] Just, W. W., *Anal. Biochem.* 1980, *102*, 134-144.

[12] Herbert, B. R., Molloy, M. P., Gooley, B. A. A., Walsh, J.; Bryson, W. G., Williams, K. L., *Electrophoresis* 1998, *19*, 845–851.

[13] Nguyen, N. Y., Chrambach, A., *Anal. Biochem.* 1976, *74*, 145-153.

[14] Mosher, R. A., Thormann, W., Graham, A., Bier, M., *Electrophoresis* 1985, *6*, 545-551.

[15] Bier, M., Ostrem, J., Marquez, R. B., *Electrophoresis* 1993, *14*, 1011-1018

[16] Righetti, P.H., Bossi, A., *Analytica Chimica Acta,* 1998; *372*, 1-19.

[17] Wu X.Z., Pawliszyn, J., *Electrophoresis*, 2002, *23*, 542-549

[18] Burggraf, D., Weber, G., Lottspeich, F., *Electrophoresis*, 1995, *16*, 1010-1015.

[19] Bier, M., *Electrophoresis*, 1998, *19*, 1057-1063.

[20] Mosher, R.A., Dewey, D., Thormann, W., Saville, D.A., Bier, M., *Anal. Chem.* 1989, 6*1,* 362-366.

[21] Mosher, R.A., Thormann, W., *Electrophoresis*, 1990, *11*, 717-723.

[22] Thormann, W., Huang, T., Pawliszyn, J., Mosher, R.A., *Electrophoresis*, 2004, *25*, 324-337.

[23] Thormann, W., Mosher, R.A., *Electrophoresis*, 2006, *27*, 968-983.

[24] Righetti, P. G., *Immobilized pH Gradients: Theory and Methodology*, Elsevier Biomedical Press, Amsterdam 1990, pp. 10-12.

[25] Bjellqvist, B., Ek, K., Righetti, P. G., Gianazza, E., Gorg, A., Westermeier, R., Postel, W., *J. Biochem. Biophys. Methods* 1982, 6, 317-339.

[26] Ogle, D., Ho, A., Gibson, T., Rylatt, D., Shave E., Lim P., Vigh, G., *J. Chromatography A*, 2002, *979*, 155-161.

[27] Martin, A. J. P., Hampson, F., US Patent 4, 243, 507, 1981.

[28] Wenger, P., de Zuanni, M., Javet, P., Gelfi, C., Righetti, P. G., *J. Biochem. Biophys. Methods,* 1987, *14*, 29-43.

[29] *Doctor pH Manual*, Amersham Pharmacia Biotech, 1993, San Francisco, CA.

[30] Righetti, P.G., Barzaghi, B., Luzzana, M., Manfredi, G., Faupel, M., *J. Biochem. Biophys. Methods*, 1987, *15*, 189-198.

[31] Faupel, M., Barzaghi, B., Gelfi, C., Righetti, P.G., *J. Biochem. Biophys. Methods*, 1987, *15*, 147-161.

[32] Righetti, P. G., Wenisch, E., Faupel, M., *J. Chromatogr.* 1989, *475*, 293-309.

[33] Lalwani, S., Shave, E., Fleisher, H. C., Nzeadibe, K., Busby, M. B., Vigh, G., *Electrophoresis* 2004, *25*, 2128-2138.

[34] Lalwani, S., Shave, E., Vigh, G., *Electrophoresis* 2004, *25*, 3323-3330.

[35] Fleisher, H. C., Vigh, G., *Electrophoresis* 2005, *26*, 2511-1519.

[36] Shave, E., Vigh, G., *Electrophoresis* 2004, *25*, 381-387.

[37] Lalwani, S., Tutu, E., Vigh, G., *Electrophoresis* 2005, *26*, 2503-2510.

[38] Lalwani, S., Tutu, E., Vigh, G., *Electrophoresis* 2005, *26*, 2047-2055.

[39] Martin, A. J. P., Hampson, F., *J. Chromatogr.* 1979, *159*, 101-110.

[40] *IsoPrime Manual*, Amersham Pharmacia Biotech, 1999, San Francsico, CA.

[41] Shang, T.Q., Ginter, J. M., Johnston, M. V., Larsen, B. S., McEwen, C. N., *Electrophoresis* 2003, 24, 2359 – 2368.

[42] Horvath, Z. S., Corthals, G L., Wrigley, C. W., Margolis, J., *Electrophoresis* 1994, *15*, 968-971.

[43] Margolis, J., Corthals, G., Horvath, Z. S., *Electrophoresis* 1995, *16*, 98-100.

[44] Horvath, Z. S., Gooley, A. A., Wrigley, C. W., Margolis, J., Williams, K. L., *Electrophoresis* 1996, *17*, 224-230.

[45] Corthals, G., Margolis, J., Williams, K. L., Gooley, A. A., *Electrophoresis* 1996, *17*, 771-775.

[46] Corthals, G. L., Molloy, M. P., Herbert, B. R., Williams, K. L., Gooley, A. A., *Electrophoresis* 1997, *18*, 317-323.

[47] Corthals, G., Collins, B. M., Mabbutt, B. C., Williams, K. L., Gooley, A. A., *J. Chromatogr. A* 1997, *773*, 299-309.

[48] Lim, S., Manusu, H. P., Gooley, A. A., Williams, K L., Rylatt, D.B., *J. Chromatogr. A* 1998, *827*, 329-333.

[49] Rylatt, D. B., Napoli, M., Ogle, D., Gilbert, A., Lim, S., Nair, C. H., *J. Chromatogr. A* 1999, *865*, 133-145.

[50] Thomas, T. M., Shave, E., Bate, I. M., Gee, S. C., Franklin, S., Rylatt, D. B., *J. Chromatogr. A* 2002, *964*, 161-168.

[51] Rothemund, D. L., Thomas, T M., Rylatt, D. B., *Protein Expression and Purification* 2002, *26*, 149-152.

[52] Rothemund, D. L., Locke, V. L., Liew, A., Thomas, T. M., Wasinger, V., Rylatt, D. B., *Proteomics* 2003, *3*, 279-287.

[53] Moller, C. C., Thomas, D., Van Dyk, D., Rylatt, D., Sheehan, M., *Electrophoresis* 2005, *26*, 35-46.

[54] Daw, R., Finkelstein, J., *Nature,* 442, 367-368.

[55] Whitesides, G. M., *Nature,* 442, 368-373.

[56] Craighead, H., *Nature,* 442, 387-393.

[57] *IsoelectriQ² Manual*, Proteome Systems Ltd., 2003, Woburn, MA.

[58] Sloane, A. J., , Duff, J. L., Wilson, N. L., Gandhi, P. S., Hill, C. J., Hopwood, F. G., Smith, P. E., Thomas, M. L., Cole, R. A., Packer, N. H., Breen, E. J., Cooley, P. W., Wallace, D. B., Williams, K. L., Gooley, A. A., *Molecular & Cellular Proteomics* 2002, 1, 490-499.

[59] Zuo, X., Speicher, D. W., *Anal. Biochem.* 2000, *284*, 266-278.

[60] Zou, X., Speicher, D.W., *Proteomics*, 2002, *2*, 58-68.

[61] *ZOOM™ Manual*, Invitrogen, 2004, Carlsbad, CA.

[62] Tan, A., Pashkova, A., Zang, L., Foret, F., Karger, B. L., *Electrophoresis* 2002, 23, 3599-3607.

[63] Michel, P.E., Reymond, P., Arnaud, I.L., Josserand, J., Girault, H.H., Rossier, J.S., *Electrophoresis*, 2003, *24*, 3-11.

[64] Zilberstein, G., Korol, L., Bukshpan, S., Baskin, E., *Proteomics* 2004, 4, 2533-2540.

[65] Stevens, L., *Comp. Biochem. Physiol.,* 1991, *100B*, 1-9.

[66] Desert, C., Guerin-Dubiard, C., Nau, F., Jan. G., Val, F., Mallard, J., *J. Agric. Food. Chem.* 2001, *49*, 4553-4561.

[67] Croguennec, T., Nau, F., Pezennec, S., Piot, M., Brule, G., *Eur. Food. Res. Technol.* 2001, *212*, 296-301.

[68] Lalwani, S., Vigh, G., *Electrophoresis* 2005, *26*, 3-9.

[69] Fountoulakis, M., Langen, H.; Evers, S., Gray, C., Takàcs, B., *Electrophoresis* 1997, *18,* 1193–1202.

[70] Fountoulakis, M.; Takács, B., *Protein Expression Purif.* 1998, *14,* 113–119.

[71] Karlsson, K., Cairns, N., Lubec, G., Fountoulakis, M., *Electrophoresis*, 1999, *20,* 2970-2976.

[72] Fountoulakis, M., Takács, M-F., Takács, B., *J. Chromatography A,* 1999, 833, 157–168.

[73] Fountoulakis, M., Takács, M-F., Berndt, P., Langen, H., Takács, B., *Electrophoresis*, 1999, *20*, 2181-2195.

[74] Badock, V., Steinhusen U, Bommert K, Otto A., *Electrophoresis,* 2001, *22*, 2856-2864.

[75] Michielsen, E., Diris, J., Hackeng, C. M., Wodzig, W., Van Dieijen-Visser, M.P. *Clinical Chemistry*, 2005, 51, 222-224.

[76] Righetti, P. G., Boschetti, E., Lomas, L., Citterio, A., *Proteomics* 2006, *6*, 3980-3992.

[77] Shave, E. E., *pH-Biased Isoelectric Trapping Separations*. Dissertation, Texas A&M University. 2005.

VITA

Peniel Jason Lim received his B.S. in chemistry degree from The University of San Carlos, Philippines in 1998. After teaching freshman chemistry at his alma mater, he moved to the United States and joined the graduate chemistry program at Texas A&M University in June 2001.Under the direction of Professor Gyula Vigh in the Separation Science group, his research interests focused on the design, manufacture and characterization of analytical-scale electrophoretic devices for protein separations. Peniel may be reached at: 404 Oxford St., #2209, Houston, TX 77007 or by email: pjlim3@yahoo.com.